

# "FEDERICO II" UNIVERSITY OF NAPLES



**Doctorate Program in Neuroscience  
Coordinator: Prof Lucio Annunziato  
XXX Cycle**

**“Characterization of the Role Played by  
NCX Isoform 3 in a Transgenic Model of  
Alzheimer’s Disease by  
Electrophysiological  
and Biochemical Studies”**

**TUTOR:**

**Prof Anna Pannaccione**

**PhD STUDENT:**

**Dr Ilaria Piccialli**

**ACADEMIC YEAR 2016-2017**

# TABLE OF CONTENT

<b>List of abbreviations</b>	Pag. 1
<b>Summary</b>	Pag. 4
<b>Introduction</b>	Pag. 7
<b>Chapter 1: Alzheimer's disease</b>	Pag. 8
<b>1.1 Overview</b>	Pag. 8
1.1.1 Neuritic plaques	Pag. 10
1.1.2 'Diffuse' plaques	Pag. 11
1.1.3 Neurofibrillary tangles	Pag. 12
1.1.4 AD clinico-pathological features and diagnostic criteria	Pag. 13
<b>1.2 Genetics of Alzheimer's disease</b>	Pag. 15
1.2.1 Mutations of APP	Pag. 16
1.2.2 Mutations of presenilins	Pag. 20
1.2.3 Apolipoprotein E4 allele	Pag. 21
<b>1.3 Animal models of AD</b>	Pag. 22
<b>1.4 Amyloid cascade hypothesis</b>	Pag. 24
1.4.1 Intracellular A $\beta$	Pag. 27
1.4.1.1 Accumulation of intracellular A $\beta$	Pag. 27
1.4.1.2 Pathogenic role of intracellular A $\beta$	Pag. 28
1.4.2 Dysregulation of ionic homeostasis	Pag. 29
1.4.2.1 Potassium dysregulation in AD	Pag. 29
1.4.2.2 Sodium dysregulation in AD	Pag. 31
1.4.2.3 Calcium dysregulation in AD: the 'Calcium hypothesis'	Pag. 32
<b>1.5 Neuronal hyperexcitability and epilepsy in AD</b>	Pag. 35
1.5.1 Role of Na $v$ currents in neuronal hyperexcitability	Pag. 37
<b>Chapter 2: The Na<math>^+</math>/Ca<math>^{2+}</math> exchanger</b>	Pag. 39
<b>2.1 Overview</b>	Pag. 39
<b>2.2 Molecular biology of NCX</b>	Pag. 41
2.2.1 NCX topology	Pag. 41
2.2.2 NCX genes and splice variants	Pag. 43
<b>2.3 NCX regulation</b>	Pag. 45
2.3.1 Ca $^{2+}$ regulation	Pag. 45
2.3.2 Na $^+$ regulation	Pag. 46

2.4 Pharmacological modulation of NCX	Pag. 47
2.4.1 Inhibitors	Pag. 47
2.4.1.1 Bivalent cations	Pag. 47
2.4.1.2 Endogenous Exchanger Inhibitory peptide	Pag. 48
2.4.1.3 Amiloride derivatives	Pag. 49
2.4.1.4 Isothiourea derivatives	Pag. 50
2.4.2 Activators	Pag. 51
2.4.2.1 Inorganic cations	Pag. 51
2.4.2.2 Redox agents	Pag. 51
2.4.2.3 Organic compounds	Pag. 52
2.5 Brain distribution of NCX	Pag. 53
2.5.1 Hippocampus	Pag. 53
2.5.2 Cerebral cortex	Pag. 54
2.5.3 Cerebellum	Pag. 54
2.6 NCX function in healthy brain	Pag. 55
2.7 NCX involvement in CNS diseases	Pag. 57
2.7.1 Stroke	Pag. 57
2.7.2 Multiple sclerosis	Pag. 58
2.7.3 Alzheimer's disease	Pag. 60
<b>Aims of the study</b>	Pag. 63
<b>Materials and methods</b>	Pag. 66
3.1 Drugs and chemicals	Pag. 67
3.2 Mice	Pag. 67
3.2.1 Genotyping: PCR analysis	Pag. 68
3.3 Mouse hippocampal neurons	Pag. 69
3.4 Electrophysiological recordings	Pag. 70
3.4.1 NCX currents	Pag. 70
3.4.2 Na <sup>+</sup> currents	Pag. 71
3.5 [Ca <sup>2+</sup> ] <sub>i</sub> and [Na <sup>+</sup> ] <sub>i</sub> measurements	Pag. 72
3.5.1 [Ca <sup>2+</sup> ] <sub>i</sub> measurement	Pag. 72
3.5.2 [Na <sup>+</sup> ] <sub>i</sub> measurement	Pag. 73
3.6 Western blotting	Pag. 74
3.7 Immunohistochemistry	Pag. 75
3.8 RNA silencing	Pag. 76

3.9 Statistical analysis	Pag. 76
<b>Results</b>	Pag. 77
4.1 A $\beta$ accumulation and oligomerization in hippocampal neurons from Tg2576 mice	Pag. 78
4.2 NCX activity in Tg2576 hippocampal neurons	Pag. 80
4.3 Effect of NCX3 silencing on I <sub>NCX</sub> up-regulation in Tg2576 hippocampal neurons	Pag. 82
4.4 SBFI-Na <sup>+</sup> detection and Nav <sub>v</sub> recording in Tg2576 hippocampal neurons	Pag. 84
4.5 Assessment of [Ca <sup>2+</sup> ] <sub>i</sub> and ER Ca <sup>2+</sup> content in Tg2576 hippocampal neurons	Pag. 86
4.6 NCX3 protein expression in the hippocampus of 3 and 8-month-old Tg2576 mice	Pag. 89
4.7 NCX3 protein expression in the hippocampus of 3 and 8-month-old Tg2576 mice	Pag. 92
<b>Discussion</b>	Pag. 94
<b>References</b>	Pag. 101

## LIST OF ABBREVIATIONS

$[Ca^{2+}]_i$	Intracellular calcium concentration
$[Na^+]_i$	Intracellular sodium concentrations
AAO	Age at onset
AD	Alzheimer's disease
APOE	Apolipoprotein E
APOE- $\epsilon$ 4	Apolipoprotein E type 4 allele
APP	Amyloid- $\beta$ precursor protein
A $\beta$	Amyloid $\beta$ protein
A $\beta$ <sub>1-40</sub>	Amyloid $\beta$ peptide 1-40
A $\beta$ <sub>1-42</sub>	Amyloid $\beta$ peptide 1-42
CNS	Central nervous system
CTF	Carboxy-terminal fragment
EAE	Experimental autoimmune encephalitis
$E_m$	Membrane potential
EOAD	Early-onset Alzheimer's disease
EOFAD	Early-onset familial Alzheimer's disease
ER	Endoplasmic reticulum
FAD	Familial Alzheimer's disease
$I_A$	Fast inactivating $K^+$ currents
IC <sub>50</sub>	Half maximal inhibitory concentration
$I_{NaP}$	Persistent sodium current
$I_{NCX}$	NCX currents
IP <sub>3</sub>	Inositole triphosphate
IP <sub>3</sub> R	Inositole triphosphate receptor

K <sub>d</sub>	Dissociation constant
K <sub>i</sub>	Inhibitory constant
K <sub>v</sub>	Voltage-gated potassium channel
LOAD	Late-onset Alzheimer's disease
LTD	Long term depression
LTP	Long term potentiation
MAPs	Microtubule-associated proteins
MOG	Myelin oligodendrocyte glycoprotein
MS	Multiple sclerosis
Nav	Voltage-gated sodium channel
NCX	Na <sup>+</sup> /Ca <sup>2+</sup> exchanger
NFTs	Neurofibrillary tangles
NGF	Nerve growth factor
NMDA	N-methyl D-aspartate
OPC	Oligodendrocyte precursor cells
PC12	Rat pheochromocytoma
PHF	Paired helical filaments
PIP2	Phosphatidylinositol 4,5-bisphosphate
PM	Plasma membrane
PMCA	Plasma membrane Ca <sup>2+</sup> -ATPase
pMCAO	Permanent middle cerebral artery occlusion
pNCX3	Proteolytic fragment of NCX3
PS1	Presenilin 1
PS2	Presenilin 2
ROS	Reactive oxygen species
RyR	Ryanodine receptor

SDS	Sodium dodecyl sulphate
SDS-PAGE	Sodium dodecyl sulphate-PolyAcrylamide gel electrophoresis
SERCA	Sarco-endoplasmic reticulum Ca <sup>2+</sup> pumps
SLC8A	Solute carrier family 8A or NCX gene family
Tg	Thapsigargin
TMS	Trans membrane domain
TTX	Tetrodotoxin
VGCC	Voltage-gated calcium channel
WT	Wild Type
XIP	Exchanger Inhibitory Peptide

# SUMMARY

Alzheimer's disease (AD), the most common neurodegenerative disorder is characterized by progressive memory loss and impairment of cognitive ability. A $\beta_{1-42}$  deposition, the principal hallmark of AD, triggers several mechanisms, including dysregulation of ionic homeostasis, contributing to neuronal dysfunction and death. In particular, the dysregulation of intracellular calcium concentrations ([Ca $^{2+}$ ]<sub>i</sub>) triggers a series of events including oxidative damage and activation of apoptotic machinery. Furthermore, the dysregulation of intracellular sodium concentrations ([Na $^{+}$ ]<sub>i</sub>) affects neuronal excitability and contributes to epileptogenesis in AD. The Na $^{+}$ /Ca $^{2+}$  exchanger (NCX) couples in a bidirectional manner the exchange of 3Na $^{+}$  for 1Ca $^{2+}$ , thereby playing a relevant role in maintaining intracellular Na $^{+}$  and Ca $^{2+}$  homeostasis. For this reason, we investigated the role of NCX3 in A $\beta_{1-42}$ -induced ionic dysregulation in primary hippocampal neurons from Tg2576 mice, a transgenic animal model of AD. First, we validated primary hippocampal neurons from Tg2576 mice, here set up for the first time, as an *in vitro* model of AD by confirming the presence of A $\beta_{1-42}$  oligomers through western blot experiments. In particular, we observed A $\beta_{1-42}$  trimers, detectable as a ~ 12 kDa band, in Tg2576 primary hippocampal neurons, whereas they were absent in Wild Type (WT) neurons. Importantly, the same band has been detected in the hippocampus of 3-month-old Tg2576 mice. Patch clamp experiments revealed that NCX activity was progressively up-regulated in the reverse mode of operation in Tg2576 hippocampal neurons compared to WT, at 8 and 12 DIV, whereas no modulation occurred in the forward mode. Furthermore, silencing experiments with a specific siRNA directed against NCX3,

revealed that this increase of NCX currents was mediated by only NCX isoform 3. However, as revealed by western blot analyses, the up-regulation of NCX3 activity was not accompanied by a significant increase of NCX3 protein expression. Interestingly,  $[\text{Na}^+]_i$  detection with SBFI probe showed a significant increase of  $[\text{Na}^+]_i$  in Tg2576 hippocampal neurons at 12 DIV compared to WT, thus indicating that the up-regulation of NCX activity was  $\text{Na}^+$ -dependent. Moreover, electrophysiological experiments revealed that  $\text{Na}_v$  currents were progressively up-regulated in Tg2576 hippocampal neurons compared to WT at 8 and 12 DIV. To determine whether the up-regulation of NCX activity results in increased  $[\text{Ca}^{2+}]_i$  or rather in  $\text{Ca}^{2+}$  refilling into ER, we performed Fura-2 AM measurements to determine both  $[\text{Ca}^{2+}]_i$  and ER  $\text{Ca}^{2+}$  content. In particular, we found a significant reduction of  $[\text{Ca}^{2+}]_i$  in Tg2576 hippocampal neurons at 8 DIV compared to WT and a significant increase in ER  $\text{Ca}^{2+}$  content at 12 DIV. Western blot on Tg2576 mouse brain, revealed that NCX3 protein expression was significantly increased in the hippocampus of 3-month-old Tg2576 mice compared to WT. Importantly, immunohistochemical analyses confirmed western blot results. In fact, in both CA1 and CA3 hippocampal regions as well as within the *corpus callosum* of 3-month-old Tg2576 mice, the anti-NCX3 antibody revealed an increased NCX3 immunoreactivity signal, which was mainly confined along the processes of cells and dendrites of pyramidal cells. By contrast, we observed a significant reduction of NCX3 protein expression in the hippocampus of 8-month-old Tg2576 compared to WT, although an increase in the hippocampus of 8-month-old WT mice has been observed in comparison with 3-month-old WT mice. Importantly, immunohistochemical analyses confirmed western blot results. In fact, in both CA1 and CA3 hippocampal regions as well as within the *corpus callosum* of 8-month-old Tg2576 mice, NCX3 immunostaining

appeared robustly decreased. Moreover, western blot experiments did not detect any modulation of NCX3 protein expression in the cerebral cortex of both 3 and 8-month-old Tg2576 mice compared to WT. On the other hand, a clear loss of intensity of immunoreactivity signal has been observed in cortical sections from both 3 and 8-month-old Tg2576 mice. All together, these results suggest that NCX3 up-regulation could represent a protective mechanism against Na<sup>+</sup> disruption occurring in Tg2576 hippocampal neurons. Notably, this evidence points to a possible role of NCX3 in neuronal survival against hyperexcitability and subsequent epileptiform activity observed in AD. Moreover, the role of NCX3 in Ca<sup>2+</sup> refilling into ER further supports its positive implication.

# **INTRODUCTION**

# CHAPTER 1: ALZHEIMER'S DISEASE

## 1.1 Overview

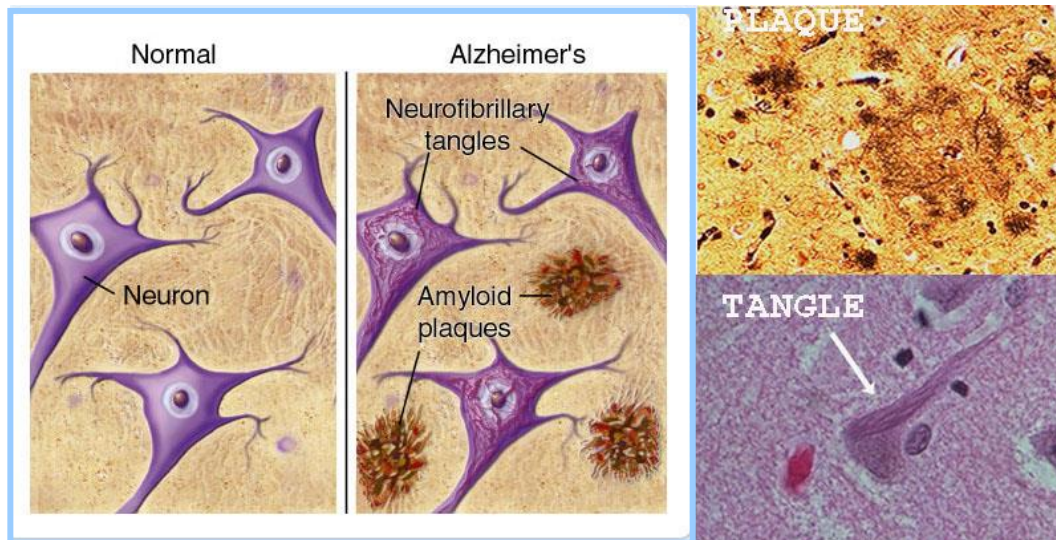
Alzheimer's disease (AD) is one of the most common neurodegenerative diseases and the most prevalent form of late-life mental disorder. With the increasing longevity of our population, AD is reaching epidemic proportions with no cure or preventative therapy yet available (Tanzi and Bertram, 2005). The clinical symptomatology results from the failure of selective cognitive domains, in particular those related to memory (LaFerla *et al.*, 2007)

The first to describe this clinicopathological syndrome was a Bavarian psychiatrist, Alois Alzheimer, who named the disease. Alzheimer's original patient presented several salient features of the disorder observed in most patients nowadays: progressive memory impairment; cognitive dysfunctions; altered behaviour; and a progressive decline in language function. With the progression of the disease, other symptoms may arise, including a tendency to slow motor functions and other disorders culminating in some forms of Parkinsonism. After Alzheimer's original description, the progress in defining the pathogenesis of AD has been slow, until two researchers, Michael Kidd in England and Robert Terry in the United States, described with electron microscopy the ultrastructural changes underlying the two typical lesions linked to AD: senile (neuritic) plaques and neurofibrillary tangles. In the mid 1970s, the identification of cholinergic neurons as the outbreak of neurodegeneration contributed to the knowledge of neurochemical features of AD. Indeed, a decrease in the activities of the synthetic and degradative enzymes choline acetyltransferase and acetylcholinesterase was observed in the limbic and

cerebral cortices, along with the loss of cholinergic cell bodies in the subcortical nuclei that project to these regions. A little later in the years, it became clear that AD also involved the degeneration of other neurotransmitter systems, and this explained the failure to produce benefits in patients treated with cholinergic drugs. Despite since 1980s increasing progresses toward approaching and understanding molecular pathogenesis of AD have occurred, the study of the disease showed many controversies. Furthermore, given the cytological and biochemical complicacy of AD, it has been difficult to reach certain conclusions about the temporal sequence of events that lead to dementia. However, in recent years, a consensus has developed that some molecular events occur several years before the onset of symptoms.

For many years, the researchers tried to identify the composition and molecular origin of the amyloid plaques and neurofibrillary tangles (**Fig. 1**) by isolating the subunit proteins of these lesions, and to understand which of the two lesions might precede the other. Despite this, it seemed clear that these two lesions observed in the *post mortem* brain occur late in the disease, so providing little useful information about the etiology and early pathogenesis of AD. Afterwards, thanks to the use of immunocytochemistry and compositional analyses, the subunit composition of the plaques and tangles has been defined, while the progress in molecular genetics of AD provided further information about the role of these subunit proteins in the pathogenesis of AD. In particular, the understanding of the relationships between each genetic alteration and the familial forms of AD helped to reveal the progression of the pathogenetic events (Selkoe *et al.*, 2001; Selkoe, 2011).

**Fig. 1**



### 1.1.1 Neuritic plaques

Neuritic plaques, one of the two lesions observed in *post mortem* brain of Alzheimer's original patient, consist of microscopic *foci* of extracellular amyloid deposition associated with dystrophic neurites and altered microglia and astrocytes. This type of lesion, which evolves as neuritic plaques very gradually over many months or years, is generally found most in the limbic and association cortices (Dodel *et al.*, 2000). The extracellular deposits of amyloid  $\beta$ -protein ( $A\beta$ ) contain skeins of insoluble amyloid fibrils, intermixed with non-fibrillar ("amorphous") forms of the peptide (Master *et al.*, 1985). Dystrophic neurites are located within this amyloid deposit but also around it. Such plaques are also associated with activated microglia, adjacent to the central amyloid core, and surrounded by reactive astrocytes that often ring the outside of the plaque. Much of the fibrillar  $A\beta$  which constitutes the neuritic plaques is the peptide ending at

amino acid 42, ( $A\beta_{1-42}$ ), the longer, more hydrophobic form of  $A\beta$  that has a strong tendency to aggregate (Jarrett *et al.*, 1993). However, the  $A\beta$  peptide ending at amino acid 40 ( $A\beta_{1-40}$ ), which is generally more abundant in cells than  $A\beta_{1-42}$ , is often co-localized with  $A\beta_{1-42}$  in the plaques.

### 1.1.2 “Diffuse” plaques

Such lesions, generally called “diffuse” or “pre-amyloid” plaques, are constituted by  $A\beta$  deposits that are mostly in a non-fibrillar, granular form (Tagliavini *et al.*, 1988). Many of the plaques found in those regions of Alzheimer’s brain that are not strongly implicated in the typical symptomatology of AD, are of the diffuse type, without a fibrillar core of  $A\beta$ , and accompanied by very little or not detectable dystrophic neurites. Unlike the  $A\beta$  deposits generally found in the fibril-rich neuritic plaques, that have a mixed composition of  $A\beta_{1-42}$  plus  $A\beta_{1-40}$ , the material comprising the diffuse plaques has only the peptide  $A\beta_{1-42}$  as subunit, with little or no  $A\beta_{1-40}$  (Iwatsubo *et al.*, 1995; Lemere *et al.*, 1996). However,  $A\beta$  deposits do not occur simply in these two distinct forms (diffuse and neuritic) but rather as a mixture of fibrillar, granular, and even soluble forms of the peptide, that are variously associated with surrounding glial and neuritic alteration. The fact that diffuse plaques are the sole form found in those brain regions lacking neuritic dystrophy, glial alterations, and neurofibrillary tangles, leads to the hypothesis that diffuse plaques represent the precursors of neuritic plaques and are not clearly implicated in the typical symptomatology of AD. Furthermore, healthy aged brains free of AD, but also other dementing processes, often showed only diffuse plaques in the same regions where Alzheimer patients share both diffuse and neuritic plaques: this evidence supports the hypothesis

that diffuse plaques could be earlier lesions that precede further alterations (Selkoe *et al.*, 2001).

### 1.1.3 Neurofibrillary tangles

Neurofibrillary tangles (NFTs) are the second lesion detectable in AD *post mortem* brains, particularly in entorhinal cortex, hippocampal formation, amygdala, association cortices, and certain subcortical nuclei that project to these regions. Many neurons in these regions contain large bundles of abnormal fibers, identified by electron microscopy as paired helical filaments (PHF) located in the perinuclear cytoplasm. Immunocytochemical and biochemical analyses begun in 1985 suggested that NFTs were composed of the microtubule-associated protein tau (Kosik *et al.*, 1986; Wood *et al.*, 1986). This was confirmed by the isolation of a subset of PHF that, solubilized in strong solvents such as sodium dodecyl sulphate (SDS) or digested with proteases (Kondo *et al.*, 1988; Wischik *et al.*, 1988), released tau proteins that had a higher molecular weight than the normal tau prepared from tangle-free human brains. This higher molecular weight was shown to result from increased phosphorylation of tau, in fact *in vitro* dephosphorylation with alkaline phosphatases restored the normal weight to this PHF-derived tau. However, although some PHF can be solubilized by boiling in SDS (Lee *et al.*, 1991), much of the tau filaments present in tangles are insoluble and resistant to detergents such as SDS and to chaotropic solvents such as guanidine hydrochloride (Selkoe *et al.*, 1982).

It has been shown that tau can be phosphorylated *in vitro* by a variety of kinases at various sites. Nevertheless, it is not clear whether one or more kinases are responsible for initiating the hyperphosphorylation of tau *in vivo* that leads to its dissociation from microtubules and aggregation into insoluble PHF. PHF are not

limited to the tangles found in neuronal cell bodies but also occur in dystrophic neurites that are present within and outside of the amyloid plaques.

However, the two classical lesions of AD, neuritic plaques and NFTs, can occur independently of each other in humans. Tau aggregates similar to or indistinguishable from the tangles observed in AD have been described also in other, less common, neurodegenerative diseases in which no A $\beta$  deposits and neuritic plaques are observed. Conversely, A $\beta$  deposits can be found in cognitively normal-aged brains without the presence of tangles (Selkoe *et al.*, 2001; Selkoe, 2011).

#### **1.1.4 AD clinico-pathological features and diagnostic criteria**

NFTs and A $\beta$  plaques are accompanied by additional changes in the brain of AD patients that may contribute to cognitive impairment, such as amyloid angiopathy, age-related brain atrophy, synaptic pathology, white matter rarefaction, neuronal loss, neuroinflammation and others (Hirano *et al.*, 1968; Masliah *et al.*, 1995; Nunomura *et al.*, 2006; Thal *et al.*, 2011). However, these are not considered pathognomic features of AD (Montine *et al.*, 2012).

NFTs are not specific for AD (Buée *et al.*, 2000, Goedert, 2004), in fact they are found in every class of brain diseases such as focal cortical dysplasia, prion diseases, some brain tumors, viral encephalitis and others (Baner *et al.*, 1996; Cairns *et al.* 2007). Furthermore, NFTs are universal in normal aging subjects. In fact, a modest number of NFTs present in the medial temporal lobe occur in subjects older than 70 years (Bouras *et al.*, 1994). This evidence suggests that NFTs are, at least in some circumstances, a secondary response to injury. Nevertheless, NFTs may be directly linked to primary neurodegenerative changes, since tau gene mutations can produce clinical dementia with NFTs

(Cairns *et al.*, 2007). However, the density and neuroanatomic localization of NFTs are determining parameters in AD neuropathology. Indeed, NFTs are found in both healthy and demented subjects in the hippocampus, but elsewhere in the cortex they are observed only in demented.

Unlike the NFTs, A $\beta$  plaques are extracellular (Selkoe, 2008). They are found in a large percentage of elderly persons, despite they are not universal (Braak *et al.*, 2011; Jicha *et al.*, 2012).

The “neuritic plaques” are more likely to correlate with cognitive impairment than “diffuse plaque” (Terry *et al.*, 1991). Moreover, many of the degenerating axons and dendrites surrounding A $\beta$  deposits in neuritic plaques often contain hyperphosphorylated tau aggregates. This subset of A $\beta$  plaques represents a current diagnostic criterion for AD, even if the extension and density of dystrophic neurites that contain altered forms of tau varie among AD cases, depending on the evolution of the neuritic plaques in AD pathological process (Thal *et al.*, 2000; Thal *et al.*, 2006).

A $\beta$  plaques alone are not considered a sufficient substrate for severe dementia. However, unlike to NFTs pathology, A $\beta$  plaques formation seems to strongly correlate with AD genetics. In fact, all high-penetrance AD risk alleles, such as Amyloid- $\beta$  precursor protein (APP), Presenilin 1 (PS1), Presenilin 2 (PS2) mutations, Apolipoprotein (APOE)  $\epsilon$ 4 allele and Down syndrome, have been linked in several experimental systems to increased A $\beta$  deposition and increased production of toxic A $\beta$  peptide species (Hardy, 2006; Selkoe, 2008; Reitz *et al.*, 2009).

Now it is well established that both A $\beta$  plaques and NFTs are hallmark features of AD but they develop independently of each other in the human brains, showing different temporal patterns of progression (Braak *et al.*, 1991; Ohm *et al.*,

1995). This evidence would provide the answer to some controversies that have evolved over the past decades. However, some debates persist in the field of clinico-pathological correlation research, which aims to assess how and how much AD neuropathologic changes (A $\beta$  plaques and NFTs) correlate with dementia. Indeed, it is possible to observe subjects without dementia with advanced AD pathologic changes at autopsy and, *vice versa*, dementing subjects with clinical AD symptoms without AD pathologic changes at autopsy. For these reasons, it is crucial to define the so-called “advanced AD pathologic changes” (Nelson *et al.*, 2012). In this regard, it must be emphasized that A $\beta$  plaques without other neuropathologic lesions are not sufficient for the development of a severe dementia, thus they cannot be considered “advanced AD pathologic changes”. By contrast, high levels of neocortical neurofibrillary tangles are strongly associated with dementia and thus, according to new diagnostic criteria, are part of the “advanced AD pathologic changes” (Montine *et al.*, 2012). It is clear that dementia, though in a form clinically similar to AD, may occur without AD pathologic changes; in this case, it cannot be diagnosed as AD but presumably as one among many other diseases that cause symptoms of dementia.

## **1.2 Genetics of Alzheimer’s Disease**

It is known for several decades that AD may occur in a sporadic form, also described as late-onset Alzheimer’s disease (LOAD), or be specifically inherited in an autosomal dominant fashion as a familial form, also known as early onset Alzheimer’s disease (EOAD). What is not yet clear is how frequently genetic factors underlie the disease in the late-onset forms. However, the certainty that

polymorphic alleles of APOE can strongly predispose to AD in the 60s and 70s (Strittmatter *et al.*, 1993) suggests that also other polymorphic genes may constitute predisposing factors for the disorder. However, since these genetic factors do variably cause the disease, they would be difficult to detect in genetic epidemiological studies. Despite this, it has become clear that familial AD and apparently non-familial (“sporadic”) forms are phenotypically similar and indistinguishable in certain cases, save for the earlier age of onset of the autosomal dominant forms. In fact, when the age of the patient at the onset of disease is not known, it is very difficult to discriminate between the phenotype of early onset cases and that of common LOAD. Although also clinical manifestations of familial AD are very similar to those of sporadic cases, some families may show peculiar clinical signs such as extrapyramidal signs, seizures, etc. However, this phenotypical similarity suggests that information about the mechanism of autosomal dominant AD caused by APP, PS1 and PS2 gene mutation, may be helpful to better understand the pathogenesis of sporadic, non-familial forms (Selkoe *et al.*, 2001).

### **1.2.1 Mutations of APP**

The first specific genetic factor predisposing for AD to be identified have been missense mutations in APP gene (Goate *et al.*, 1991). Missense mutations in APP account for about 0,01% of all Alzheimer’s cases but the identification of their genotype-to-phenotype relationships has provided important information about the mechanisms underlying AD pathology. In particular, these mutations cause AD by altering proteolytic processing of APP in different ways.

The 37-43 amino acid A $\beta$  peptide is generated in a physiologic pathway by the proteolytic processing of its precursor, the APP (Haass *et al.*, 1992; Seubert *et al.*,

1992; Haass and Selkoe, 1993). The APP is a transmembrane protein with its amino terminus within the extracellular space and its carboxyl terminus within the cytosol (Kang *et al.*, 1987). Although APP is trafficked through the secretory pathway, in which it is transported from endoplasmic reticulum (ER) to the plasma membrane (PM), it is posttranslationally modified at different subcellular sites (Weidemann *et al.*, 1989). In fact, it can undergo several proteolytic cleavages, whose secreted products are released into vesicle lumen and extracellular space, thus only a small fraction of nascent APP molecules reach the PM (Lai *et al.*, 1995).

Two principal processing pathways have been identified: the amyloidogenic pathway, which leads to A $\beta$  generation; and the anti-amyloidogenic pathway, in which A $\beta$  generation is prevented. The three proteases involved in these processing pathways are called  $\alpha$ -,  $\beta$ -, and  $\gamma$ -secretase. The A $\beta$  is produced in the amyloidogenic pathway by the consecutive action of  $\beta$ - and  $\gamma$ -secretase (Haass, 2004). The  $\beta$ -secretase initiates A $\beta$  generation by cleaving APP within the extracellular domain, thus shedding a large part of APP ectodomain (APPs $\beta$ ) in the lumen (Seubert *et al.*, 1993) and generating a 99-residue APP-carboxy-terminal fragment (CTF) called  $\beta$ CTF or C99, which is then cleaved by  $\gamma$ -secretase. On  $\gamma$ -secretase cleavage, A $\beta$  is generated and released into vesicle lumen and extracellular fluids such as plasma or cerebrospinal fluid. In the anti-amyloidogenic pathway,  $\alpha$ -secretase cleaves APP in the A $\beta$  region (Esch *et al.*, 1990; Sisodia *et al.*, 1990), thus generating a truncated 83-residue APP CTF ( $\alpha$ CTF or C83), lacking the amino-terminal portion of the A $\beta$  domain. The subsequent intramembrane cleavage by  $\gamma$ -secretase generates a truncated A $\beta$  peptide called p3 (Haass *et al.*, 1993), which has no evident pathological relevance. Even if the amyloidogenic and the anti-amyloidogenic processing

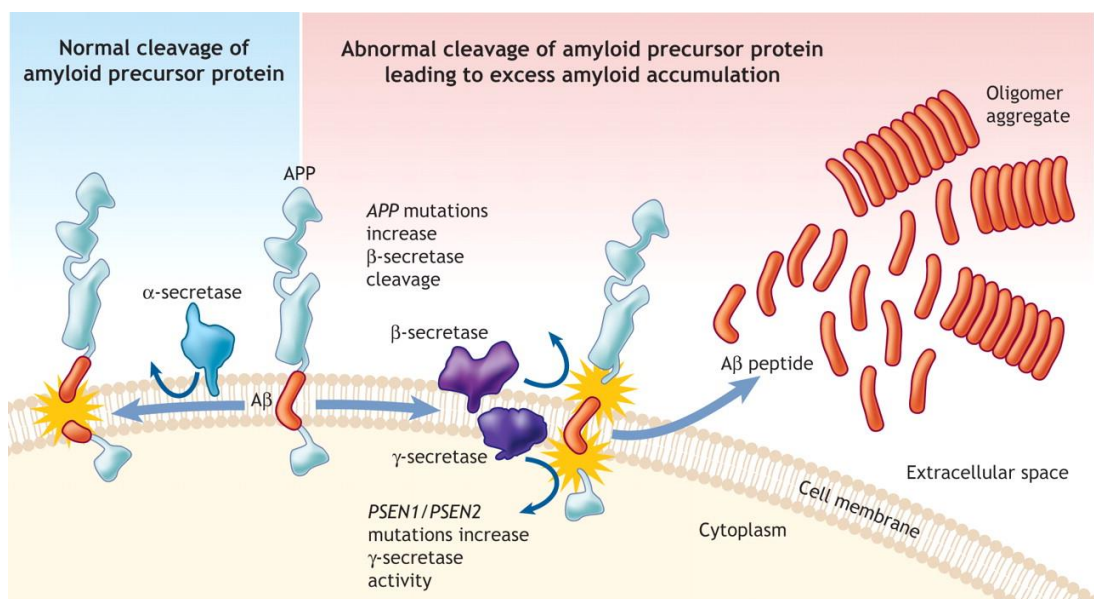
pathways compete with each other, in most cells a much bigger portion of total APP undergoes cleavage by  $\alpha$ -secretase rather than by  $\beta$ -secretase.

The nine known missense mutations of APP have been found within and around A $\beta$  domain. These mutations are responsible of a number of familial Alzheimer's disease (FAD) cases (Chartier-Harlin *et al.*, 1991; Schenk *et al.*, 2011), by affecting A $\beta$  generation and aggregation. The Swedish mutation (so called because of the ethnic origin of the family in which it occurs) is a double mutation, which falls at amino terminus of the A $\beta$  region (Mullan *et al.*, 1992), more specifically in the two amino acids just before the  $\beta$ -secretase cleavage site, and results in a significant increase of A $\beta$ <sub>1-40</sub> and A $\beta$ <sub>1-42</sub> production, since it provides a better substrate for the  $\beta$ -secretase activity (Citron *et al.*, 1992; Cai *et al.*, 1993). The five mutations located just beyond the carboxyl terminus of A $\beta$ , near to the  $\gamma$ -secretase (the so-called Austrian, French, London, Iranian and Florida mutations) selectively increase the production of A $\beta$ <sub>1-42</sub>, which has a higher tendency to aggregate and is considered to have the greatest neurotoxicity among all A $\beta$  species (Suzuki *et al.*, 1994). The mutations falling in the mid region of A $\beta$ , such as Arctic (Nilsberth *et al.*, 2001) and Dutch mutations (Levy *et al.*, 1990) change the structure of A $\beta$ , by affecting its primary sequence, and enhance its aggregational propensity. Some of these intra-A $\beta$  mutations can lead to mixed amyloid pathologies, with marked cerebral angiopathy with abundant amyloid plaques. In particular, the Dutch mutation causes hereditary cerebral hemorrhage with amyloidosis (Levy *et al.*, 1990). The Flemish mutation results in a particular pathologic mechanism, leading to AD type plaques and tangles associated with dementia, and microvascular  $\beta$ -amyloidosis with sporadic cerebral hemorrhage (Hendriks *et al.*, 1992). This mutation is located in a substrate inhibitory domain that negatively regulates  $\gamma$ -secretase activity by binding to an allosteric site within

the  $\gamma$ -secretase complex. As consequence, the Flemish mutation reduces the inhibitory potency of APP substrate inhibitory domain thus promoting  $\gamma$ -secretase activity (De Jonghe *et al.*, 1998).

Another alteration in the APP gene that can predispose to AD is the overexpression of structurally normal APP, which occurs in trisomy 21 (Down's syndrome), leading usually to premature AD neuropathology (neuritic plaques and neurofibrillary tangles) during middle adult years (Tokuda *et al.*, 1997). Down's subjects display early appearance of many  $A\beta_{1-42}$  diffuse plaques, which can occur as soon as age of 12 years (Lee *et al.*, 1991), whereas the appearance of NFTs can be delayed until the late 20s, 30s or beyond in most Down's patients. However because the entire chromosome 21 is duplicated in most cases of Down's syndrome, it is difficult to assess if Alzheimer syndrome that they develop is correlated directly to APP gene dosage.

**Fig. 2**



Christopher Patterson *et al.*, *cmaj* (2008)

### 1.2.2 Mutations of presenilins

The mechanism by which mutations in presenilins produce an AD phenotype, leading to several forms of early onset familial Alzheimer's disease (EOFAD), has always been intensely debated. While the functional role of presenilins was unknown when they have been discovered, it was nevertheless found that presenilin mutations enhanced the production of  $A\beta_{1-42}$ , thus rendering it the predominant  $A\beta$  specie at the expense of  $A\beta_{1-40}$ . In fact, direct assays of  $A\beta_{1-42}$  and  $A\beta_{1-40}$  levels in the plasma and cultured skin fibroblasts media of subject harboring these mutations, revealed a selective and approximately twofold elevation of  $A\beta_{1-42}$ .

Presenilin is an aspartyl protease, identified as the catalytic subunit of  $\gamma$ -secretase. In mammals there are two presenilin isoforms, PS1 and PS2, characterized by nine transmembrane domains, a cytosolic loop domain, and two aspartate residues, critical for  $\gamma$ -secretase catalytic function. Although presenilin has been intensely studied because of its role in APP proteolytic cleavage, it is involved in a wide variety of cellular processes also independently of  $\gamma$ -secretase activity, such as protein trafficking (Naruse *et al.*, 1998), calcium homeostasis (Yu, 2009) and lysosomal function (Lee *et al.*, 2010; Zhang *et al.*, 2012).

Mutations in PS1 are the most common cause of EOFAD, accounting for 18-50% of autosomal dominant EOAD cases (Cruts *et al.*, 1996). Patients with mutations in this gene display progressive dementia and Parkinsonism and, in some cases, other atypical AD symptoms like ataxia or epilepsy may appear (Langheinrich *et al.*, 2011; Borroni *et al.*, 2012). More than 180 mutations in PS1 have been reported (Cruts *et al.*, 2012); the majority are missense mutations that cause amino acid substitutions throughout PS1 protein, so leading to PS1 "gain" or "loss of function".

Missense mutations in the PS2 gene are a rare cause of EOAD and what makes them different from PS1 mutations is the age of onset, that is generally more advanced and highly variable (45-88 years), even among patients of the same family (Bekris *et al.*, 2010). Although both PS1 and PS2 increase the ratio of A $\beta$ <sub>1-42</sub> to A $\beta$ <sub>1-40</sub>, presenilin mutations affect APP processing by  $\gamma$ -secretase in a differential manner (De Strooper *et al.*, 1998; Baulac *et al.*, 2003).

### 1.2.3 Apolipoprotein E4 Allele

The APOE type 4 allele (APOE- $\epsilon$ 4) is the major genetic factor predisposing to the common late onset familial and sporadic forms of AD. APOE has three alleles: APOE- $\epsilon$ 2, APOE- $\epsilon$ 3, and APOE- $\epsilon$ 4. APOE- $\epsilon$ 4 is overrepresented in 80% of familial and 64% of sporadic AD late onset cases compared with the general population. Furthermore, inheritance of one or two APOE- $\epsilon$ 4 alleles determines an age at onset earlier than that observed in subjects harboring  $\epsilon$ 2 and/or  $\epsilon$ 3 alleles (Corder *et al.*, 1993; Saunders *et al.*, 1993).

The mechanism by which APOE4 protein leads to increased A $\beta$  deposition has been difficult to identify. However, APOE4 seems to enhance the steady-state level of A $\beta$  peptides, in particular of A $\beta$ <sub>1-40</sub> (Gearing *et al.*, 1996), probably by affecting its clearance from the brain tissue.

### 1.3 Animal model of AD

The progresses reached in the last two decades in elucidating AD susceptibility and causative genes as well as other proteins involved in AD pathogenesis, have facilitated the development of genetically modified mouse models. Moreover, animal models have played an important role in identify mechanisms underlying AD pathology and in evaluating novel therapeutic approaches.

Importantly, neuropathology and clinical phenotype are generally identical in the EOFAD versus the sporadic form of AD (SAD), except for the age at onset (AAO) (Selkoe, 2002). However, unlike the FAD, the etiology of SAD is unknown. For this reason, animal models harboring genetic mutations associated with FAD are used with the rationale that the events underlying AD pathology are quite similar in the two forms, although the initial trigger is not the same. In fact, despite a single mouse model does not recapitulate the wide *spectrum* of pathogenic mechanisms, each model can contribute to analyse one or more components of the disease, which is not possible with human patients.

Transgenic mice overproducing mutant APP develop a pathology similar to that found in humans. In particular, plaque formation occurs in mid to late adulthood in the majority of these mice. Notably, the accumulation of A $\beta$  into extracellular plaques is accelerated when A $\beta$ <sub>1-42</sub> is more abundant than A $\beta$ <sub>1-40</sub>, as in the case of mice carrying APP mutations. Working with transgenic mic highlighted the nature of A $\beta$  plaques and contributed to clarify the factors determining aggregation of A $\beta$  into plaques.

However, most AD transgenic mice exhibit memory impairments and cognitive deficits long before the appearance of extracellular plaques. For this reason, the researchers tried to identify the precursors to plaque formation and, especially, they focused on soluble oligomeric species of A $\beta$ . In fact, it is well known that

cognitive decline in humans, as well as in mice, correlates with the presence of soluble A $\beta$ , rather than with A $\beta$  plaques. In humans, but not in AD transgenic mice, a large quantity of A $\beta$  accumulation is needed for cognitive decline beginning. However, mouse models still provided much of the information about the toxicity of A $\beta$  oligomers. Many APP transgenic mice exhibit intraneuronal accumulation of A $\beta$ , similarly as human AD and Down syndrome patients. Importantly, the accumulation of intracellular A $\beta$  has been shown to precede extracellular deposition in both mice and human patients, to correlate with early memory deficits, and to be more toxic than extracellular A $\beta$ .

## 1.4 Amyloid cascade hypothesis

The amyloid  $\beta$ -protein hypothesis (Hardy and Allsop, 1991; Selkoe, 1991; Hardy and Higgins, 1992) is one of the dominant models of AD pathogenesis and the most influential concept guiding the development of potential AD therapies. Since brain tissues from AD patients are only studied *post mortem*, it has been difficult to identify the sequence of pathogenic events occurring in the disorder. However, important results have come from analysing the very similar, almost indistinguishable neuropathological processes that occur in Down's syndrome. Other information about the disease cascade have come from the study of mice transgenic for mutant human APP, either with or without presenilin mutations. In particular, although lesion formation occurs in a shorter period in these mice than in human (Hsiao *et al.*, 1996), they are a useful model to deduce some features of the cellular and protein changes that often precede neuronal/neuritic alteration. The amyloid cascade hypothesis (**Fig. 2**) postulates that an abnormal accumulation of A $\beta$  peptide in various brain areas is responsible for AD

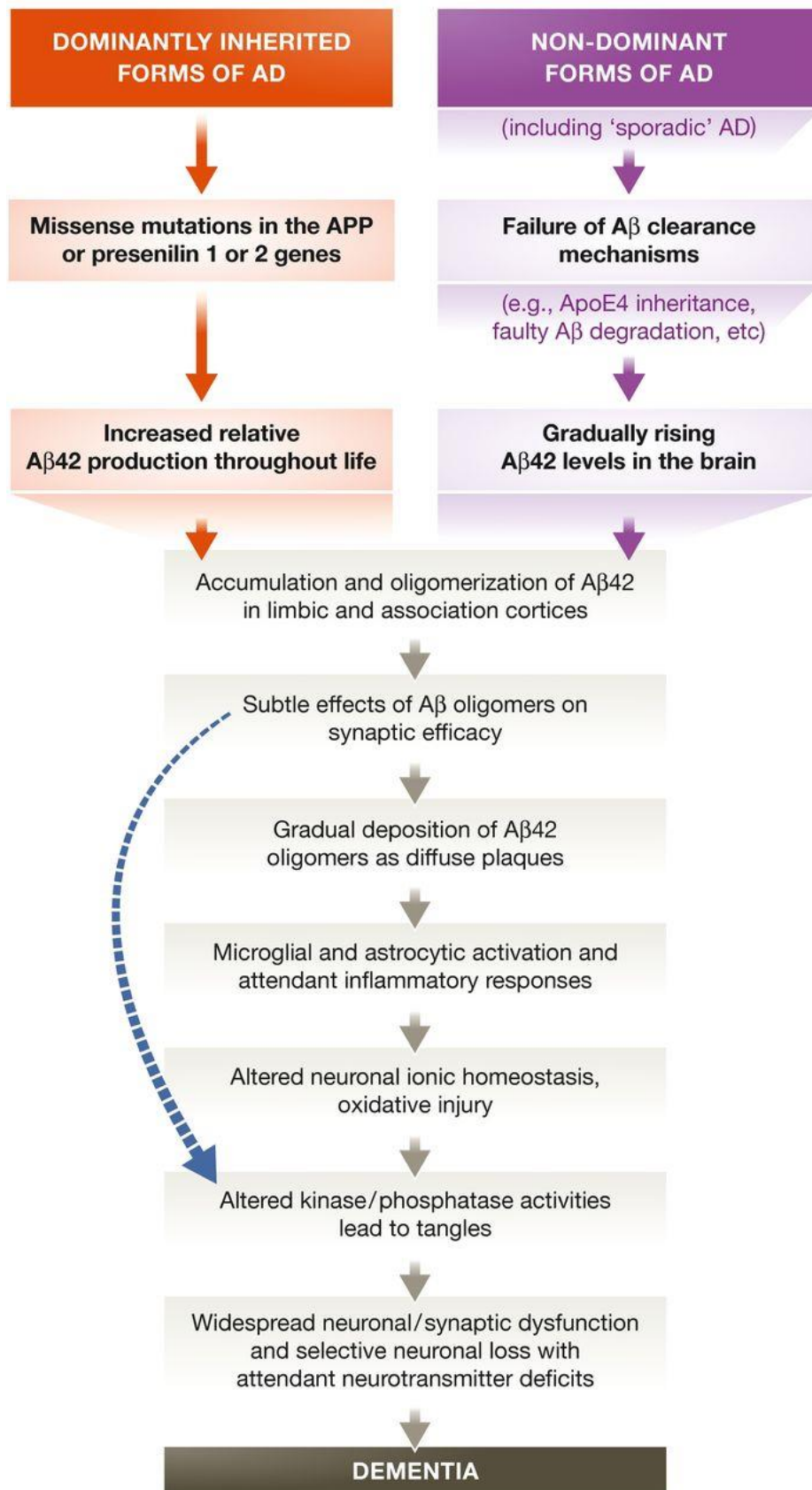
neurodegeneration (Hardy and Higgins, 1992; Evin and Weidemann, 2002). According to this hypothesis, the accumulation of A $\beta$  peptide triggers a cascade of events that include neuritic injury and formation of neurofibrillary tangles, culminating in neuronal dysfunction and cell death (Hardy and Higgins, 1992; Selkoe, 1999).

A $\beta$  peptides, the main component of A $\beta$  plaques (Masters *et al.*, 1985), are 39-43 amino acid residue peptides proteolitically derived from the secretase-mediated processing of APP (Coulson *et al.*, 2000). The length of A $\beta$  peptide varies at C-terminal depending on the cleavage pattern of APP. The A $\beta$ <sub>1-40</sub> isoform is the most prevalent, followed by A $\beta$ <sub>1-42</sub>, which is the more hydrophobic isoform and more prone to aggregation than A $\beta$ <sub>1-40</sub>. Within the plaques, A $\beta$  peptide has a  $\beta$ -sheet conformation and aggregates into several distinct forms including fibrillar, protofibrils and polymorphic oligomers (Glennner *et al.*, 1984; Selkoe, 1994). The A $\beta$  deposition and diffuse plaque formation lead to microglial activation, reactive astrocytosis, cytokine release, inflammatory response and altered neuronal ionic homeostasis accompanied by oxidative stress. A $\beta$  aggregation also results in various biochemical and structural changes in surrounding dendrites, axons and neuronal cell bodies, which eventually lead to synapse loss and neuronal death (Braak and Braak, 1994).

Although the amyloid cascade hypothesis is the most important model proposed to explain AD pathogenesis nowadays, it has been difficult to demonstrate the direct correlation between A $\beta$  accumulation and neurodegeneration leading to cognitive deficits (Serrano-Pozo *et al.*, 2014). However, genetic studies suggest that neurodegeneration in AD is the consequence of an imbalance between A $\beta$  peptide production and clearance, thus providing important evidence for amyloid cascade hypothesis. In particular, autosomal dominant mutations in APP, PS1

and PS2 genes lead to an abnormal A $\beta$  peptide production in the familial forms of AD (Selkoe, 1994; Bertram *et al.*, 2010). In addition, the APOE $\epsilon$ 4, which predisposes to AD in more than 40% of cases as a dose-dependent risk factor for late-onset FAD (Saunders, 2000), increases A $\beta$  peptide aggregation and impairs its clearance in the brain (Castano *et al.*, 1995).

**Fig. 3**



**Selkoe and Hardy, *EMBO Mol Med* (2016)**

### 1.4.1 Intracellular A $\beta$

The A $\beta$  peptide was first identified as a component of extracellular amyloid plaques in the mid-1980s. Then, a large number of studies on *post mortem* AD, Down syndrome and transgenic mouse brains provided evidence for the presence of intraneuronal A $\beta$ . Furthermore, several results suggested that the accumulation of intraneuronal A $\beta$  is an early event in AD progression, which occurs before the formation of extracellular A $\beta$  deposits (Gyure *et al.*, 2001; Gouras *et al.*, 2000). Moreover, a comprehensive study, in which 99 brains from controls and from AD and Down syndrome patients were analyzed, found that most of the intraneuronal A $\beta$  is the A $\beta$ <sub>1-42</sub> peptide.

#### 1.4.1.1 Accumulation of intracellular A $\beta$

Despite the A $\beta$  generation from APP is known to take place at the extracellular side of plasma membrane, it may occur also in several cellular compartments, where APP and  $\beta$ - and  $\gamma$ - secretases are localized. Moreover, it is conceivable that secreted A $\beta$  is taken back up by the cell to form A $\beta$  intracellular pools.

Wertkin *et al.* in 1993 provided the first evidence that A $\beta$  may be generated intracellularly under certain conditions. In particular, they demonstrated that cells harbouring WT APP and APP<sub>Swe</sub> process APP differently: cells expressing APP<sub>Swe</sub> display A $\beta$  formation, whereas WT APP do not (Wertkin *et al.*, 1993). Importantly, A $\beta$  may be produced intracellularly in the endosome compartments following the internalization of APP by endocytosis (Koo and Squazzo, 1994). In fact, it has been demonstrated that reducing APP internalization by site-directed mutagenesis correlates with a reduction of A $\beta$ <sub>1-42</sub> levels (Perez *et al.*, 1999). In addition, strong evidence suggests that A $\beta$  is generated along the secretory pathway (Busciglio *et al.*, 1993). Moreover, it has been shown that retention of

APP in the ER blocks the production of A $\beta$ <sub>1-40</sub> but not of A $\beta$ <sub>1-42</sub>, thus suggesting that A $\beta$ <sub>1-42</sub> can be also produced in the ER (Wild-Bode *et al.*, 1997).

As said previously, the generation of intracellular pools of A $\beta$  can result from a re-uptake of previously secreted A $\beta$ . A $\beta$  can be internalized into the cell by binding to several biomolecules, including various receptors and transporters, such as to the  $\alpha$ 7 nicotinic acetylcholine receptor (Nagele *et al.*, 2002), low density lipoprotein receptor and NMDA receptor (Snyder *et al.*, 2005). In fact, blocking this internalization mechanism prevents the pathogenicity, as confirmed by the protective effect of memantine against A $\beta$ -mediated cognitive decline (Reisberg *et al.*, 2003; Minkeviciene *et al.*, 2004).

#### **1.4.1.2 Pathogenic role of intracellular A $\beta$**

It is widely accepted that the oligomeric species of A $\beta$ , from dimer and trimers to dodecamers, are more pathological than protofibrils and fibrils. The intracellular oligomerization of A $\beta$  is a crucial event and, importantly, it initiates before than the oligomerization in the extracellular space (Walsh *et al.*, 2000). A number of data suggest that increased levels of A $\beta$  within the neurites and synapses lead to their dysfunction and subsequent destruction. The remnant amorphous neurites are shaped as plaques by activated microglia (Meyer-Luehmann *et al.*, 2008), a crucial player in A $\beta$  plaques formation and other AD processes. The accumulation and the oligomerization of A $\beta$ <sub>1-42</sub> peptides in neurons are associated with subcellular pathology, such as reduction or loss of microtubule-associated proteins (MAPs) (Takahashi *et al.*, 2002; Capetillo-Zarate *et al.*, 2011). In particular, Takahashi *et al.* in 2013 provided evidence that localized accumulation of A $\beta$ <sub>1-42</sub> peptides is associated with early alterations of MAP2, an important MAP in dendrites, thus confirming the significant role of intracellular A $\beta$

in synaptic loss (Takahashi *et al.*, 2013). Moreover, their anatomical studies on Tg2576 mouse brain revealed that the increase in A $\beta$ <sub>1-42</sub> peptides levels was concomitant with the reduction of MAP2 in the *stratum lacunosum moleculare*, the region containing distal dendrites from the CA1 pyramidal cells and their synaptic compartments (Takahashi *et al.*, 2013). This result was consistent with several evidence demonstrating the reduction of dendritic architecture in APP mutant transgenic mice.

### **1.4.2 Dysregulation of ionic homeostasis**

According to the amyloid cascade hypothesis, altered ionic homeostasis is one of the metabolic consequences of progressive A $\beta$  accumulation and aggregation, contributing to neuronal dysfunction and death.

Although the study of ionic homeostasis in AD is somewhat recent and more limited in the field of calcium homeostasis, also potassium and sodium channels are interesting objects of study given their implication in memory and learning processes and neuron excitability, respectively.

Very recently, it has been speculated that an imbalance of Na<sup>+</sup> and K<sup>+</sup>, that are critical for nerve signal transduction, electrophysiological activity, membrane transport and other processes, occurs in AD brains after A $\beta$  accumulation (Vitvitsky *et al.*, 2012).

#### **1.4.2.1 Potassium dysregulation in AD**

The first to study potassium channels dysfunction in AD has been Renè Etcheberrigaray in 1993. Starting from the assumption that K<sup>+</sup> has a central role in memory acquisition in both molluscs and mammals (Alkon, 1984; Alkon, 1989; Collin *et al.*, 1988; Etcheberrigaray *et al.*, 1992; Sanchez-Andres and Alkon,

1991), he investigated K<sup>+</sup> channel dysfunction as a possible downstream event of A $\beta$  metabolism disruption contributing to memory impairment. In particular, he found that a 113-pS tetraethylammonium (TEA)-sensitive K<sup>+</sup> channel was dysregulated in AD patients fibroblasts compared to non-AD fibroblasts, together with altered intracellular Ca<sup>2+</sup> release (Etcheberrigaray, 1993). Moreover, he revealed that soluble A $\beta$  was responsible for K<sup>+</sup> channel dysfunction, thus suggesting that A $\beta$  could affect memory mechanisms in early phases of AD, before plaque formation and cell death. Subsequently, accumulating evidence supported the systemic K<sup>+</sup>-dysregulation hypothesis for AD postulated by Etcheberrigaray and Bhagavan in 1999 (Etcheberrigaray and Bhagavan, 1999). More recently, a crucial role for intracellular K<sup>+</sup> in the regulation of cell cycle progression and apoptosis has been observed in several neurodegenerative disease, including AD (Yu, 2003). Furthermore, treatment with A $\beta$  peptide has been found to enhance voltage-gated potassium channel (K<sub>v</sub>) activity in rat cerebellar granule cells (Ramsden *et al.*, 2001), as well as in rat cortical astrocytes (Jalonen *et al.*, 1997) and microglial cells (Chung *et al.*, 2001). Interestingly, in most of these neurotoxicity models, the inhibition of elevated K<sup>+</sup> efflux exerted a neuroprotective effect by preventing cell death (Pike *et al.*, 1996; Colom *et al.*, 1998; Yu, 2003). Interestingly, Pannaccione *et al.* in 2005 demonstrated that A $\beta$  peptides cause a dose-dependent and time-dependent enhancement of K<sub>v</sub> currents, in nerve growth factor (NGF)-differentiated rat pheochromocytoma (PC-12) cells and in hippocampal neurons. In particular, this up-regulation of both inactivating and non-inactivating component of K<sub>v</sub> currents is triggered by reactive oxygen species (ROS) production caused by the A $\beta$ -induced Ca<sup>2+</sup> increase. In fact, Ca<sup>2+</sup>-dependent ROS production activates NF- $\kappa$ B transcription factors so leading to enhanced expression of K<sub>v</sub> channels in the

neuronal membrane. More specifically, it has been shown that the Kv3.4 channel subunit, a component of Kv3 family underlying the fast-inactivating K<sup>+</sup> currents (*I<sub>A</sub>*), and its accessory subunit MIRP2 are involved in A $\beta$ -induced *I<sub>A</sub>* modulation (Pannaccione *et al.*, 2007). In fact, both NGF-differentiated PC12 cells and hippocampal neurons treated with A $\beta$ <sub>1-42</sub> peptide display a selective up-regulation of Kv3.4 channel subunits and an altered subcellular distribution of this protein. In addition, the involvement of Kv3.4 in AD pathogenesis (Angulo *et al.*, 2004; Boda *et al.*, 2012; Pannaccione *et al.*, 2005, 2007) is further supported by data provided by Diochot *et al.* in 1998, as well as by results from our laboratory, that BDS-I, a Kv3.4 blocker, exerts a potent neuroprotective action in hippocampal neurons and NGF-differentiated PC12 cells exposed to A $\beta$ <sub>1-42</sub> peptide. Furthermore, Boscia *et al.* recently demonstrated that the expression and activity of Kv3.4 are intensely up-regulated in primary astrocytes exposed to A $\beta$  oligomers and in Tg2576 primary astrocytes, thus suggesting the involvement of Kv3.4 channel dysregulation in astrocyte dysfunction occurring in AD (Boscia *et al.*, 2017).

#### **1.4.2.2 Sodium dysregulation in AD**

Interestingly, several evidence suggest a dysregulation of intracellular sodium concentrations in AD brain. In particular, [Na<sup>+</sup>] was found 26% higher in brain tissue from patients with severe AD than controls, thus suggesting that disruption of Na<sup>+</sup> homeostasis may be a late-stage event, with a significant positive correlation with Braak stage (Graham *et al.*, 2015). Nevertheless, the increase of intracellular sodium concentrations ([Na<sup>+</sup>]<sub>i</sub>) seems not simply to be a consequence of late-stage neurodegeneration. Aberrant increases in network excitability and compensatory inhibitory mechanisms in the hippocampus, due to

an A $\beta$ <sub>1-42</sub>-induced Nav up-regulation, may contribute to cognitive deficits in AD and, more importantly, they may explain the high incidence of epileptic seizures in patients with EOAD who overexpress human APP (Palop and Mucke, 2010). In addition, it has been well documented that AD is associated with depressed ATPase activity in the brain (Hattori *et al.*, 1998) and increased Na<sup>+</sup> dependent Ca<sup>2+</sup> uptake has been reported in AD brain tissue (Colvin *et al.*, 1991). Indeed, membrane lipid peroxidation due to the generation of ROS during A $\beta$  formation, impairs the function of membrane proteins involved in ion transport, such as the Na<sup>+</sup>/Ca<sup>2+</sup>-ATPase and Ca<sup>2+</sup>-ATPase, and glutamate and glucose transporters (Mark *et al.*, 1995; 1997). In addition, the impairment of glucose energy metabolism caused by mitochondrial dysfunction and reduced glucose uptake, deprives the pumps from ATP, thus affecting their functioning (Mark *et al.*, 1997). The impairment of ion-motive ATPases, observed in both primary cultures and synaptosomes from adult post-mortem hippocampus (Mark *et al.* 1995), results in membrane depolarization and in the opening of N-methyl D-aspartate (NMDA) receptor-channels and voltage-gated Ca<sup>2+</sup> channels. Collectively, these processes may alter Na<sup>+</sup> and Ca<sup>2+</sup> homeostasis.

#### **1.4.2.3 Calcium dysregulation in AD: the “calcium hypothesis”**

Khachaturian first proposed the “calcium hypothesis” of AD in which he postulated that calcium dysregulation had a central role in the pathophysiology of AD (Khachaturian *et al.*, 1989). Although this hypothesis was initially proposed without any supporting experimental evidence, such evidence has since emerged (Mattson *et al.*, 2000), including the fact that every gene that is known to be a predisposing factor for AD also modulates some aspects of calcium signalling.

According to this hypothesis, calcium dyshomeostasis is an early event that can influence A $\beta$  accumulation and hyperphosphorylation of tau. Results obtained from both human subjects and experimental models support this aspect, showing that alterations in calcium signalling occur during the early phases of AD, even before the development of overt symptoms (Etcheberrigaray *et al.*, 1998). Moreover, animal models of AD revealed how the calcium hypothesis can explain both the early cognitive decline and later cell death. The concept is that the activation of amyloidogenic pathway leads to a remodelling of the neuronal Ca<sup>2+</sup> signalling, in particular to an up-regulation of Ca<sup>2+</sup> signalling, despite a down-regulation is also described.

Intracellular Ca<sup>2+</sup> concentrations ([Ca<sup>2+</sup>]<sub>i</sub>) are normally maintained at nanomolar levels. Nonetheless, they can be specifically increased to micromolar level within distinct microdomains (Yuste *et al.*, 2000). Calcium entry in the cytosol is predominantly mediated by ligand-gated channels, such as the NMDA receptors, or voltage-gated calcium channels (VGCC) located on the plasma membrane. Calcium release from intracellular ER stores occurs via inositol triphosphate receptors (IP<sub>3</sub>R) and ryanodine receptors (RyR), located on ER membrane. The activation of both IP<sub>3</sub>R and RyR by inositol triphosphate (IP<sub>3</sub>) and cytosolic calcium, respectively, is enhanced by the mechanism known as calcium-induced calcium release (Verkhratsky, 2002).

The first mechanism by which A $\beta$  can disrupt calcium homeostasis is the formation of cation-selective ion channel (Kagan *et al.*, 2002). In particular, it has been demonstrated that nanomolar levels of A $\beta$ <sub>1-42</sub> form calcium-permeable pores (Bhatia *et al.*, 2000) able to mediate simple calcium signals at low concentrations and calcium waves at higher concentrations of A $\beta$ <sub>1-42</sub>.

Furthermore, A $\beta$  oligomers are able to increase non-selectively Ca<sup>2+</sup> permeability of cellular membranes, thus increasing Ca<sup>2+</sup> influx from the extracellular space but also Ca<sup>2+</sup> leakage from intracellular Ca<sup>2+</sup> stores (Demuro *et al.*, 2005). Moreover, A $\beta$  can increase NMDA receptor-dependent Ca<sup>2+</sup> influx (De Felice *et al.*, 2007) and promote Ca<sup>2+</sup> entry through voltage-gated Ca<sup>2+</sup> channels.

Another mechanism by which A $\beta$  affects calcium signalling is the generation of oxidative damage. In fact, aggregated A $\beta$  induces the formation of ROS that can lead to membrane-lipid peroxidation (Hensley *et al.*, 1994). This process in turn can affect the function of membrane ATP-ases and other transporters, so leading to an increase of basal intracellular calcium levels (Mattson *et al.*, 1992; Mark *et al.*, 1995). Indeed, the A $\beta$ -mediated impairment of ion ATPases has been observed in both neuronal primary cultures and synaptosomes from adult post-mortem hippocampus (Mark *et al.*, 1995).

However, A $\beta$  peptide is not the only link between APP metabolism and calcium dynamics. Indeed, also other metabolic derivatives of APP influence calcium homeostasis and *vice versa* calcium modulates APP processing, in particular A $\beta$  production. In fact, every important derivative of APP, including A $\beta$ , the  $\beta$ -CTFs, and the secreted ectodomain, has been demonstrated to affect calcium signalling in a different way (LaFerla, 2002). Secreted APP molecules normalize cytosolic calcium levels, particularly by attenuating the elevated intracellular calcium levels evoked by A $\beta$ , thus sharing a neuroprotective role (Goodman and Mattson, 1994). Unlike APPs, A $\beta$ -containing fragments increase [Ca<sup>2+</sup>]<sub>i</sub>, as said previously, thus triggering several neurotoxic processes culminating with cell death (Mattson, 1994). In fact, altered calcium dynamics have a number of consequences: dysregulated activation of cellular enzymatic systems (such as proteases, phospholipases, kinases and phosphatases), including calpain system (Nixon *et*

*al.*, 1994; Bano *et al.*, 2005; Atherton *et al.*, 2009) cytoskeleton modifications; generation of free radicals (Mattson, 1995); triggering of apoptotic machinery (Mattson, 1994).

However, unlike for presenilin mutations, few studies have focused on the consequences of FAD-causing mutations in APP gene for calcium signalling. Indeed, it is deeply investigated the role of mutated presenilins, since they may affect calcium signalling by interacting with three different key components of Ca<sup>2+</sup> signalling: the IP<sub>3</sub>R (Stutzmann, 2005; Cheung *et al.*, 2008), RyR (Stutzmann *et al.*, 2006; Hayrapetyan *et al.*, 2008), and the sarco/endoplasmic reticulum Ca<sup>2+</sup> pumps (SERCA) (Green *et al.*, 2008). In fact, potentiation of IP<sub>3</sub>R-mediated Ca<sup>2+</sup> signals by presenilin mutations has been demonstrated in several experimental systems.

## **1.5 Neuronal hyperexcitability and epilepsy in AD**

As the main cause of dementia (Reitz *et al.*, 2011), AD is still intensely investigated, also as regards its complex relationship with seizures and epilepsy. Indeed, since dementia is a major cause of seizures in elderly population and, conversely, seizures have a deleterious impact on cognitive performances in demented patients, it has become crucial to establish a correct diagnosis of epileptic activity in AD patients and, consequently, to treat them with suitable antiepileptic drugs. In fact, it is established that AD patients have a greater risk of having seizures than non-AD patients of similar age. Myoclonus, that is generally considered a consequence of cortical hyperexcitability, is also common in AD patients, with a prevalence of 7-10%. Moreover, seizures and myoclonus show to have a greater incidence in younger AD patients (Vossel *et al.*, 2013; Sherzai *et*

*al.*, 2014) and, more interestingly, to be associated with reduced survival (Samson *et al.*, 1996).

Although initial studies focused on seizures in patients with advanced AD, transgenic mouse models of AD showed that seizures and epileptiform activity can occur early in the disease (Sanchez *et al.*, 2012), before A $\beta$  plaques deposition. This finding induced the researchers to pay closer attention to seizures occurring in the early stages of dementia (Vossel *et al.*, 2013; Sanchez *et al.*, 2016). Animal model of AD overexpressing human APP and/or PS1 or expressing genetic mutations linked to FAD can exhibit a variety of seizures types (Palop and Mucke, 2010; Minkeviciene *et al.*, 2009; Vogt *et al.*, 2011). Evidence from these animal models show that the mechanisms that lead to epileptogenesis in AD are distinct from those derived from epilepsy models. In fact, the trigger for many of these mechanisms seem to be the oligomeric species of A $\beta$ , even if the relative implication of A $\beta$ , APP and other APP derivatives to network hyperexcitability is not fully clear (Minkeviciene *et al.*, 2009; Vogt *et al.*, 2011). Palop *et al.* in 2007 showed that A $\beta$  accumulation in the brain could cause epileptiform activity, thus correlating epileptic seizures with an excitatory effect of A $\beta$  on brain networks rather than with a neurodegenerative mechanism (Palop *et al.*, 2007). In fact, AD mouse models with epileptic seizures exhibit little neuronal loss, further suggesting that seizures are not related to end-stage degeneration (Chin, 2011). Furthermore, Palop and Mucke in 2009 suggested that A $\beta$ -induced aberrant networks are associated with sprouting of inhibitory neurons in the dentate gyrus of the hippocampus (Palop and Mucke, 2010). In addition, exposure to soluble A $\beta$  peptides in hippocampal CA1 cells in mice has been demonstrated to alter intrinsic excitability towards hyperexcitability patterns (Tamagnini *et al.*, 2015). Moreover, *in vitro* experiments with mouse models

showed that the increase of L-type calcium channel currents depends on APP expression but not on A $\beta$  production, suggesting a prominent role of APP in neuronal network imbalance (Santos *et al.*, 2009).

### **1.5.1 Role of Na<sub>v</sub> currents in hyperexcitability**

As said previously, neuronal network dysfunction may play a critical role in AD pathogenesis, since it has been demonstrated to be altered in transgenic mice overexpressing human APP. In particular, it has been shown that alterations in neuronal network activity contributing to cognitive impairment associated with AD, may result from an A $\beta$ -induced aberrant increase in neuronal activity and resulting compensatory responses. In fact, mouse models of AD that have elevated levels of A $\beta$  exhibit altered neuronal activity, spontaneous seizures and epileptiform discharges (Palop *et al.*, 2006; 2007), which further contribute to cognitive deficits. Accumulating evidence suggests that soluble A $\beta$ , rather than A $\beta$  plaques, correlates with neuronal hyperactivation. In fact, it has been found that extracellular application of A $\beta$ <sub>1-42</sub> induces hyperactivity on hippocampal CA1 neurons in WT mice (Busche *et al.*, 2012). Furthermore, Busche *et al.* in 2015 demonstrated that A $\beta$ <sub>1-42</sub>-induced hyperexcitation was due to an increase in the amplitude of persistent sodium current ( $I_{NaP}$ ), a slow inactivating component of Tetrodotoxin (TTX)-sensitive sodium current, important for regulating neuronal excitability (Busche *et al.* 2015; Crill *et al.*, 1996; Driscoll *et al.*, 2013). In fact,  $I_{NaP}$  depolarizes membrane potential toward the threshold for action potential initiation, thus regulating several neuronal functions, generating subthreshold oscillatory activity, amplifying synaptic potentials, and facilitating repetitive firing patterns (Yue *et al.*, 2005). For these reasons,  $I_{NaP}$  represents a crucial player involved in both acquired and genetically determined epilepsy (Stafstrom, 2007).



# CHAPTER 2: Na<sup>+</sup>/Ca<sup>2+</sup> EXCHANGER

## 2.1 The Na<sup>+</sup>/Ca<sup>2+</sup> exchanger: a brief background

The regulation of intracellular concentrations of Na<sup>+</sup> and Ca<sup>2+</sup> ions is a crucial physiological phenomenon that maintains cellular homeostasis in excitable cells. In fact, Ca<sup>2+</sup> represents a second messenger in cytosolic and nuclear signaling (Choi, 1988), whereas Na<sup>+</sup> plays a key role in regulating cellular osmolarity, in inducing action potential (Lipton, 1999), and in transduction signaling (Yu *et al.*, 1997).

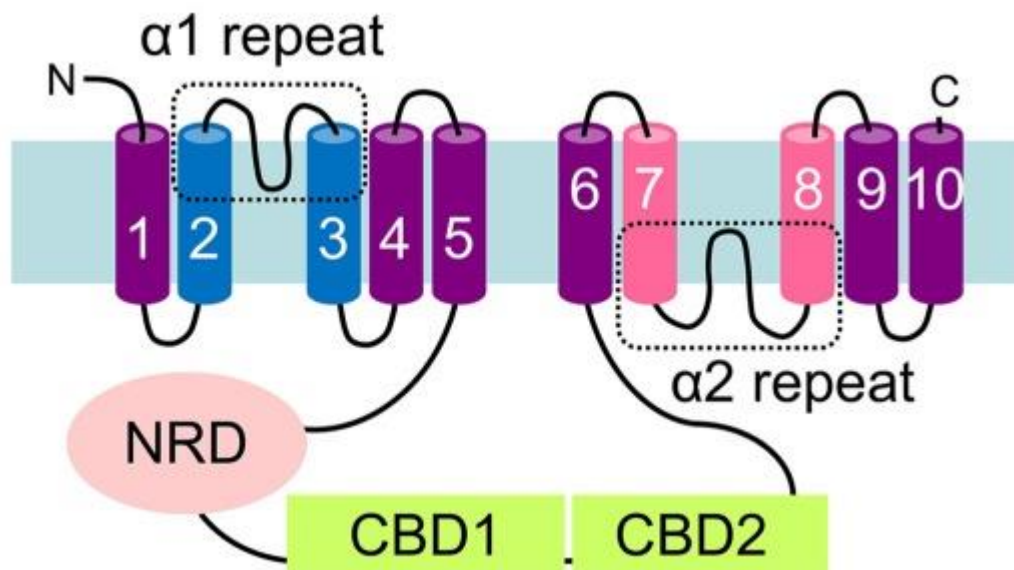
The Na<sup>+</sup>/Ca<sup>2+</sup> exchanger (NCX) (**Fig. 4**), together with selective ion channels and ATP-dependent pumps, contributes to the regulation of Na<sup>+</sup> and Ca<sup>2+</sup> physiological concentrations. (Blaustein and Lederer, 1999). In particular, the NCX catalyzes the countertransport of Na<sup>+</sup> for Ca<sup>2+</sup> ions across the plasma membrane in a bidirectional way (Blaustein and Lederer, 1999; Philipson and Nicoll, 2000). In vertebrate species, NCX is present in most tissues, where its abundance depends on the importance of Na<sup>+</sup>/Ca<sup>2+</sup> exchange in that cell type. In particular, its expression is high in excitable tissues (heart, brain) and in those involved in osmoregulation (kidney), but is low in other tissues (Quednau *et al.*, 1997; Kofuji *et al.*, 1992).

Na<sup>+</sup>/Ca<sup>2+</sup> exchange is electrogenic, thus the net direction in which the NCX transports Ca<sup>2+</sup> is dependent on the membrane potential ( $E_m$ ) in addition to intracellular and extracellular concentrations of Na<sup>+</sup> and Ca<sup>2+</sup>. The stoichiometry of this exchange is generally accepted to be 3Na<sup>+</sup> ions/1Ca<sup>2+</sup> (Philipson and Nicoll, 2000; Blaustein and Lederer, 1999); however a stoichiometry of 4:1 may

be also possible (Lytton and Dong, 2002; Fujioka *et al.*, 2000; Kang and Hilgemann, 2004).

In excitable cells, after an increase of  $[Ca^{2+}]_i$ , the NCX provides the return of  $[Ca^{2+}]_i$  at resting levels (Carafoli, 1985), by coupling  $Ca^{2+}$  extrusion to  $Na^+$  influx into the cells, following their electrochemical gradient. This mode of operation is defined as the forward mode (Blaustein and Santiago, 1977). By contrast, when an increase in intracellular sodium concentrations ( $[Na^+]_i$ ) or membrane depolarization occurs, the NCX mediates  $Na^+$  extrusion and  $Ca^{2+}$  influx, following the reduced  $Na^+$  electrochemical gradient across the plasma membrane, thus operating in the so-called reverse mode (Baker and McNaughton, 1976; DiPolo, 1979).

**Fig. 4**



Emery *et al.*, *Front in plant science* (2012)

## 2.2 Molecular biology of NCX

The NCX is a member of the superfamily of membrane proteins comprising: 1) the NCX family (Reeves and Hale, 1984; Fujioka *et al.*, 2000; Kang and Hilgemann, 2004); 2) the K<sup>+</sup>-dependent Na<sup>+</sup>/Ca<sup>2+</sup> exchanger family (Schnetkamp *et al.*, 1989; Lytton *et al.*, 2002); 3) the bacterial family which probably promotes H<sup>+</sup>/Ca<sup>2+</sup> exchange (Cunningham and Fink, 1996); 4) the nonbacterial H<sup>+</sup>/Ca<sup>2+</sup> exchange family, which is also the Ca<sup>2+</sup> exchanger of yeast vacuoles (Pozos *et al.*, 1996); and 5) a group provisionally named cation/Ca<sup>2+</sup> exchanger, an electrogenic exchanger of protons with Mg<sup>2+</sup> and Zn<sup>2+</sup> ions (Shaul *et al.*, 1999).

### 2.2.1 NCX Topology

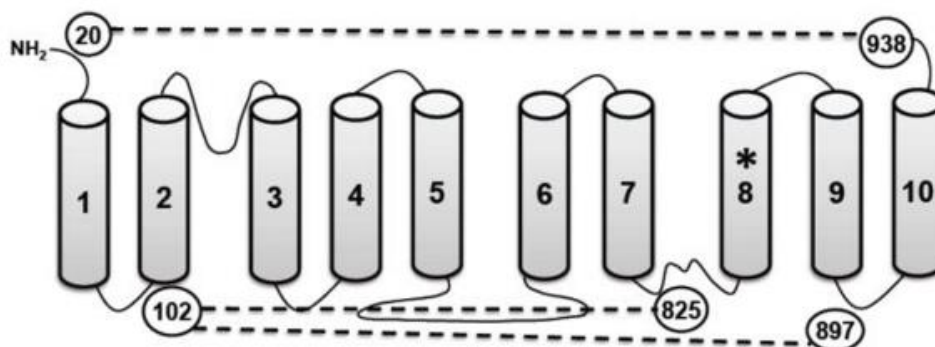
The most current NCX topology refers to the data provided by Nicoll *et al.* 1990 and Iwamoto *et al.* in 1999.

The NCX protein varies in size anywhere from 880 to 970 residues, depending on the isoform, with a molecular weight of ~108 kDa. Initial purification of native NCX from cardiac sarcolemma and subsequent SDS-PolyAcrylamide Gel Electrophoresis (SDS-PAGE) allowed identifying proteins of 70, 120, and 160 kDa; the smallest of them is thought to be a proteolytic fragment (Philipson *et al.*, 1988; Bano *et al.*, 2005; Pannaccione *et al.*, 2012). NCX undergoes several post-translational modifications, which may explain the difference between the expected and the actual molecular weight of the protein.

Initial analyses of NCX structure identified a mature protein with 12 trans membrane domains (TMS) (Nicoll *et al.*, 1990), whereas later studies indicated 9 putative TMS organized in N and C- terminal hydrophobic domains of 5 and 4 TMS, respectively (Iwamoto *et al.*, 1999; Nicoll *et al.*, 1999; Doering *et al.*, 1998).

However, to better understand structure/function correlation, Ren and Philipson in 2013 re-examined the membrane topology of NCX1. According to their results, NCX1 is modelled to have 10 TMS (**Fig.5**) (Ren and Philipson, 2013). Within the hydrophobic domains are the  $\alpha$ -1 and  $\alpha$ -2 repeats, which are crucial for ion translocation across the plasma membrane (Nicoll *et al.*, 1996). These two repeats are located on opposite sides of the membrane with  $\alpha$ -1 spanning the TMS2 and 3 and  $\alpha$ -2 spanning the TMS 8 and 9. The large hydrophilic intracellular loop, named the f loop, contains sites important for NCX activity regulation elicited by several cytoplasmic messengers, including Na<sup>+</sup> and Ca<sup>2+</sup> ions, and for alternative splicing. Some groups have provided evidence about an exchange activity in truncated NCX lacking the C-terminal portion of the protein (Gabellini *et al.*, 1996; Li and Lytton, 1999; Van Eylen *et al.*, 2001). In fact, these researchers showed that dimerization of the N-terminus TMS region can form a functional exchanger. However, other investigator, such as Ottolia *et al.* in 2001 and Kasir *et al.* in 1999 refuted this possibility.

**Fig. 5**



Ren and Philipson, *J Mol Cell Cardiol* (2013)

### 2.2.2 NCX genes and splice variants

The NCX family, also named Solute carrier family 8A (SLC8A), includes three separate gene products, NCX1 (Nicoll *et al.*, 1990), NCX2 (Li *et al.*, 1994), and NCX3 (Nicoll *et al.*, 1996). Apparently, two sequential gene replication events generate the three NCX genes, even if the evolutionary timeframe of these replications has not been identified.

The three NCX isoforms display differential expression patterns in mammalian tissues. NCX1 is the most well characterized, since it has been found in virtually all tissues, including heart, brain, skeletal muscle, smooth muscle, kidney, spleen, liver, intestine and pancreas (Quednau *et al.*, 1997). The location of all three NCX genes on human chromosomes has been determined: NCX1, NCX2 and NCX3 have 2p23-p22, 19q13.3, 14q24.1 as gene loci, respectively. The protein products of all three genes display ~70% identity, which become greater than 80% in the TMS (Nicoll *et al.*, 1996).

NCX1 gene has a differential expression, which is directed by three 5' untranslated exons under the control of tissue specific promoters (Barnes *et al.*,

1997; Lee *et al.*, 1994; Nicholas *et al.*, 1998). Less is known about the regulation of NCX2 and NCX3 gene expression, which are found exclusively in brain and skeletal muscle (Quednau *et al.*, 1997; Nicoll *et al.*, 1996; Lee *et al.*, 1994). In addition, tissue specific expression of NCX is further diversified through alternative splicing (Quednau *et al.*, 1997; Lee *et al.*, 1994; Kofuji *et al.*, 1994). NCX splice variants originate from different combinations of exons 3-8, also known as exons A-F, which encode a region of C-terminal portion of f loop commonly known as alternative splice region. Exons A and B are mutually exclusive and, to give rise to tissue specific splice variants, they are used in combination with exons C-F (Kofuji *et al.*, 1994). In general, excitable tissues express exon A, whereas splicing variants with exon B are predominant in other tissues (Quednau *et al.*, 1997). In addition, all NCX1 splice variants contain the 6-mer, exon D, which seems to have no functional role.

Alternative splicing in NCX2 and NCX3 is less extensive. NCX2 expresses only exons A and C since no alternative splicing has been identified to date (Quednau *et al.*, 1997). In contrast, four splice variants of NCX3 have been detected in brain and skeletal muscle (Quednau *et al.*, 1997; Gabellini *et al.*, 2002).

The physiological significance of NCX alternative splicing is not clear, despite potential roles of the region in Protein Kinase A (PKA) sensitivity and  $\text{Ca}^{2+}$  and  $\text{Na}^{+}$ -dependent activity regulation have been proposed (Ruknudin *et al.*, 2000; Schulze *et al.*, 2002; Dyck *et al.*, 1999; Maack *et al.*, 2005). What is very interesting is that there are more functional differences among splice variants of the same NCX gene than between NCX genes. Therefore, it has been hypothesized that the structural complexity of NCX genes allows them to respond independently to specific ionic environments and exchange requests in a tissue specific or cell specific manner (Lee *et al.*, 1994).

## 2.3 NCX regulation

NCX function is dynamically regulated by several factors including the intracellular pH (Philipson *et al.*, 1982), ATP (Hilgemann, 1990; DiPolo and Beauge, 1998), Phosphatidylinositol 4,5-bisphosphate (PIP<sub>2</sub>) (Hilgemann and Ball, 1996; He *et al.*, 2000), proteinase treatment (Philipson and Nishimoto, 1984), phospholipases (Philipson and Nishimoto, 1984) and eXchanger Inhibitory peptide (XIP) (Li *et al.*, 1991). In addition, Na<sup>+</sup> and Ca<sup>2+</sup> have their own autoregulatory effects on NCX currents. This regulation arises from the f loop, since its deletion abolishes allosteric regulation of NCX activity by intracellular Na<sup>+</sup> and Ca<sup>2+</sup> (Matsuoka *et al.*, 1993).

### 2.3.1 Ca<sup>2+</sup> Regulation

Early studies showed stimulation of NCX currents by intracellular Ca<sup>2+</sup> (DiPolo, 1979; Reeves and Poronnik, 1987; Miura and Kimura, 1989), suggesting the regulatory role of this ion in exchange activity. In fact, submicromolar concentrations (0,1-0,3 μM) of intracellular Ca<sup>2+</sup> are needed to activate NCX (Hilgemann *et al.*, 1992). This regulatory function of low micromolar Ca<sup>2+</sup> is especially evident when NCX is working in the reverse mode, whereas it is not fully clear how it can regulate NCX when it operates in the forward mode (Matsuoka *et al.*, 1995).

Levitsky *et al.* in 1994 identified in the centre of f loop a high affinity Ca<sup>2+</sup> binding region of 130 residues, which display high identity among NCX isoforms (Levitsky *et al.*, 1994). Mutations in this region do not affect ion translocation but do alter Ca<sup>2+</sup> binding and regulatory properties (Matsuoka *et al.*, 1995).

### 2.3.2 Na<sup>+</sup> Regulation

In addition to intracellular Ca<sup>2+</sup>, an increase in [Na<sup>+</sup>]<sub>i</sub> can also regulate the NCX (Hilgemann, 1990). In particular, when intracellular Na<sup>+</sup> increases, it binds to the transport site of NCX molecule at the intracellular surface, and after an initial fast outward current, it induces a state of inactivation (Hilgemann *et al.*, 1992). The physiological significance of this phenomenon, named Na<sup>+</sup>-dependent inactivation, is unclear since it predominates only at [Na<sup>+</sup>]<sub>i</sub> (i.e. >30 mM) that are unlikely to be reached during normal conditions (Bers, 2002). The region responsible for Na<sup>+</sup>-dependent inactivation has been identified as a 20-amino acid site of the N-terminal portion of f loop, usually named XIP site (Matsuoka *et al.*, 1997) because it shares the same sequence of a small peptide, XIP, which is able to inhibit NCX (Li *et al.*, 1991) probably binding this site (Hale *et al.*, 1997). The inhibitory action of the peptide is non-competitive with Na<sup>+</sup> and Ca<sup>2+</sup> binding. In addition, mutational analysis of the XIP region confirmed that this site does not affect ion translocation *per se*, but rather modulates Na<sup>+</sup>-dependent inactivation (Matsuoka *et al.*, 1993; He *et al.*, 1997). However, the XIP site shows relatively low evolutionary conservation compared to other regions of NCX molecule, which could involve potentially be due to a Na<sup>+</sup>-dependent inactivation involving a different binding site. Interestingly, Ca<sup>2+</sup>, at low micromolar concentrations, binding its regulatory site, can decrease the extent of this Na<sup>+</sup>-dependent inactivation. In fact, mutations in the Ca<sup>2+</sup> regulatory site alter the activation and inactivation kinetics of NCX currents by modulating Na<sup>+</sup>-dependent inactivation (Matsuoka *et al.*, 1995).

## 2.4 Pharmacological modulation of NCX

After the discovery of NCX activity in 1969, several studies have reported that some compounds can affect the activity of this antiporter (Kaczorowsky *et al.*, 1989). In fact, in the last 35 years, many inorganic and organic compounds have been found to be able to activate or block NCX activity.

### 2.4.1 Inhibitors

#### 2.4.1.1 Bivalent cations

Among the NCX inhibitors, many inorganic cations have been reported to block NCX (Iwamoto and Shigekawa, 1998). In particular, the inhibitory effect of divalent cations can be due either to a direct action on NCX molecule or to the replacement of  $\text{Ca}^{2+}$  ions as a substrate for the exchanger.  $\text{Cd}^{2+}$ ,  $\text{Mn}^{2+}$  and  $\text{Ni}^{2+}$ , for instance, may function as substrates for the antiporter (Iwamoto and Shigekawa, 1998). Notably,  $\text{Ni}^{2+}$  is the element most commonly used for blocking NCX activity during electrophysiological recordings (Fujioka *et al.*, 1998; Main *et al.*, 1997). However, the use of  $\text{Ni}^{2+}$  as NCX inhibitor is limited because it has an inhibitory effect at concentrations in order of 2 to 5 mM, a range in which it is able to inhibit also other membrane currents (Iwamoto and Shigekawa, 1998). Furthermore, the half maximal inhibitory concentration ( $\text{IC}_{50}$ ) value of  $\text{Ni}^{2+}$  for NCX inhibition is enhanced 2- to 3-fold by membrane depolarization, thus suggesting that its affinity for the inhibitory site is affected by membrane potential (Iwamoto and Shigekawa, 1998). In addition,  $\text{Ni}^{2+}$  affinity for NCX differs among the three isoforms; in fact, NCX3 is 10-fold less sensitive to  $\text{Ni}^{2+}$  inhibition than NCX1 and NCX2 (Iwamoto and Shigekawa, 1998).

#### 2.4.1.2 Endogenous Exchange Inhibitory peptides

As mentioned above, the first 20 amino acids of the f loop, named XIP, represents an autoinhibitory region involved in the Na<sup>+</sup>-dependent inactivation of NCX (Nicoll *et al.*, 1990, Matsuoka *et al.*, 1997). Several studies have shown that a synthetic peptide having the same amino acid sequence as the XIP region exerts an inhibitory effect on NCX activity (Li *et al.*, 1991; DiPolo and Beaugè, 1994), so the researchers made a great effort to synthesize and to characterize the molecular pharmacology of different XIP analogs. XIP, an amphipathic molecule, potently inhibits both modes of operation of NCX activity in a noncompetitive manner with an inhibitory constant ( $K_i$ ) of 0,1 to 1,0  $\mu$ M (Li *et al.*, 1991). NCX1, NCX2 and NCX3 have homologous XIP regions. The three corresponding inhibitory peptides, XIP1, XIP2, and XIP3 have some residue variations, despite having well conserved sequences. Concerning the mechanism by which XIP inhibits NCX activity, some authors have suggested that XIP is able to induce a conformational change in the C-terminal portion of f loop, by occupying its binding site, thus inhibiting the ion transport (Li *et al.*, 1991).

Since XIP hardly penetrates the cell membrane because of its prevalent hydrophilia, a XIP bearing a molecule of glucose attached to the Tyr-6 residue has recently been synthesized. In fact, the peptide more easily penetrates into the cell, since the molecule of glucose is actively transported into the cell through glucose transporters (1 and 3), thus carrying the attached peptide (Namane *et al.*, 1992). Interestingly, Pignataro *et al.* in 2004 exploited this strategy in *in vivo* experiments. In particular, the administration of this Tyr-6-glycosilated form of XIP intracerebroventricularly in male rats bearing permanent middle cerebral artery occlusion (pMCAO) caused a dramatic increase in infarct volume

(Pignataro *et al.*, 2004), thus suggesting that NCX plays a pivotal role in the mechanisms leading to neuronal death under ischemic conditions.

Interestingly, starting from this evidence, Molinaro *et al.* in 2015 tested the hypothesis that it was possible to increase NCX1 activity by blocking the regulatory cytosolic f loop of NCX1 (XIP<sub>NCX1</sub>), thereby preventing its binding to the inhibitory site, that has been hypothesized to correspond to the N-terminal portion of the f loop (P1 domain, 562-688aa). In particular, they demonstrated that a synthetic P1 peptide is able to up-regulate NCX1 activity, by directly binding XIP<sub>NCX1</sub> domain, thus counteracting its autoinhibitory action (Molinaro *et al.*, 2015).

#### **2.4.1.3 Amiloride derivatives**

Amiloride and its analogues were synthesized as K<sup>+</sup>-sparing diuretics capable to inhibiting kidney epithelia Na<sup>+</sup> channels (Cragoe *et al.*, 1967). Subsequently, these compounds have been found to have an inhibitory effect on other ion transport processes such as NCX, Na<sup>+</sup>/H<sup>+</sup> exchanger, and voltage-gated Ca<sup>2+</sup> channels (Murata *et al.*, 1995). Despite amiloride has been used for some time as an NCX blocker to assess NCX activity (Sharikabad *et al.*, 1997), its employment has two major limits. Firstly, its inhibitory activity requires millimolar concentrations; secondly, it lacks specificity. For these reasons two classes of amiloride analogues were developed. First class derivatives, such as 5-[N-methyl-N-(guanidinocarbonylmethyl)] amiloride, bear substituent on the 5-amino nitrogen atom of the pyrazine ring (Taglialatela *et al.*, 1988). They are not able to inhibit Na<sup>+</sup> channels and NCX, but they display great effectiveness in inhibiting the Na<sup>+</sup>/H<sup>+</sup> exchange in a range of 1 to 10 μM (Taglialatela *et al.*, 1988, 1990; Amoroso *et al.*, 1990). On the contrary, second class compounds, bearing

substituents on the terminal guanidino nitrogen, behave as specific inhibitors ( $K_i = 1\text{--}10\ \mu\text{M}$ ) of the epithelial  $\text{Na}^+$  channels and NCX, having no inhibitory effect on the  $\text{Na}^+/\text{H}^+$  exchanger. Among these compounds, dimethylbenzamiloride (DMB), 3',4'-dichlorobenzamyl, and  $\alpha$ -phenylbenzamyl have been shown to be selective inhibitors of NCX in excitable cells, such as neurons, in which the kidney epithelial  $\text{Na}^+$  channels are not expressed (Taglialatela *et al.*, 1988, 1990). By contrast, [*N*-(4-chlorobenzyl)]2,4-dimethylbenzamyl (CB-DMB) appears to be the most specific inhibitor of NCX activity ( $K_i = 7.3\ \text{M}$ ), for it has no inhibitory properties against the  $\text{Na}^+/\text{H}^+$  antiporter ( $K_i > 500\ \mu\text{M}$ ) and the epithelial  $\text{Na}^+$  channels ( $K_i > 400\ \mu\text{M}$ ) (Sharikabad *et al.*, 1997). Notably, the amiloride derivatives are able to inhibit both the forward (Taglialatela *et al.*, 1990) and the reverse mode of NCX activity (Amoroso *et al.*, 1997). Furthermore, they share a reversible inhibition of NCX activity, and this inhibition is competitive with respect to  $\text{Na}^+$  ion. In fact, it has been hypothesized that these derivatives function as  $\text{Na}^+$  analogues and interact at a  $\text{Na}^+$  binding site of NCX molecule thereby binding the transporter in an inactive complex (Kaczorowski *et al.*, 1985).

#### **2.4.1.4 Isothiourea derivatives**

A 2-[2-[4-(4-nitrobenzyloxy)phenyl]ethyl]isothiourea methanesulfonate derivative, named KB-R7943 was identified by Shigekawa's group (Iwamoto and Shigekawa, 1998) because they screened a compound library for the inhibition of  $\text{Na}^+$ -dependent  $\text{Ca}^{2+}$  uptake. This compound has the particular feature to inhibit NCX with a different potency depending on its mode of operation. In particular it has an  $\text{IC}_{50}$  value of 1.1 to 2.4  $\mu\text{M}$  when NCX operates in the reverse mode and an  $\text{IC}_{50}$  value  $> 30\ \mu\text{M}$ , when NCX operates in the forward mode (Iwamoto *et al.*, 1996). Furthermore, this compound seems to have a different ability to block the

three NCX isoforms. In fact, NCX3 inhibition requires concentrations 3-fold lower than those necessary to inhibit NCX1 and NCX2 (Iwamoto and Shigekawa, 1998). Regarding the inhibitory mechanism, KB-R7943 interacts with NCX molecule at the extracellular side, at the  $\alpha$ -2 repeat, between the TMS7 and TMS8 of the exchanger (Iwamoto *et al.*, 2001; Shigekawa *et al.*, 2002).

## **2.4.2 Activators**

Pharmacological agents able to stimulate NCX activity, either in the reverse or in the forward mode of operation, may represent a helpful strategy in some pathophysiological conditions, such as cardiac or brain ischemia by re-establishing intracellular  $\text{Na}^+$  and  $\text{Ca}^{2+}$  homeostasis.

### **2.4.2.1 Inorganic cations**

$\text{Li}^+$ , the lightest of alkaline cations, is able to stimulate  $\text{Na}^+$ -dependent  $\text{Ca}^{2+}$  uptake of all three NCX isoforms with low affinity, even if its extent of stimulation is somewhat smaller in NCX1 than in NCX2 and NCX3 (Iwamoto and Shigekawa, 1998). In particular, the  $\alpha$ -2 repeat seems to be responsible for the  $\text{Li}^+$ -induced NCX stimulation in NCX1 and NCX3.

### **2.4.2.2 Redox agents**

As mentioned above, changes in the redox state may stimulate NCX activity. Therefore, the simultaneous presence of reducing compounds, such as,  $\text{Fe}^{2+}$ , and  $\text{O}_2^-$  superoxide, and of oxidizing agents, such as  $\text{Fe}^{3+}$ ,  $\text{H}_2\text{O}_2$ , GSSG, and  $\text{O}_2$ , is able to stimulate NCX activity (Reeves *et al.*, 1986).

At first, when the researchers identified the property of redox agents to stimulate NCX activity, it was proposed that these agents could activate the exchange

activity by promoting thiol-disulfide interchange in the protein carrier (Reeves *et al.*, 1986). In particular, it was hypothesized that the stimulation of NCX came from the reduction of a disulfide bond and from the formation of a new disulfide bond (Reeves *et al.*, 1986). More recently, the cysteine residues involved in this disulfide bond have been identified as Cys-14, Cys-20, and Cys-780. They are located on the extracellular side, where Cys-780 is connected either to Cys-14 or to Cys-20 (Santacruz-Toloza *et al.*, 2000). However, the analysis of mutated exchangers indicated that the stimulation of WT exchanger induced by a mixture of redox agents (Fe-DTT) is not to be attributed to cysteines but rather is mainly due to the removal of the Na<sup>+</sup>-dependent inactivation process (Santacruz-Toloza *et al.*, 2000). Since redox changes in NCX activity have been implicated in many aspects of cell physiology and pathophysiology, it is possible to speculate that NCX activators might constitute a possible therapeutic strategy in those pathological conditions in which oxidative stress is involved. In this regard, evidence that the stimulation of NCX activity by the oxidant agent Fe<sup>3+</sup> may exert a neuroprotective effect has been provided both in *in vitro* and *in vivo* models of hypoxia and ischemia. Thus, in C6 glioma cells, it has been demonstrated that SNP, by stimulating NCX activity through its K<sub>3</sub>Fe(CN)<sub>6</sub> portion-containing iron, is able to significantly reduce cellular injury elicited by chemical hypoxia (Amoroso *et al.*, 2000). This protective effect is certainly due to NCX activation as a Na<sup>+</sup> efflux-Ca<sup>2+</sup> influx pathway, since it is abolished by NCX inhibitors (Amoroso *et al.*, 2000).

#### **2.4.2.3 Organic compounds**

It has been reported that the agonists of G-protein-coupled receptors, such as α- and β-receptors, histamine, 5HT<sub>2c</sub>, and endothelin-1 and angiotensin-II receptors,

are able to stimulate NCX activity by a pathway involving either PKA and/or protein kinase C (Ballard and Schaffer, 1996; Smith and Armstrong, 1996; Stengl *et al.*, 1998; Eriksson *et al.*, 2001a,b; Woo and Morad, 2001).

Among the peptides capable of stimulating NCX activity, only insulin and concanavalin A have been proven to exert such effect. In fact, both peptides stimulate Na<sup>+</sup>-dependent Ca<sup>2+</sup> uptake (Gupta *et al.*, 1986; Makino *et al.*, 1988).

## **2.5 Brain distribution of NCX**

The three NCX isoform appear to be differentially expressed in several regions of central nervous system (CNS), suggesting that each NCX subtype play a different functional role in distinct CNS region.

### **2.5.1 Cerebral cortex**

In the cerebral cortex, the expression of the mRNA encoding for all three NCX isoforms has different patterns. In particular, the upper neurons of the motors system and the terminal neurons of the sensory system display a differential expression of NCX isoforms. In fact, pyramidal neurons of layers III and V of motor cortex appear to be most intensively stained with NCX1 specific ribo-probe, whereas neurons within the somatosensory cortical area express mainly NCX2 transcripts. More specifically, the molecular layer of motor cortex, which contains the terminal dendritic field of the pyramidal cells, displays a more intense NCX1 immunoreactivity than that of NCX2, a result consistent with the preferential expression of NCX1 transcripts in neurons that have their cell bodies in layers III and V of this cortical area. In contrast, NCX2 isoform is preferentially expressed

in neurons of layer V and VI of the sensory cortex (Canitano *et al.*, 2002; Papa *et al.*, 2003)

### **2.5.2 Hippocampus**

Within the hippocampus, ribo-probes for all three NCX isoforms showed an intense labeling of most neuronal populations, whereas in immunohistochemistry experiments the hippocampal circuitry components exhibited differential expression of selective NCX isoforms. NCX1 protein expression is particularly intense in the granule cell layer and hilus of dentate gyrus, which represent the terminal field of the perforant pathway, the major excitatory input of the hippocampus, originating from the entorhinal cortex. In addition, neurons within this cortical area display an intense positivity for NCX1 transcripts. Furthermore, both NCX1 and NCX3 antibody intensively label the mossy fiber projections to the CA3 region, whereas CA1 field show mainly NCX3 protein expression. This particular distribution suggests that distinct NCX isoforms may play a crucial role in regulating the intracellular Na<sup>+</sup> and Ca<sup>2+</sup> homeostasis of the major afferent, intrinsic and efferent hippocampal projections. These circuits are crucial for synaptic plasticity phenomena, such as long-term potentiation (LTP) and long-term depression (LTD) (Madison *et al.*, 1991).

### **2.5.3 Cerebellum**

The cerebellum shows the more intense protein expression of all NCX isoforms. In particular, the analysis of the expression of NCX transcripts and proteins in the cerebellum reveals their presence in the afferent projections and in the intrinsic neurons of this crucial brain region (Canitano *et al.*, 2002; Papa *et al.*, 2003). More specifically, NCX1 protein is expressed in the excitatory mossy

fibers that originate in the extracerebellar structures and that branch off to the granule cell layer, a site where the glomerular structure is formed by the mossy fiber terminals, the granule cell dendrites, and the Golgi cell axons (Canitano *et al.*, 2002; Papa *et al.*, 2003). This distribution is consistent with functional studies performed on cerebellar granule cells, suggesting that  $[Ca^{2+}]_i$  increase induced by glutamate may occur through the NCX operating in the reverse mode (Kiedrowski *et al.*, 1994).

## 2.6 NCX functions in healthy brain

NCX protein plays important functions in different neurophysiological conditions. In particular, the level of NCX expression in neurons is particularly high in the sites where a large movement of  $Ca^{2+}$  ions occurs across the plasma membrane. This is what happens at synaptic level (Juhaszova *et al.*, 1996; Canitano *et al.*, 2002) where, during an action potential or after a glutamate-activated channel activity,  $Ca^{2+}$  ions massively enter the plasma membrane. This phenomenon leads to the fusion of synaptic vesicles with the plasma membrane thus promoting neurotransmitter exocytosis. After this event, outward  $K^+$  currents provide plasma membrane repolarization, thus triggering voltage-gated  $Ca^{2+}$  channels closure. According to the principle of diffusion,  $Ca^{2+}$  ions are distributed in the cytosolic compartments, reversibly interacting with  $Ca^{2+}$ -binding proteins. Residual  $Ca^{2+}$  ions are rapidly extruded by the plasma membrane  $Ca^{2+}$  ATPase (PMCA) (Tolosa de Talamoni *et al.*, 1995) and by NCX (Sanchez-Armass and Blaustein, 1987; Reuter and Porzig, 1995).

These two pathway have complementary characteristics. In fact, while NCX has a relatively low affinity for cytosolic calcium (dissociation constant  $K_d \sim 0,6-2$  mM)

and a relatively high transport ('turnover') ( $\gg 1000\text{-}5000\text{ Hz}$ ), the PMCA has a higher affinity for calcium ( $K_d \sim 0,1\text{ mM}$ ) but lower turnover ( $\sim 150\text{ Hz}$ ) (Reeves and Hale, 1984; Niggli and Lederer, 1993). For these reasons, NCX is well suited for rapid recovery from high levels of  $[\text{Ca}^{2+}]_i$ , while PMCA is of crucial importance in the establishment of submicromolar resting  $[\text{Ca}^{2+}]_i$  (Penniston *et al.*, 1997; Yamoah *et al.*, 1998).

In particular, NCX becomes the dominant  $\text{Ca}^{2+}$  extrusion mechanism when a train of action potentials reaches the nerve terminals and the  $[\text{Ca}^{2+}]_i$  exceeds the value of  $500\text{ nM}$ . In fact, it has been calculated that for these  $[\text{Ca}^{2+}]_i$  values, more than 60% of  $\text{Ca}^{2+}$  extrusion is mediated by NCX families. This experimental evidence agrees with localization studies showing that NCX and PMCA have a differential localization in nerve terminal. In particular, Juhaszova *et al.* in 2000 suggested that, while the PMCA may be located near the active zones, at the sites of neurotransmitter vesicles release, NCX does not. Moreover, it has been suggested that a particularly favourable location for NCX would be in the domains of PM that are closely associated with the specialized PM-ER junctions, as appears to be in neuronal cell bodies (Juhaszova *et al.*, 1996). Indeed, Blaustein in 1993 first proposed that the most important role for NCX may be in regulating ER  $\text{Ca}^{2+}$  content, more specifically, in mediating  $\text{Ca}^{2+}$  sequestration in the ER in order to counteract excessive  $[\text{Ca}^{2+}]_i$  increases (Blaustein, 1993).

Notably, Reuter and Porzig in 1995 provided evidence that NCX contributes to reduction of  $[\text{Ca}^{2+}]_i$  after excitation in dendritic boutons of hippocampal neurons. In addition, Bouron and Reuter in 1996 hypothesized NCX involvement in  $\text{Na}^+$ -mediated increase in neurotransmitter release from nerve terminal. In fact, after a  $\text{Na}^+$  load, they observed increased  $[\text{Ca}^{2+}]_i$  and accelerated turnover rate of the vesicular pools in presynaptic boutons, and that both the effects were prevented

by TTX and enhanced by ouabain (Bouron and Reuter, 1996). These results suggested that NCX could be involved in Na<sup>+</sup>-induced Ca<sup>2+</sup> increase by operating in the reverse mode.

## **2.7 NCX involvement in CNS diseases**

As a pivotal player in the maintaining Na<sup>+</sup> and Ca<sup>2+</sup> homeostasis in excitable cells, NCX is involved in many pathophysiological conditions and diseases in which an imbalance of [Ca<sup>2+</sup>]<sub>i</sub> and/or [Na<sup>+</sup>]<sub>i</sub> occurs. Since NCX plays a central role in muscle cells, particularly in regulating Ca<sup>2+</sup> balance during excitation-contraction coupling, it is involved in cardio-vascular diseases, including heart failure, arrhythmias and hypertension, but also in skeletal muscle diseases. Moreover, several lines of studies highlight the involvement of NCX in CNS disorders, such as stroke and many neurodegenerative diseases.

### **2.7.1 Stroke**

Stroke may be a very traumatic event for healthy brain, since it induces a rapid cell death in the core of the injured region and triggers several mechanisms in surrounding *penumbra* area, including dysregulation of intracellular ionic homeostasis and ROS production (Donnan *et al.*, 2008). In particular, a progressive increase in [Na<sup>+</sup>]<sub>i</sub> is a critical factor in determining neuronal death during cerebral ischemia, because it leads to cell swelling and microtubular disorganization, thereby leading to cell necrosis. In addition, also dysregulation of Ca<sup>2+</sup>, K<sup>+</sup>, and H<sup>+</sup> ions may trigger several death pathways, including oxidative stress, mitochondrial dysfunction and apoptosis (Annunziato *et al.*, 2007a;

2007b). Additionally, a large amount of papers showed that the increase of extracellular glutamate concentrations during acute brain injury triggers an influx of  $\text{Ca}^{2+}$  and  $\text{Na}^+$  ions into neurons (Olney, 1973), thus leading, according to the glutamate excitotoxicity paradigm, to neuronal cell death.

Several *in vitro* and *in vivo* models of hypoxia-anoxia highlighted the involvement of NCX in neuronal and glial injury after stroke. In particular, it has been demonstrated that, after pMCAO, all three NCX transcripts are down-regulated by 90% in the ischemic core, although NCX2 reduction occurs earlier (Boscia *et al.*, 2006). By contrast, in other brain regions belonging to the peri-infarct zone, NCX1 and NCX3 mRNAs display an up-regulation, whereas NCX2 mRNA is decreased (Boscia *et al.*, 2006).

Moreover, *in vitro* models of hypoxia showed that NCX3 more significantly contributes to the maintenance of  $[\text{Ca}^{2+}]_i$  homeostasis than NCX1 and NCX2. In fact, unlike NCX1 and NCX2, NCX3 is capable of preventing  $\text{Ca}^{2+}$  overload induced by hypoxia plus reoxygenation, thanks to its ability to work in the forward mode in presence of reduced ATP levels (Secondo *et al.*, 2007; Condrescu *et al.*, 1995).

### **2.7.2 Multiple sclerosis**

Multiple sclerosis (MS) is an inflammatory demyelinating disease of the CNS. MS clinical manifestations result from an aberrant immune response induced by both environmental factors and predisposing genetic factors. In MS, blood-circulating effector T cells infiltrate into the CNS and attack the myelin-forming cells, or oligodendrocytes. This aberrant immune attack leads to demyelination, thus compromising the saltatory conduction along the axon, and, ultimately, causing neurodegeneration. For these reasons, MS patients exhibit a number of

debilitating symptoms, including motor, sensory, and cognitive deficits (Compston and Coles, 2008; Milo and Kahana, 2010; Zozulya and Wiendl, 2008). Currently, an important therapeutic goal is to promote remyelination by boosting endogenous oligodendrocytes precursor cells (OPC), before axons are irreversibly damaged.

It has been recently demonstrated that axonal pathology underlies the development of non-remitting deficits in MS (Davie *et al.*, 1995; Ganter *et al.*, 1999; Bjartmar *et al.*, 2000; Lovas *et al.*, 2000; Wujek *et al.*, 2002), although the mechanisms leading to axonal degeneration are not completely known. Imaizumi *et al.* in 1998 provided evidence that sodium channels and NCX are involved in axonal degeneration of spinal cord dorsal columns exposed to anoxia (Imaizumi *et al.*, 1998). In addition, Craner and colleagues in 2003 provided evidence that the number of axons displaying a diffuse expression of Nav channels increases in the spinal cord of mice with autoimmune encephalomyelitis (EAE) and that here they are co-localized with NCX, suggesting that this co-incident distribution of Nav channels and NCX along demyelinated axons may contribute to the development of axonal degeneration in EAE (Craner *et al.*, 2003). Furthermore, it has been speculated that increased sodium influx into injured axons induces NCX to work in the reverse mode thus leading to the accumulation of intra-axonal calcium (Stys *et al.*, 1991, 1992; Stys and Lopachin, 1998).

The involvement of NCX in pathophysiology of EAE has been confirmed by Casamassa *et al.* in 2016 in myelin oligodendrocyte glycoprotein (MOG)-induced EAE, an animal model of MS. In fact, they showed that mice lacking *ncx3* gene displayed increased susceptibility and more severe symptomatology after MOG-induced EAE. Moreover, ablation of *ncx3* gene in these mice not only induced and exacerbated development of EAE, but was also accompanied by a

significant reduction in OPCs and premyelinating cells in the spinal cord during the chronic stage. This finding is in accordance with several studies indicating that NCX3 is a protein component of the myelin membrane (Gopalakrishnan *et al.*, 2013) and that NCX-mediated calcium signaling plays an important role during oligodendrocyte development (Boscia *et al.*, 2012; 2013). Altogether, these observations suggest that NCX3 play a role in oligodendrocyte response after MOG-induced demyelination.

### **2.7.3 Alzheimer's disease**

According to the amyloid cascade hypothesis, the neurotoxicity exerted by A $\beta$  protein is intimately correlated with a dysregulation of ionic homeostasis. In particular, the 'calcium hypothesis' of AD proposes that the amyloidogenic pathway contributes to the remodeling of Ca<sup>2+</sup> signaling responsible for cognitive dysfunction. In fact, several studies showed that alterations in Ca<sup>2+</sup> signaling, often detected as changes in intraneuronal calcium concentrations, occur early in the disease and correlate with synaptic degeneration and subsequent cognitive deficits (DeKosky *et al.*, 1996). In addition, together with Ca<sup>2+</sup> disruption, A $\beta$  is also able to induce a dysregulation of sodium homeostasis by triggering an aberrant increase of inward currents through Nav channels. Despite the mechanisms underlying the A $\beta$ -induced Ca<sup>2+</sup> alteration are not completely known, it is clear that some of these mechanisms involve complex interaction between Ca<sup>2+</sup> binding proteins, Ca<sup>2+</sup> sequestering organelles and Ca<sup>2+</sup> transport proteins. Since NCX play a fundamental role in buffering intracellular Ca<sup>2+</sup> and Na<sup>+</sup> overload occurring under physiological and pathophysiological conditions (Condrescu *et al.*, 1995; Secondo *et al.*, 2007), some researchers decided to investigate the involvement of NCX in AD pathogenesis.

Colvin *et al.* in 1991 first assessed NCX activity in cerebral plasma membrane vesicles purified from human *post mortem* AD brains. In particular, they reported an increased NCX activity of surviving neurons in brain areas affected by neurodegeneration. According to their observations, neuronal cells with increased NCX activity were more likely to survive  $\text{Ca}^{2+}$  disruption and subsequent neurodegenerative processes occurring in AD. Moreover, they suggested that the increase in NCX activity could result from the modulation of specific NCX isoforms (Colvin *et al.*, 1991). However, they were unable to further investigate their hypothesis because of the lack of NCX isotype-specific antibodies. Since then, NCX1, NCX2 and NCX3 have been identified and the generation of isoform-specific antibodies has allowed later investigators to study their specific expression in several AD experimental models. Among these, Sokolow *et al.* in 2011 demonstrated that selective changes in the pattern of NCX1-3 protein expression occur in synaptosomes from AD patients. Indeed, since several studies of synapses in AD patients and animal models suggest that synapses are the primary sites of  $\text{Ca}^{2+}$  dysregulation in AD (Mattson and Chan, 2003; Kuchibhotla *et al.*, 2008),  $\text{Ca}^{2+}$  transport systems, such as NCX, become of crucial importance at synaptic level where elevated  $[\text{Ca}^{2+}]_i$  lead to cell demise. In particular, the results provided by Sokolow *et al.* demonstrated that a selective regulation of NCX1, NCX2 and NCX3 isoforms occurs in AD cortex. More specifically, they observed a reduction of NCX3 protein expression in the parietal cortex of AD patients and, interestingly, an up-regulation of NCX2 levels, maybe as result of a compensatory mechanism to balance the loss of NCX3 expression. Additionally, they demonstrated the co-localization of NCX1, NCX2 and NCX3 with  $\text{A}\beta$  protein. Recently, important evidence about NCX role IN AD pathogenesis has been provided by Pannaccione *et al.* in 2012, who investigated

the mechanisms underlying the effects of A $\beta$ <sub>1-42</sub> on NCX activity in NGF-differentiated PC12 cells and primary hippocampal neurons. In particular, they observed a significant up-regulation of NCX activity in the reverse mode of operation after A $\beta$ <sub>1-42</sub> exposure in both the experimental models. Interestingly, NCX3 was the only NCX isoform displaying an increased activity. Moreover, according to the authors, this up-regulation of NCX currents was due to the over-expression of a hyperfunctional proteolytic fragment of NCX3 (pNCX3), generated by calpain, a Ca<sup>2+</sup>-activated proteolytic enzyme. In fact, the selective calpain inhibitor calpeptin completely prevented both the generation of pNCX3 and the up-regulation of NCX currents in the reverse mode. Importantly, the increased activity of pNCX3 during the early phases of A $\beta$ <sub>1-42</sub> insult resulted in Ca<sup>2+</sup> accumulation into the ER, a particular mechanism aimed to prevent ER stress and caspase-12 activation. Indeed, alterations in ER Ca<sup>2+</sup> homeostasis play an important role in A $\beta$ <sub>1-42</sub>-induced neurodegenerative processes and may represent a trigger for apoptotic neuronal death.

Although further investigation is needed, it can be said that NCX could be a relevant player in A $\beta$ <sub>1-42</sub>-induced neurodegeneration. In fact, albeit few, these observations highlight the crucial role of NCX in responding to the abnormal Ca<sup>2+</sup> signaling occurring in AD.

# **AIMS OF THE STUDY**

## Aims of the study

Starting on these promises, the present study has been aimed to investigate the involvement of NCX in a mouse model of AD, the Tg2576 mice. In fact, this animal model is characterized by a progressive accumulation of A $\beta$  thus allowing to deeply study the effects of amyloid protein aggregation and deposition in both early and late stages of AD pathology. In particular, we wanted to study the mechanisms underlying the A $\beta$ -induced dysregulation of neuronal ionic homeostasis in AD and to assess the NCX behavior profile in A $\beta$  pathology, as NCX is a crucial player in regulating intraneuronal Ca<sup>2+</sup> and Na<sup>+</sup> concentrations. Furthermore, a recent genetic study (Saad *et al.*, 2015) corroborated the hypothesis suggested by Pannaccione *et al.* in 2012 that the NCX isoform 3 is specifically involved in ionic dysregulation induced by the neurotoxic peptide A $\beta$ <sub>1-42</sub>. Indeed, Saad *et al.* identified several genes in which variations may affect the age at onset (AAO) of FAD. Among them, multiple rare variants in SLC8A3 have been found to be associated with the AAO of AD. Since this evidence suggests that NCX3 may play a functional role in modifying the AAO of AD, we first evaluated the possible involvement of NCX isoform 3 in Tg2576 AD pathology. However, it has been widely accepted that intraneuronal accumulation of A $\beta$  is involved in synaptic dysfunction and cognitive deficits even before plaques formation, and specially, that soluble intraneuronal A $\beta$  oligomers, rather than A $\beta$  plaques, are the critical neurotoxic entity in AD pathogenesis. Starting from this assumption, we focused our attention on the early and more advanced, but 'pre-plaque' stages of AD in Tg2576 mice, as they display very early neuronal hyperexcitability and cognitive dysfunction. We both conducted anatomical studies in Tg2576 brains and performed *in vitro* experiments in Tg2576 hippocampal neurons. Importantly, Takahashi *et al.* in 2004 demonstrated that

primary neurons from Tg2576 mice recapitulate the *in vivo* localization and accumulation of A $\beta$ <sub>1-42</sub> with time in culture and, moreover, that intraneuronal accumulation and oligomerization of A $\beta$ <sub>1-42</sub> are associated with synaptic destruction. In conclusion, the present study has been aimed to:

1. measure NCX currents in primary hippocampal neurons from Tg2576 mice at different time in culture
2. assess NCX3 protein expression in Tg2576 primary hippocampal neurons at different time in culture
3. measure intracellular [Ca<sup>2+</sup>] and [Na<sup>+</sup>] in Tg2576 primary hippocampal neurons at different time in culture
4. investigate the role of NCX3 in ER Ca<sup>2+</sup> refilling
5. determine the protein expression profile of NCX3 in the hippocampus, cerebral cortex and cerebellum of 3-month-old and 8-month-old Tg2576 mice

# **MATERIALS AND METHODS**

### 3.1 Drugs and chemicals

Poly(D)-lysine Hydrobromide Mol Wt 30,000-70,000 (P7280), Poly(D)-lysine Hydrobromide Mol Wt >300,000 (P7405), Poly-L-lysine hydrochloride (P2658), Cytosine  $\beta$ -D-arabinofuranoside (Ara-C), Nimodipine, Bovine Serum Albumin (BSA), Proteinase K from *Tritirachium album*, TRI Reagent Solution, mouse monoclonal anti- $\alpha$ -Tubulin as well as all other materials for solution preparation, were from Sigma Aldrich (Milan, Italy). Tetrodotoxin (TTX), rabbit polyclonal anti-NCX3, rabbit polyclonal anti-NCX1 antibodies were from Alomone Labs (Jerusalem, Israel). Hanks' Balanced Salt Solution (HBSS), Minimum Essential Medium (MEM), Opti-MEM I Reduced Serum Medium, Horse Serum (HS), Fetal Bovine Serum (FBS), L-glutamine, Penicillin-Streptomycin, Trypsin-EDTA (0.05%), Phosphate-Buffered Saline (PBS), Lipofectamine 2000, Lipofectamine 3000 were purchased from Thermo Fischer (Massachusetts, USA), Invitrogen (California, USA). Rabbit polyclonal anti-caspase 12, rabbit polyclonal anti-GRP78, and rabbit monoclonal anti-A $\beta$  (17-42) antibodies were purchased from Cell Signaling (Massachusetts, USA). Rabbit monoclonal anti-Calpain 1 was purchased from abcam (Cambridge, UK). Polyclonal anti-NCX3 was provided by Dr. KD Philipson and Dr. DA Nicoll (Los Angeles, CA).

### 3.2 Mice

Animals were kept under standard conditions of temperature, humidity and light, and were supplied with standard food and water *ad libitum*. Animals were handled in accordance with the recommendations of International Guidelines for Animal Research and the experimental protocol was approved by the Animal Care and Use Committee of "Federico II" University of Naples. All efforts were

made to minimize animal suffering and to reduce the number of animal used. Heterozygous male Tg2576 mice and WT littermates, obtained backcrossing male Tg2576 mice with F1 WT female, were used for all experiments. Tg2576 mice, purchased from commercial source [B6;SJL-Tg(APP<sup>SWE</sup>)2576Kha, model 1349, Taconic, Hudson, NY], are well-established AD-related mouse model carrying the human APP Swedish 670/671 mutation (K670N e M671L; Hsiao *et al.*, 1996). F1 WT female (B6;SJL) littermates were obtained crossing female C57BL/6 with male SJL; C57BL/6 and SJL mice were purchased from Charles River.

### **3.2.1 Genotyping: PCR analysis**

Genomic DNA from mouse tails was isolated with salt precipitation method. Tails after the cut were incubated with tail digestion buffer (50 mM Tris-HCl pH 8.0, 100 mM EDTA pH 8.0, 100 mM NaCl, 1% SDS) supplemented with Proteinase K (Sigma Aldrich, Milan, Italy) at a final concentration of 0.5 mg/ml and placed in water bath at 55-60°C overnight with mixing. This step should result in the complete solubilization of the tail fragment. Embryonic brain tissue was kept during cerebral dissection and frozen immediately upon collection. After thawing, we added TRI Reagent to each sample in order to homogenize the tissue. Subsequently one volume of phenol:chloroform:isoamyl alcohol (25:24:1) was added to each sample. After centrifugation, the mixture separated into 3 phases: an aqueous phase containing the RNA, the interphase containing DNA, and an organic phase containing proteins. We discarded and collected the interphase in a new centrifuge tube for each sample. After we proceeded to DNA precipitation with 100% ethanol; we centrifuged the sample at 4°C for 30 minutes at 16,000 × g to pellet the DNA. Carefully we remove the supernatant without disturbing the

DNA pellet; after we added 70% ethanol and centrifuged each sample at 4°C for 2 minutes at 16,000 × g. We removed as much of the remaining ethanol as possible and we dried the DNA pellet at room temperature for 5–10 minutes. Finally, we resuspended the DNA pellet in TE buffer (Tris-EDTA) by pipetting up and down 30–40 times. DNA concentration and purity of each sample was quantified using Nanodrop Spectrophotometer (Thermo Fisher Scientific, Wilmington, DE, US). We used following primers to amplify the DNA region with human APP Swedish mutation on both types of genomic DNA: 5'-CTGACCACTCGACCAGGTTCTGGGT-3' and 5'GTGGATAACCCCTCCCCAGCCTAGACCA-3' (Primm, Milan, Italy). 50 ng/μL of DNA were used for PCR reaction. The amplification protocol (30 cycles) was the following: 95°C for 45 s, 55°C for 60 s, 72°C for 60 s. Each 25-μL reaction contained: 1U of AmpliTaq DNA Polymerase (Lucigen, US) and 0.5 μM of each primer. The amplification products were visualized on agarose (2%) gel by loading approximately half (10 μL) of each reaction per lane. The band of 466bp indicated the transgenic genotype, whereas its absence indicated the wild type genotype.

### **3.3 Mouse hippocampal neurons**

Primary neuronal cultures were prepared from Tg2576 and WT hippocampi of embryonic day (E). Embryonic age (E) was calculated by considering E0.5 the day when a vaginal plug was detected. Briefly, pregnant animals were anesthetized and sacrificed by cervical dislocation. Hippocampal tissues from embryos were dissected in ice-cold dissecting medium (HBSS supplemented with 27 mM glucose, 20 mM sucrose, 4 mM sodium bicarbonate), centrifuged, and the resulting pellet was mechanically dissociated with a fire polished glass pipette. Cells were resuspended in plating medium consisting in Eagle's MEM

(MEM, Earle's salts, supplied bicarbonate-free) supplemented with 5% FBS, 5% HS, 2 mM L-glutamine, 20 mM glucose, 26 mM bicarbonate, and plated on 35mm culture dishes or onto 25 mm glass coverslips (Glaswarenfabrik Karl Hecht KG, Sondheim, Germany) coated with 100 µg/ml poly(D)-lysine at a density of one embryo hippocampi/1 ml. Three days after plating, non-neuronal cell growth was inhibited by adding 10µM of cytosine AraC. 24 hours after this treatment, the planting medium was replaced by growth medium (Eagle's Minimal Essential Medium with 20 mM glucose, 26 mM NaHCO<sub>3</sub> supplemented with 2mM L-glutamine and 10% HS. Neurons were cultured at 37°C in a humidified 5% CO<sub>2</sub> atmosphere. All the experiments were performed between 8-18 days *in vitro* (DIV).

## **3.4 Electrophysiological recordings**

### **3.4.1 NCX currents**

I<sub>NCX</sub> in hippocampal mouse neurons were recorded by the patch-clamp technique in whole-cell configuration using the commercially available amplifier Axopatch200B and Digidata1322A interface (Molecular Devices), as previously described by Secondo (2009) and Molinaro (2008). I<sub>NCX</sub> were recorded starting from a holding potential of -60 mV up to a short-step depolarization at -60 mV (60 ms). A descending voltage ramp from -60 mV to -120 mV was applied. I<sub>NCX</sub> recorded in the descending portion of the ramp (from -60 mV to -120 mV) were used to plot the current–voltage (*I–V*) relation curve. The I<sub>NCX</sub> magnitude was measured at the end of -60 mV (reverse mode) and at the end of -120 mV (forward mode), respectively. The Ni<sup>2+</sup>- insensitive component was subtracted from total currents to isolate I<sub>NCX</sub>. The neurons were perfused with external

Ringer's solution containing the following (in mM): 126 NaCl, 1.2 NaHPO<sub>4</sub>, 2.4 KCl, 2.4 CaCl<sub>2</sub>, 1.2 MgCl<sub>2</sub>, 10 glucose, and 18 NaHCO<sub>3</sub>, pH7.4. Twenty millimolar tetraethylammonium (TEA), 50 nM TTX, and 10 μM nimodipine were added to Ringer's solution to abolish potassium, sodium, and calcium currents. The dialyzing pipette solution contained the following (in mM): 100 K-gluconate, 10 TEA, 20 NaCl, 1 Mg-ATP, 0.1 CaCl<sub>2</sub>, 2 MgCl<sub>2</sub>, 0.75 EGTA, and 10 HEPES.

Possible changes in cell size were taken into account by measuring, in each cell, the membrane capacitance, which is directly related to membrane surface area, and by expressing the current amplitude data as current densities [picoamperes/picofarads (pA/pF)]. Capacitive currents were elicited by 5-mV depolarizing pulses from -80 mV and acquired at a sampling rate of 50 kHz. The capacitance of the membrane was calculated according to the following equation:  $C_m = \tau_c / \Delta E_m (1 - I_\infty / I_0)$ , where  $C_m$  is membrane capacitance,  $\tau_c$  is the time constant of the membrane capacitance,  $I_0$  is the maximum capacitance current value,  $\Delta E_m$  is the amplitude of the voltage step, and  $I_\infty$  is the amplitude of the steady-state current.

### **3.4.2 Na<sup>+</sup> currents**

Na<sup>+</sup> currents in hippocampal neurons were recorded with the patch-clamp technique in whole-cell configuration using the commercially available amplifier Axopatch 200B and Digidata 1322A interface (Molecular Devices). Currents were filtered at 5 kHz and digitized using a Digidata 1322A interface (Molecular Devices). Data were acquired and analyzed using the pClamp software (version 9.0, Molecular Devices). The pipette solution contained the following (in mM): 140 CsF, 10NaCl, 1 EGTA, and 10 HEPES, pH7.30 (with CsOH), and osmolarity was adjusted to 316 mOsmol/L with dextrose. The extracellular solution

contained the following (in mM): 140 NaCl, 3 KCl, 20 TEA<sub>4</sub>Cl (tetraethylammonium chloride), 1 MgCl<sub>2</sub>, 1 CaCl<sub>2</sub>, 10 HEPES, 5 CsCl, 0.1 CdCl<sub>2</sub>, pH 7.32 (with NaOH), and the osmolarity was 330 mOsmol/L (Gasser *et al.*, 2012). Current recordings were taken using low-resistance electrodes (1.4–2.3 MΩ), sampled at a rate of 100 kHz and filtered at 5 kHz. The cells were held at –120 mV and stepped to a range of potentials (–100 to +30mV in 5mV increments) for 100 ms each (Gasser *et al.*, 2012). Possible changes in cell size occurring after specific treatments were calculated by monitoring the capacitance of each cell membrane, which is directly related to membrane surface area, and by expressing the current amplitude data as current densities (pA/pF). The capacitance of the membrane was calculated according to the following equation:  $C_m = \tau_c \cdot I_o / \Delta E_m (1 - I_\infty / I_o)$ , where  $C_m$  is the membrane capacitance,  $\tau_c$  is the time constant of the membrane capacitance,  $I_o$  is the maximum capacitance current value,  $\Delta E_m$  is the amplitude of the voltage step, and  $I_\infty$  is the amplitude of the steady-state current.

### **3.5 [Ca<sup>2+</sup>]<sub>i</sub> and [Na<sup>+</sup>]<sub>i</sub> measurement**

#### **3.5.1 [Ca<sup>2+</sup>]<sub>i</sub> measurement**

[Ca<sup>2+</sup>]<sub>i</sub> was measured by single cell computer-assisted videoimaging (Secondo *et al.* 2007). Briefly, primary hippocampal neurons, grown on glass coverslips, were loaded with 10μM Fura-2 acetoxymethyl ester (Fura-2AM) (Calbiochem, San Diego, CA, USA) for 30 minutes at 37°C. At the end of the Fura-2AM loading period, the coverslips were placed into a perfusion chamber (Medical System, Co. Greenvale, NY, USA) mounted onto a Zeiss Axiovert 200 microscope (Carl Zeiss, Germany) equipped with a FLUAR 40X oil objective lens. The experiments were

carried out with a digital imaging system composed of MicroMax 512BFT cooled CCD camera (Princeton Instruments, Trenton, NJ, USA), LAMBDA 10-2 filter wheeler (Sutter Instruments, Novato, CA, USA), and Meta-Morph/MetaFluor Imaging System software (Universal Imaging, West Chester, PA, USA). After loading, cells were alternatively illuminated at wavelengths of 340 nm and 380 nm by a Xenon lamp. The emitted light was passed through a 512 nm barrier filter. Fura-2AM fluorescence intensity was measured every 3 seconds. Ratiometric values were automatically converted by the software into  $[Ca^{2+}]_i$  using a preloaded calibration curve obtained in preliminary experiments as previously reported (Grynkiewicz *et al.* 1985). ER  $Ca^{2+}$  content was measured by inducing  $Ca^{2+}$  release from the organelle with the rapid administration of ATP (100  $\mu$ M) + thapsigargin, a selective inhibitor of the sarco(endo)plasmic reticulum  $Ca^{2+}$  ATPase (Tg, 1  $\mu$ M). The amount of  $Ca^{2+}$  extruded in the cytoplasm upon ATP+ Tg measured as  $[Ca^{2+}]_i$  increase, is widely considered as indexes of ER or  $Ca^{2+}$  efflux.

### **3.5.2 $[Na^+]_i$ measurement**

$[Na^+]_i$  was measured by single-cell computer-assisted video-imaging in primary hippocampal neurons from WT and Tg2576 mice loaded with 1,3-benzenedicarboxylic acid,4,4'-[1,4,10-trioxo-7,13-diazacyclopentadecane-7,13-diylbis(5-methoxy-6,12-benzofurandiyl)] bis-, tetrakis [(acetyloxy) methyl] ester (SBFI) at 10  $\mu$ M in the presence of pluronic acid (0.02%) for 1 h at 37°C (Pannaccione *et al.*, 2012). At the end of the SBFI loading period, the coverslips were placed into a perfusion chamber (Medical System) mounted onto a Zeiss Axiovert200 microscope (Carl Zeiss) equipped with a FLUAR 40X oil objective lens. The experiments were carried out with a digital imaging system composed

of MicroMax 512BFT cooled CCD-camera (Princeton Instruments), LAMBDA10-2 filter wheeler (Sutter Instruments), and Meta-Morph/MetaFluor Imaging System software (Universal Imaging). After loading, neurons were alternatively illuminated at wavelengths of 340 and 380 nm by a Xenon lamp. The emitted light was passed through a 512-nm barrier filter. SBF1-fluorescence intensity was measured every 3 seconds.

### **3.6 Western blotting**

To obtain total lysates for immunoblotting analysis, neurons were washed in PBS and collected by gentle scraping in ice-cold RIPA buffer containing in mM: 50 Tris pH 7.4, 100 NaCl, 1 EGTA, 1 PMSF, 1 sodium orthovanadate, 1 NaF, 0.5% NP-40, and 0.2% SDS supplemented with Protease Inhibitor Cocktail II (Roche Diagnostic, Monza, Italy). After sonication and incubation for 1 hour on ice, we centrifuged at 12,000 rpm at 4°C for 30 minutes and collected the supernatants. Mice brain tissues from Tg2576 and WT were homogenized in a glass teflon grinder (10 strokes at 500 rpm in about 1 min) using a lysis buffer containing (in mM): 250 sucrose, 10 KCl, 1.5 MgCl<sub>2</sub>, 1 EDTA, 1 EGTA, 1 dithiothreitol, 20 HEPES, pH 7.5, (Angulo *et al.* 2004) and completed with Protease Inhibitor Cocktail II (Roche Diagnostic, Monza, Italy). Tissue suspensions were then sonicated and incubated for 1 hour on ice. After centrifugation at 12,000 rpm at 4 C for 5 min, the supernatants were collected. The protein content of resulting supernatant was determined using the Bradford reagent. 70 µg of proteins were mixed with a Laemmli sample buffer; then, they are applied and resolved on SDS-PAGE polyacrylamide gels. Following transfer onto nitrocellulose membranes (Hybond-ECL, Amersham Bioscience, UK), non-specific binding sites were blocked by incubation for 2 hrs at 4°C with 5% non-fat dry milk (Bio-

Rad Laboratories, Milan, Italy) in TBS-T buffer; subsequently, incubated with primary antibodies overnight at 4°C. After three 10-min washes with TBS-T, the membranes were incubated 1h with the appropriate secondary antibody. Excessive antibodies were then washed away three times (10 min) with TBS-T. Immunoblots were visualized by enhanced chemiluminescence (ECL) (Amersham-Pharmacia-Biosciences, UK). Films were developed using a standard photographic procedure and the relative levels of immunoreactivity were determined by densitometry using ImageJ Software (NIH, Bethesda, MA, USA). Primary antibodies used were: rabbit polyclonal anti-NCX3 (1:1000, Alomone Labs), polyclonal anti-NCX3 (1:4000, provided by Dr. KD Philipson and Dr. DA Nicoll, Los Angeles, CA), polyclonal anti  $\beta$ -Amyloid (D54D2) XP rabbit mAb (1:1000 Cell Signaling), rabbit polyclonal anti-caspase-12 (1:1000, Cell Signaling), rabbit polyclonal anti-GRP78 (1:1000, Cell Signaling), rabbit monoclonal anti-calpain 1 (1:1000, abcam), mouse monoclonal anti- $\alpha$ -Tubulin (1:3000; Sigma Aldrich). Immunoreactive bands were detected using the chemiluminescence system (Amersham-Pharmacia-Biosciences, UK). Proteins were visualized with peroxidase-conjugated secondary antibodies, using the enhanced chemiluminescence system (Amersham-Pharmacia Biosciences LTD, Uppsala, Sweden). The software Image J (NIH) was used for densitometric analysis.

### **3.7 Immunohistochemistry**

Immunostaining and confocal immunofluorescence procedures in tissue sections were performed as previously described (Boscia *et al.*, 2013). In brief, WT and Tg2576 mice were euthanized at 3 and 8 months. Anesthesia was induced with 4% sevoflurane in a mixture of 60% N<sub>2</sub>O and 36% O<sub>2</sub> and maintained during

intracardiac perfusion with 2% sevoflurane in a mixture of 60% N<sub>2</sub>O and 38% O<sub>2</sub>. Transcardial perfusion was carried out with 4% paraformaldehyde in PBS. The brains were sectioned coronally and sagittally (60 µm) on a vibratome. After blocking with Rodent M block (Biocare Medical, Concord, USA), sections were incubated with the following primary antibodies: polyclonal anti-NCX3 (1:500, provided by Dr. KD Philipson and Dr. DA Nicoll, Los Angeles, CA); fluorescent DNA-binding dye Hoechst-33258 (1 µg/ml, Sigma, Milan, Italy) for nuclear staining.

### **3.8 RNA silencing**

The mammalian expression vector pSUPER.retro.puro (OligoEngine) was used to express siRNA against NCX3 and its mismatch sequence in neurons. This vectors was prepared as previously reported (Secondo *et al.*, 2007). After 15 h plating, neurons were transfected with pSUPER-NCX3, pSUPER-mismatch sequence by Lipofectamine 2000 (Invitrogen) standard protocol.

### **3.9 Statistical analysis**

Statistical analysis was performed with GraphPad Prism 5.0 (Graphpad software, Inc., San Diego, CA), using ANOVA followed by Newman-Keuls or Bonferroni, to compare more than two groups, and Student's t test to compare two groups. Data were analysed and presented as mean ± SEM, and P values of <0,05 were accepted as statistically significant.

# RESULTS

## 4.1 A $\beta$ accumulation and oligomerization in hippocampal neurons from Tg2576 mice

Several evidence demonstrated that Tg2576 primary neurons *in vitro* display intracellular A $\beta$ <sub>1-42</sub> accumulation. In particular, Takahashi *et al.* in 2004 provided evidence that A $\beta$ <sub>1-42</sub> accumulating within processes aggregates as oligomeric A $\beta$ <sub>1-42</sub> in Tg2576 cortical neurons with time in culture as well as in aging Tg2576 mouse brain. Furthermore, they highlighted the critical role of soluble, low weight, A $\beta$ <sub>1-42</sub> intracellular aggregates in synaptic disruption. For this reason, we first assessed the presence of A $\beta$ <sub>1-42</sub> oligomers in our primary cultures of Tg2576 hippocampal neurons by western blot experiments. In particular, we detected A $\beta$ <sub>1-42</sub> trimers in Tg2576 hippocampal neurons after 12 DIV (**Fig. 6, Panel A**), whereas no A $\beta$ <sub>1-42</sub> oligomers have been found, as expected, in WT neurons. Moreover, soluble A $\beta$ <sub>1-42</sub> monomers have been detected in culture medium of the same Tg2576 neurons (**Fig. 6, Panel B**), thus confirming that A $\beta$ <sub>1-42</sub> is secreted from these neurons. These results demonstrated that hippocampal neurons from Tg2576 mice, like Tg2576 cortical neurons, are a useful *in vitro* model since they can provide evidence about the effects of endogenous A $\beta$ <sub>1-42</sub> oligomers and recapitulate the *in vivo* A $\beta$  pathology better than *in vitro* models of A $\beta$  treatment.

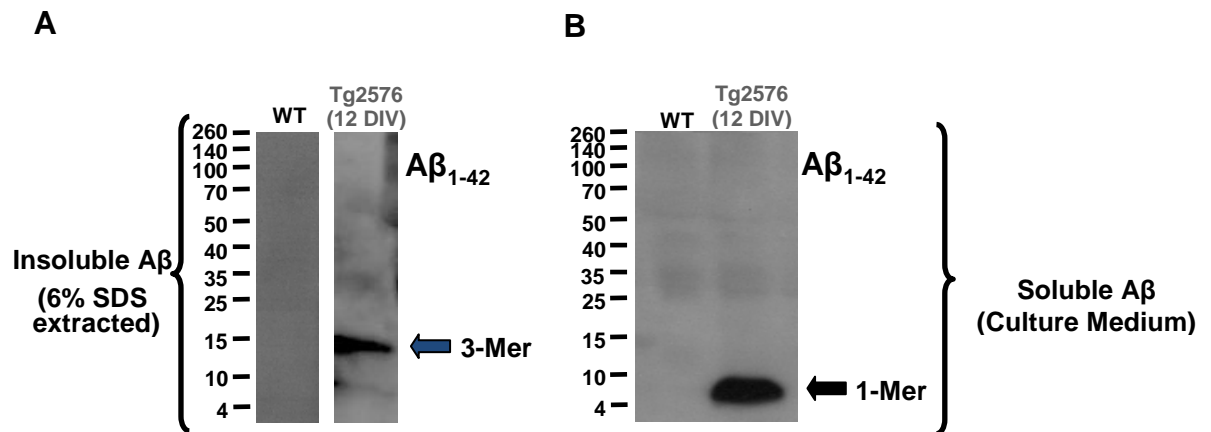


**Figure 6. Aβ accumulation and oligomerization in hippocampal neurons from Tg2576 mice. (A)** Representative Western blot of Aβ<sub>1-42</sub> intracellular deposition in primary Tg2576 hippocampal neurons at 12 DIV compared to WT. Neurons were lysed in 6% SDS containing 10 μl/ml of β-mercaptoethanol, sonicated, and then heated at 95°C for 6 min to extract insoluble intraneuronal Aβ<sub>1-42</sub>. **(B)** Representative Western blot of soluble Aβ<sub>1-42</sub> detected in the culture medium of Tg2576 hippocampal neurons at 12 DIV compared to WT.

## 4.2 NCX activity in Tg2576 hippocampal neurons

Several evidence showed that NCX activity is modulated during AD pathology. In particular, Pannaccione *et al.* in 2012 demonstrated that NCX currents ( $I_{NCX}$ ) in the reverse mode of operation were up-regulated in hippocampal neurons exposed to 5 $\mu$ M of A $\beta$ <sub>1-42</sub> oligomers for 24 hours. For this reason, we decided to record  $I_{NCX}$  in hippocampal neurons from Tg2576 mice, as they display a progressive deposition of A $\beta$ <sub>1-42</sub> oligomers with time in culture.

$I_{NCX}$  were assessed in the reverse and forward modes of operation by patch-clamp in whole-cell configuration in both WT and Tg2576 hippocampal neurons. We observed a significant increase of  $I_{NCX}$  only in the reverse mode in Tg2576 hippocampal neurons compared to WT, whereas no modulation was observed in the forward mode (**Fig. 7, Panel A and B**). In particular,  $I_{NCX}$  up-regulation in Tg2576 hippocampal neurons seemed to be correlated with time in culture. In fact, Tg2576 hippocampal neurons at 12 DIV displayed a more pronounced increase of  $I_{NCX}$  compared to 8 DIV, whereas no differences were observed in WT neurons between 8 and 12 DIV. However, as revealed by western blot analyses, the up-regulation of  $I_{NCX}$  was not accompanied by a significant increase of NCX3 protein expression in both 8 and 12 DIV Tg2576 hippocampal neurons (**Fig. 7, Panel C**).

Interestingly, after 12 DIV, WT neurons also displayed a progressive increase of  $I_{NCX}$ . Nevertheless, also in these “old” neurons, we observed a persistent up-regulation of  $I_{NCX}$  in Tg2576 hippocampal neurons compared to WT, up to 18 DIV (**Fig. 7, Panel D and E**).

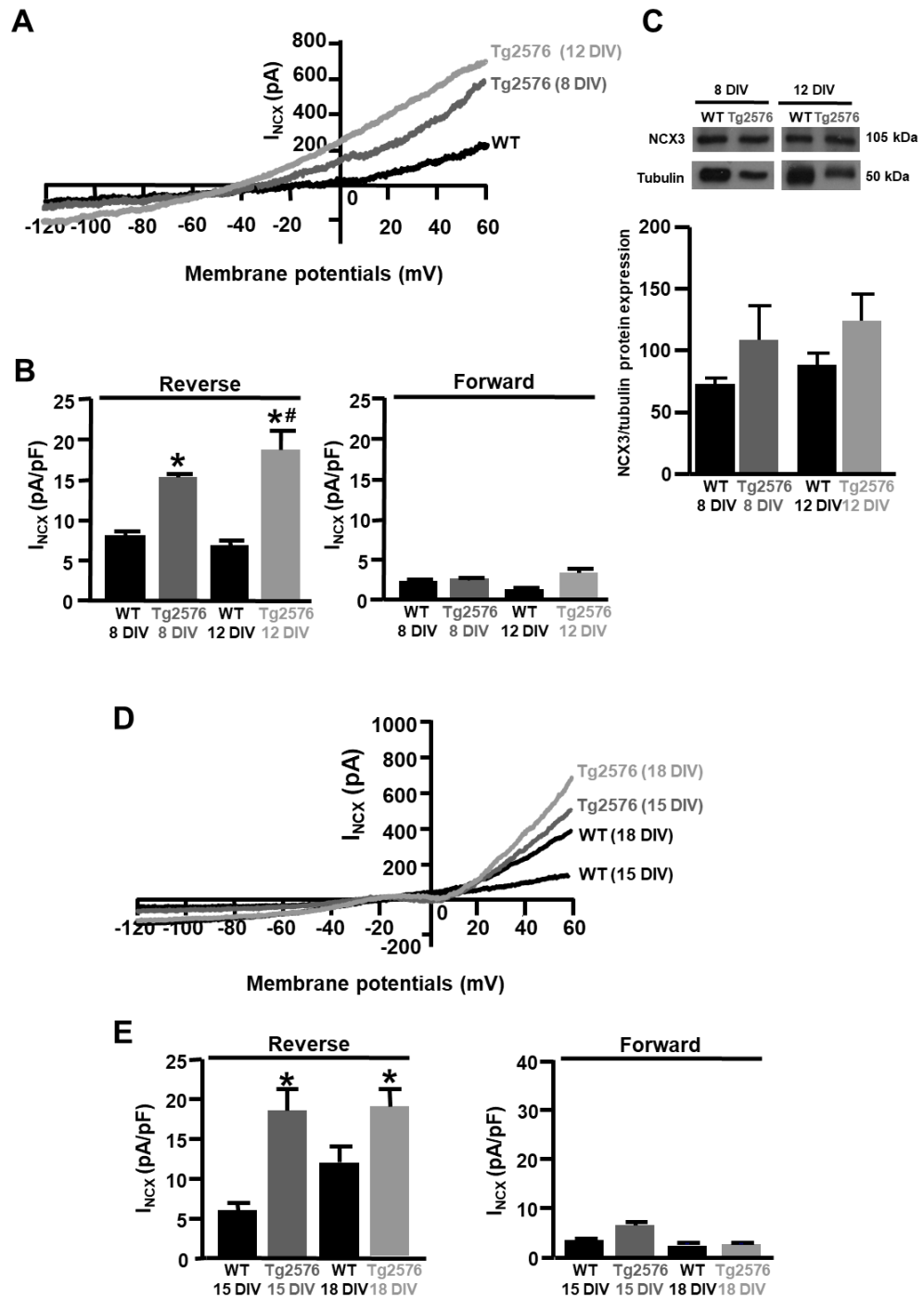


**Figure 7. NCX activity in Tg2576 hippocampal neurons.** (A) Representative  $I_{NCX}$  current traces recorded from primary WT hippocampal neurons (black trace) and from primary Tg2576 hippocampal neurons at 8 and 12 DIV (grey traces). (B) Quantification of  $I_{NCX}$  in the reverse mode of operation (left panel) and in the forward mode of operation (right panel). Values are expressed as mean $\pm$ SEM of current densities of 3 independent experimental sessions ( $n=10$  for each group). (C) Representative Western blot and densitometric quantification of NCX3 protein expression normalized to  $\alpha$ -tubulin levels evaluated in primary WT and Tg2576 hippocampal neurons at 8 and 12 DIV. (D) Representative  $I_{NCX}$  current traces recorded from primary WT hippocampal neurons (black trace) and from primary Tg2576 hippocampal neurons at 15 and 18 DIV (grey traces). (E) Quantification of  $I_{NCX}$  in the reverse mode of operation (left panel) and in the forward mode of operation (right panel) recorded from primary WT and Tg2576 hippocampal neurons at 15 and 18 DIV. Values are expressed as mean $\pm$ SEM of current densities of 3 independent experimental sessions ( $n=10$  for each group). \* $p \leq 0.05$  versus their respective WT, #  $p \leq 0.05$  versus Tg2576 at 8 DIV (Student's *t* test and ANOVA followed by Bonferroni).

### **4.3 Effect of NCX3 silencing on $I_{NCX}$ up-regulation in Tg2576 hippocampal neurons**

Patch-clamp experiments revealed that the silencing of NCX3 completely prevented the up-regulation of  $I_{NCX}$  in the reverse mode of operation in Tg2576 hippocampal neurons. In fact, Tg2576 hippocampal neurons transfected with a specific siRNA against NCX3 at 8 DIV, displayed a marked reduction of  $I_{NCX}$  in the reverse mode compared to those observed in non-transfected Tg2576 hippocampal neurons (**Fig. 8, Panel A and B**). Moreover, the siRNA caused a significant reduction of  $I_{NCX}$  in both the reverse and forward modes of operation in Tg2576 hippocampal neurons compared to WT. The reduction of NCX3 protein expression assessed through western blot confirmed siNCX3 efficacy (**Fig. 8, Panel A**).

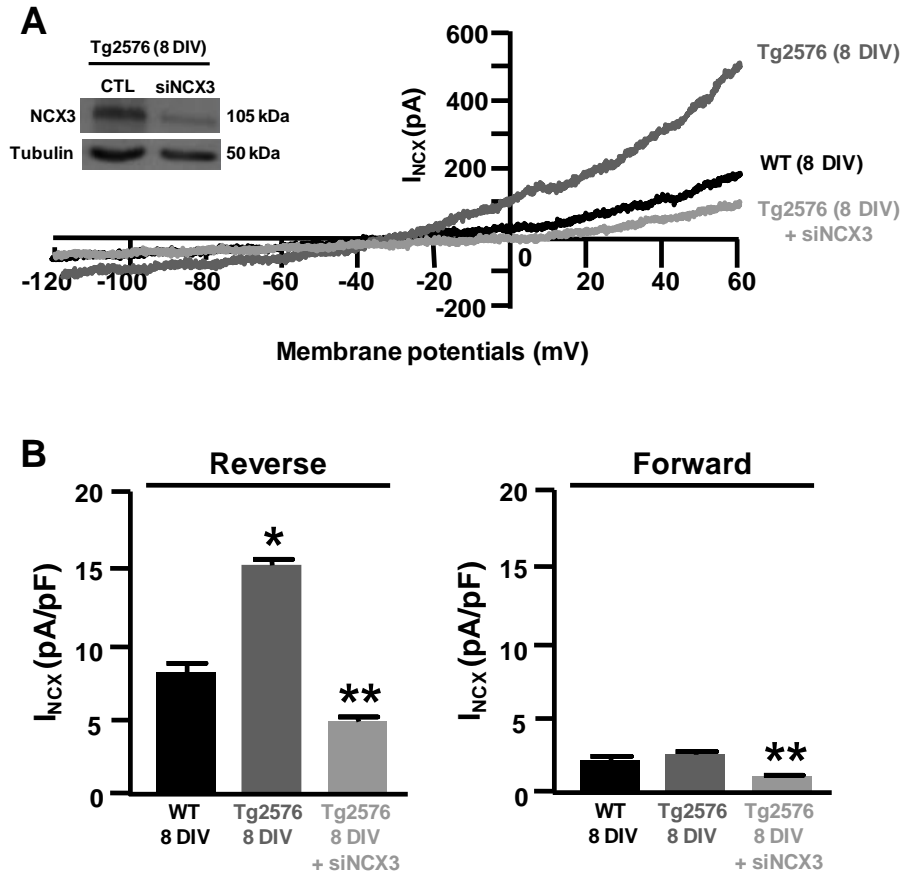


**Figure 8. Effect of NCX3 silencing on INCX up-regulation in Tg2576 hippocampal neurons.** (A) Representative Western blot of NCX3 silencing in primary Tg2576 hippocampal neurons at 8 DIV (top) and representative current traces of INCX recorded from primary WT hippocampal neurons (black trace) and from primary Tg2576 hippocampal neurons at 8 DIV in control condition and plus siNCX3 (grey traces). (B) Quantification of INCX in the reverse mode of operation (left panel) and in the forward mode of operation (right panel). Values are expressed as mean±SEM of current densities of 3 independent experimental sessions ( $n=10$  for each group). \* $p \leq 0.05$  versus their respective WT, \*\* $p \leq 0.05$  versus their respective Tg2576 (Student's t test).

#### **4.4 SBFI- $\text{Na}^+$ detection and $\text{Nav}$ recording in Tg2576 hippocampal neurons**

Since NCX activity is strictly dependent on  $\text{Na}^+$  and  $\text{Ca}^{2+}$  concentrations on the two sides of plasma membrane, we assessed  $[\text{Na}^+]_i$  in Tg2576 hippocampal neurons at 12 DIV, when the first peak of  $I_{\text{NCX}}$  was observed.  $\text{Na}^+$  detection with SBFI probe revealed a significant increase of  $[\text{Na}^+]_i$  in Tg2576 hippocampal neurons compared to WT (**Fig. 9, Panel A**), thus showing that the up-regulation of  $I_{\text{NCX}}$  in the reverse mode of operation was driven by a marked accumulation of  $\text{Na}^+$  into the neurons. To further investigate the dysregulation of intracellular  $\text{Na}^+$ , we also recorded  $\text{Nav}$  currents in Tg2576 hippocampal neurons at 8 and 12 DIV by patch-clamp in whole cell configuration. In particular, we observed a significant increase of  $\text{Nav}$  currents in Tg2576 neurons compared to WT at 8 DIV and, notably, a more pronounced increase at 12 DIV (**Fig. 9, Panel C and D**). Moreover, we observed an over-expression of  $\text{Na}^+$  channel  $\alpha$  subunits in Tg2576 hippocampal neurons at 12 DIV (**Fig. 9, Panel B**). Importantly, the progressive up-regulation of  $\text{Nav}$  currents temporally correlates with the increases of  $I_{\text{NCX}}$  observed in Tg2576 hippocampal neurons (**Fig. 9, Panel E**), thus suggesting that inward currents through  $\text{Nav}$  channels could drive reverse  $\text{Na}^+/\text{Ca}^{2+}$  exchange.

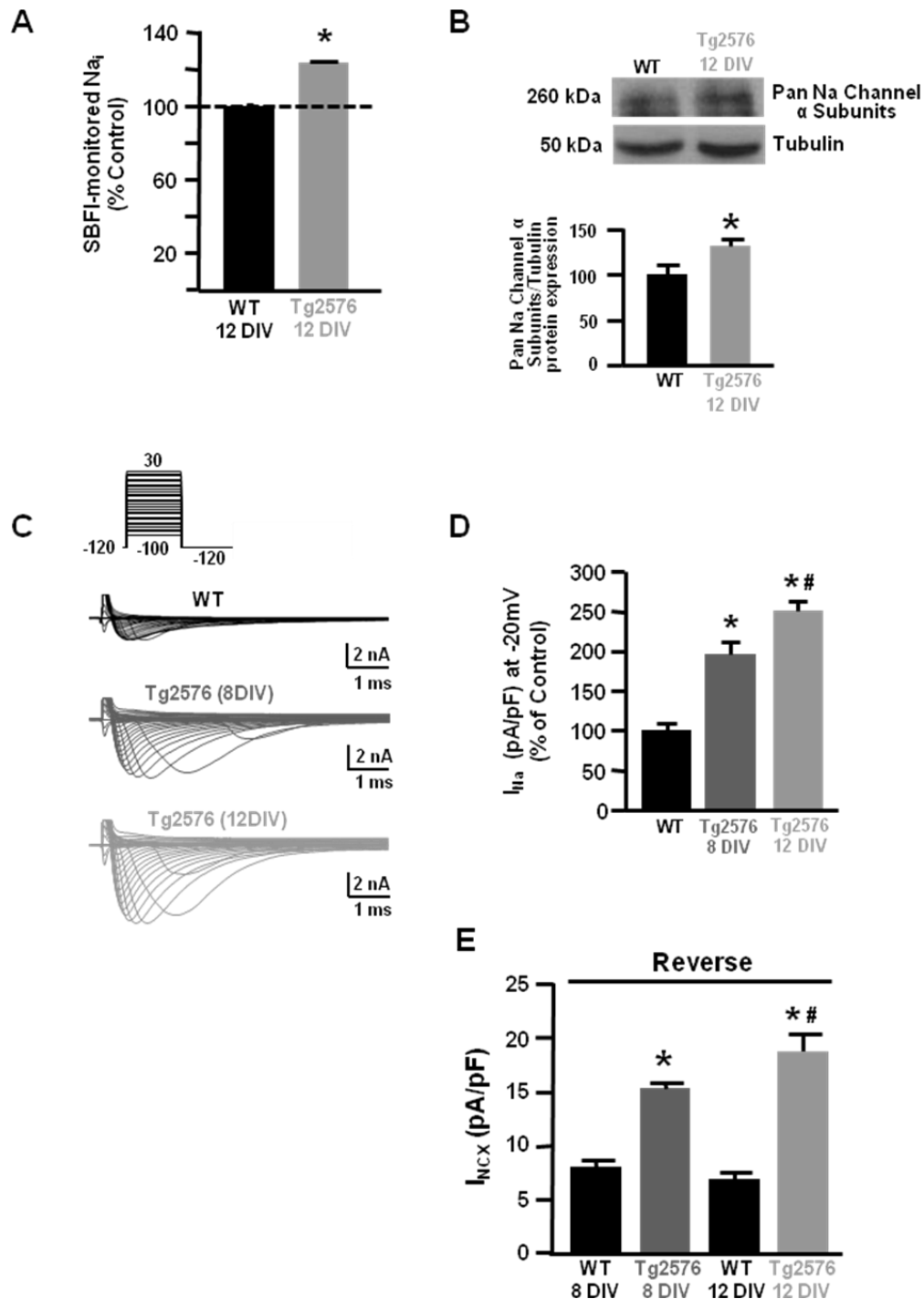


**Figure 9. SBFI- $\text{Na}^+$  detection and  $\text{Na}_v$  recording in Tg2576 hippocampal neurons.** (A) Quantification of  $[\text{Na}^+]_i$  in primary WT and Tg2576 hippocampal neurons at 12 DIV. Values are expressed as percentage mean $\pm$ SEM of 3 independent experimental sessions ( $n=50$  for each experimental group). \* $p<0.05$  versus WT group (Student's t-test). (B) Representative Western blot (top) and densitometric quantification (bottom) of Na channel  $\alpha$ -subunits protein expression normalized to  $\alpha$ -tubulin levels in primary WT and Tg2576 hippocampal neurons at 12 DIV (top) and representative current traces of  $\text{Na}^+$  evoked by the indicated voltage protocol in primary WT and Tg2576 hippocampal neurons at 8 and 12 DIV. (C) Quantification of  $\text{Na}^+$  currents ( $I_{Na}$ ) at -20mV. Values are expressed as percentage mean $\pm$ SEM of 3 independent experimental sessions ( $n=10$  for each group). (D) Quantification of  $I_{NCX}$  in the reverse mode of operation represented in Fig. 7 panel E. Values are expressed as mean $\pm$ SEM of current densities of 3 independent experimental sessions ( $n=10$  for each group). \* $p\leq 0.05$  versus their respective WT, #  $p\leq 0.05$  versus Tg2576 at 8 DIV (Student's t test and ANOVA followed by Bonferroni).



## 4.5 Assessment of $[Ca^{2+}]_i$ and ER $Ca^{2+}$ content in Tg2576 hippocampal neurons

To investigate the implications of  $I_{NCX}$  up-regulation, we assessed both  $[Ca^{2+}]_i$  and ER  $Ca^{2+}$  content in Tg2576 hippocampal neurons. In fact, several lines of evidence showed that NCX activity in the reverse mode of operation is associated with increased  $[Ca^{2+}]_i$  and subsequent calpain activation. Nevertheless, in some experimental conditions reverse  $Na^+/Ca^{2+}$  exchange has been correlated to  $Ca^{2+}$  refilling into ER. Interestingly,  $Ca^{2+}$  detection with FURA-2 AM did not reveal any significant increase of  $[Ca^{2+}]_i$  in Tg2576 hippocampal neurons at 8 and 12 DIV compared to WT, but rather a significant decrease of  $[Ca^{2+}]_i$  in Tg2576 hippocampal neurons at 8 DIV (**Fig. 10, Panel A**). Moreover, western blot experiments showed that no increase in calpain activation occurs in Tg2576 hippocampal neurons compared to WT. In fact, neither autolysed/activated calpain nor the calpain-cleaved spectrin fragment, detectable as a 145 kDa band, were modulated in Tg2576 hippocampal neurons compared to WT (**Fig. 10, Panel B and C**, respectively).

On the other hand, in Tg2576 hippocampal neurons at 8 and 12 DIV, the ER  $Ca^{2+}$  content, determined by using the SERCA inhibitor Tg was significantly higher than that observed in WT neurons (**Fig. 10, Panel D**). This demonstrated that a larger accumulation of  $Ca^{2+}$  in the ER occurs in Tg2576 hippocampal neurons in comparison with WT neurons, thus confirming that the up-regulation of  $I_{NCX}$  in Tg2576 hippocampal neurons is correlated with the  $Ca^{2+}$  refilling into ER, rather than with a cytosolic  $Ca^{2+}$  increase.

In addition, to further investigate the effects of  $A\beta_{1-42}$  oligomers on ER homeostasis in Tg2576 hippocampal neurons, we assessed the activation of ER stress markers by western blot experiments. In particular, we did not detect any

modulation of caspase 12 and GRP78 protein expression (**Fig. 10, Panel E and F**), thus confirming that ER stress does not occur in Tg2576 hippocampal neurons.

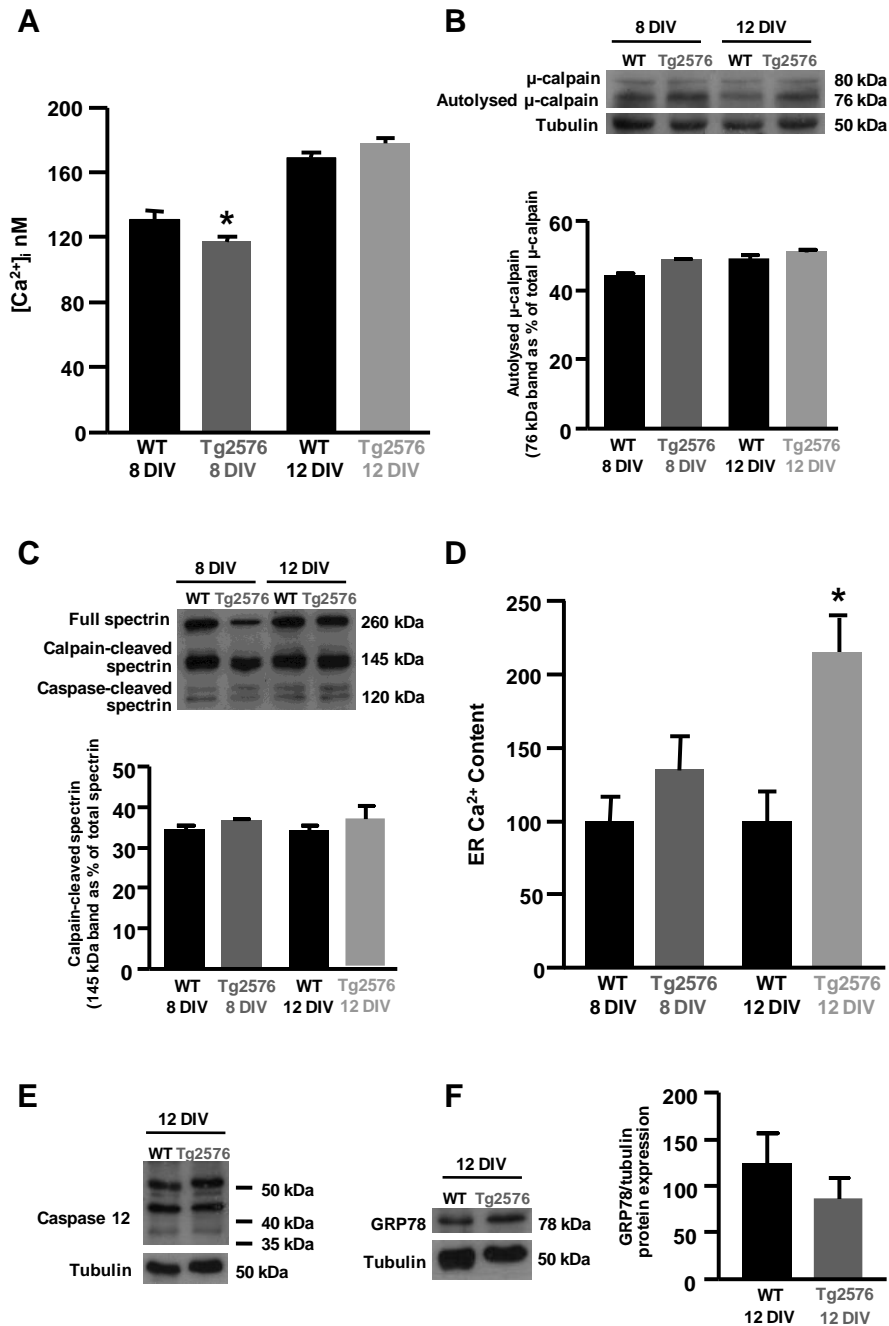


**Figure 10. Assessment of  $[Ca^{2+}]_i$  and ER  $Ca^{2+}$  content in Tg2576 hippocampal neurons.** (A) Quantification of  $[Ca^{2+}]_i$  in primary WT and Tg2576 hippocampal neurons at 8 DIV and 12 DIV. Values are expressed as mean $\pm$ SEM of 3 independent experimental sessions ( $n=50$  for each experimental group). (B) Representative Western blot (top) and densitometric quantification (bottom) of autolysed  $\mu$ -calpain protein expression normalized to  $\alpha$ -tubulin levels in primary WT and Tg2576 hippocampal neurons at 8 DIV and 12 DIV. Values of autolysed  $\mu$ -calpain are expressed as % of total  $\mu$ -calpain. (C) Representative Western blot (top) and densitometric quantification (bottom) of calpain-cleaved spectrin protein expression normalized to  $\alpha$ -tubulin levels in primary WT and Tg2576 hippocampal neurons at 8 DIV and 12 DIV. Values of calpain-cleaved spectrin are expressed as % of total spectrin. (D) Quantification of ER  $Ca^{2+}$  content in primary WT and Tg2576 hippocampal neurons at 8 DIV and 12 DIV. Values are expressed as percentage mean $\pm$ SEM of 3 independent experimental sessions ( $n=50$  for each group). (E) Representative Western blot of caspase 12 protein expression in primary WT and Tg2576 hippocampal neurons at 12 DIV. (F) Representative Western blot (left) and densitometric quantification (right) of GRP78 protein expression normalized to  $\alpha$ -tubulin levels in primary WT and Tg2576 hippocampal neurons at 12 DIV. \* $p \leq 0.05$  versus their respective WT. (Student's t test).

## 4.6 NCX3 protein expression in the hippocampus of 3 and 8-month-old Tg2576 mice

In order to obtain preliminary information about NCX involvement in AD *in vivo* pathology, we decided to determine the NCX3 protein expression profile in brain areas of 3 and 8-month-old Tg2576 mice. We first assessed A $\beta$ <sub>1-42</sub> deposition in the hippocampus of Tg2576 mice by western blot experiments. Notably, with a specific A $\beta$  antibody, we observed trimers deposition in the hippocampus of 3-month-old Tg2576 mice, whereas no A $\beta$ <sub>1-42</sub> deposition has been detected in the hippocampus of WT mice, as expected (**Fig. 11, Panel A**).

Western blot analyses revealed that NCX3 protein expression is significantly increased in the hippocampus of 3-month-old Tg2576 mice compared to WT (**Fig. 11; Panel B**). By contrast, we observed a significant reduction of NCX3 protein expression in the hippocampus of 8-month-old Tg2576 mice compared to WT, although an increase in the hippocampus of 8-month-old WT mice has been observed in comparison with 3 month-old WT mice (**Fig. 11, Panel C**).

To improve western blot results, Immunohistochemical analyses have been performed in the hippocampus of Tg2576 mice. In particular, we observed that, although NCX3 immunoreactivity was scarcely detected in the soma of pyramidal cells of both 3 and 8-month-old WT mice, several scattered cells including pericytes along vessels- and glia-shaped cells appeared very intensely stained (**Fig. 11, Panel D**). Similarly, NCX3 was moderately expressed in the *corpus callosum* of both 3 and 8 months old WT mice (**Fig. 11, Panel D, c and m**, respectively). Moreover, NCX3 immunosignal seems to be increased in the hippocampus of 8-month-old WT mice (**Fig. 11, Panel D, i-n**) compared to 3-month-old WT mice (**Fig. 11, Panel D, a-d**).

Interestingly, a divergent modulation of NCX3 expression was observed in the hippocampal region and *corpus callosum* at 3 or 8-month-old Tg2576 mice. Indeed, in both CA1 and CA3 hippocampal regions as well as within the *corpus callosum* of 3-month-old Tg2576 mice, the anti-NCX3 antibody revealed an increased NCX3 immunoreactivity signal, which was mainly confined along the processes of cells and dendrites of pyramidal cells (**Fig. 11, Panel D, e-h**). By contrast, in both CA1 and CA3 hippocampal regions as well as within the *corpus callosum* of 8-month-old Tg2576 mice, NCX3 immunostaining appeared robustly decreased (**Fig. 11, Panel D, o-r**).

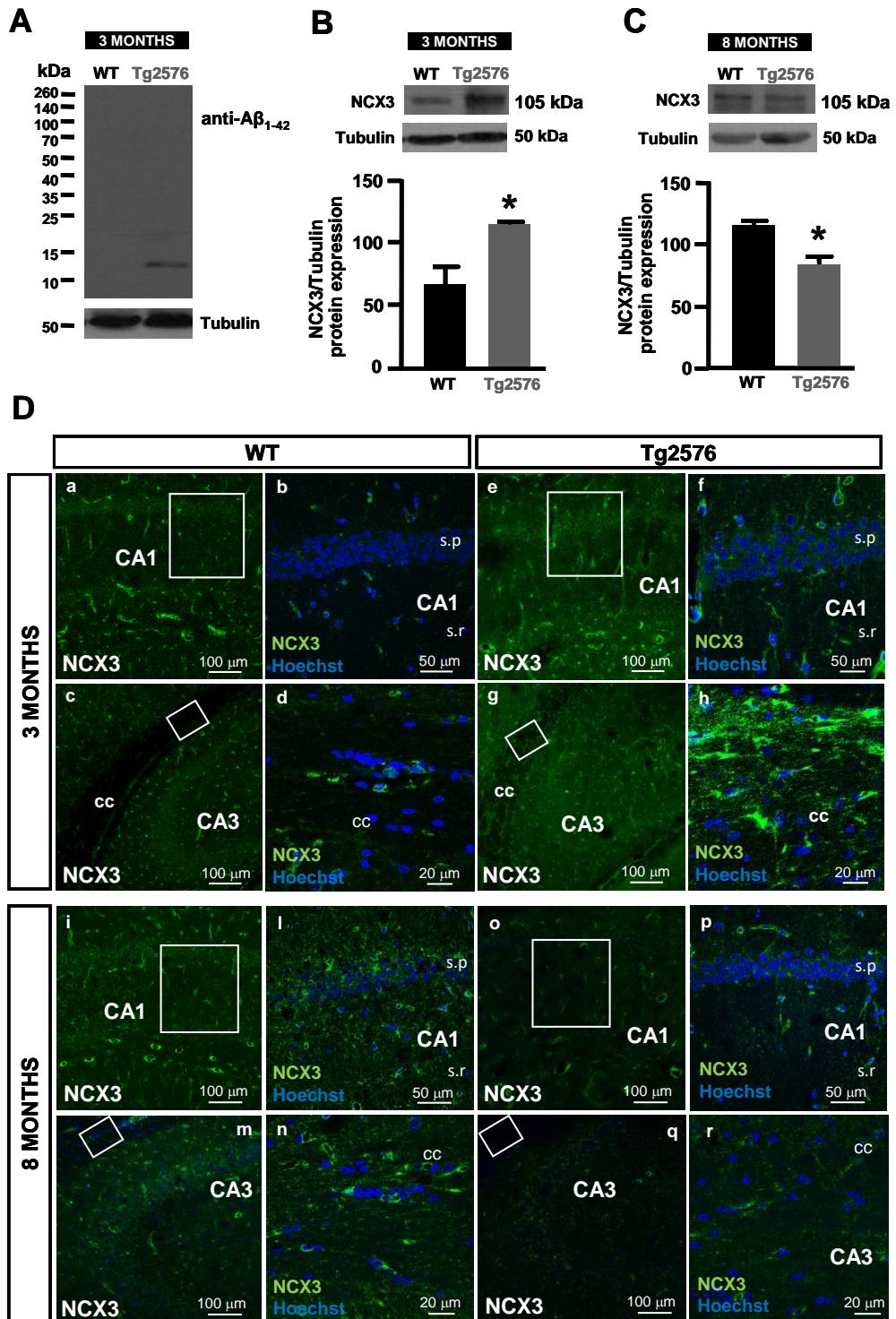


**Figure 11. NCX3 protein expression in the hippocampus of 3 and 8-month-old Tg2576 mice.** (A) Representative Western blot of A $\beta_{1-42}$  protein levels in the hippocampus of 3-months old WT and Tg2576 mice. (B) Representative Western blot (top) and densitometric quantification (bottom) of NCX3 protein expression normalized to  $\alpha$ -tubulin levels in the hippocampus of 3-months old WT and Tg2576 mice. (C) Representative Western blot (top) and densitometric quantification (bottom) of NCX3 protein expression normalized to  $\alpha$ -tubulin levels in the hippocampus of 8-months old WT and Tg2576 mice. (D) Confocal immunofluorescence images displaying the expression of NCX3 (green) within the CA1 and CA3 hippocampal region of 3-months old WT mice (a-d), 3-months old Tg2576 mice (e-h), 8-months old WT mice (i-n), 8-months old Tg2576 mice (o-r). Scale bars, a, c, e, g, i, m, o, q: 100  $\mu$ m; b, f, l, p: 50  $\mu$ m; d, h, n, r: 20  $\mu$ m. Abbreviations: s.p., stratum pyramidale; s.r., stratum radiatum; cc, corpus callosum. \* $p < 0.05$  versus their respective WT. (Student's t test).

#### **4.7 NCX3 protein expression in the cerebral cortex of 3 and 8-month-old Tg2576 mice**

Western blot experiments revealed A $\beta$ <sub>1-42</sub> trimers deposition also in the cerebral cortex of Tg2576 mice (**Fig. 12, Panel A**). However, we did not detect any modulation of NCX3 protein expression in the cerebral cortex of both 3 and 8-month-old Tg2576 mice compared to WT (**Fig. 12, Panel B and C**). On the other hand, a clear loss of intensity of immunoreactivity signal has been observed in cortical sections from both 3 and 8 month's old Tg2576 mice (**Fig. 12, Panel D, c-d and g-h**, respectively) compared to WT mice (**Fig. 12, Panel a-b and e-f**). However, similarly to what has been observed in the hippocampus, a significant increase of NCX3 protein expression has been found in the cerebral cortex of 8-month-old WT mice compared to 3-month-old mice.

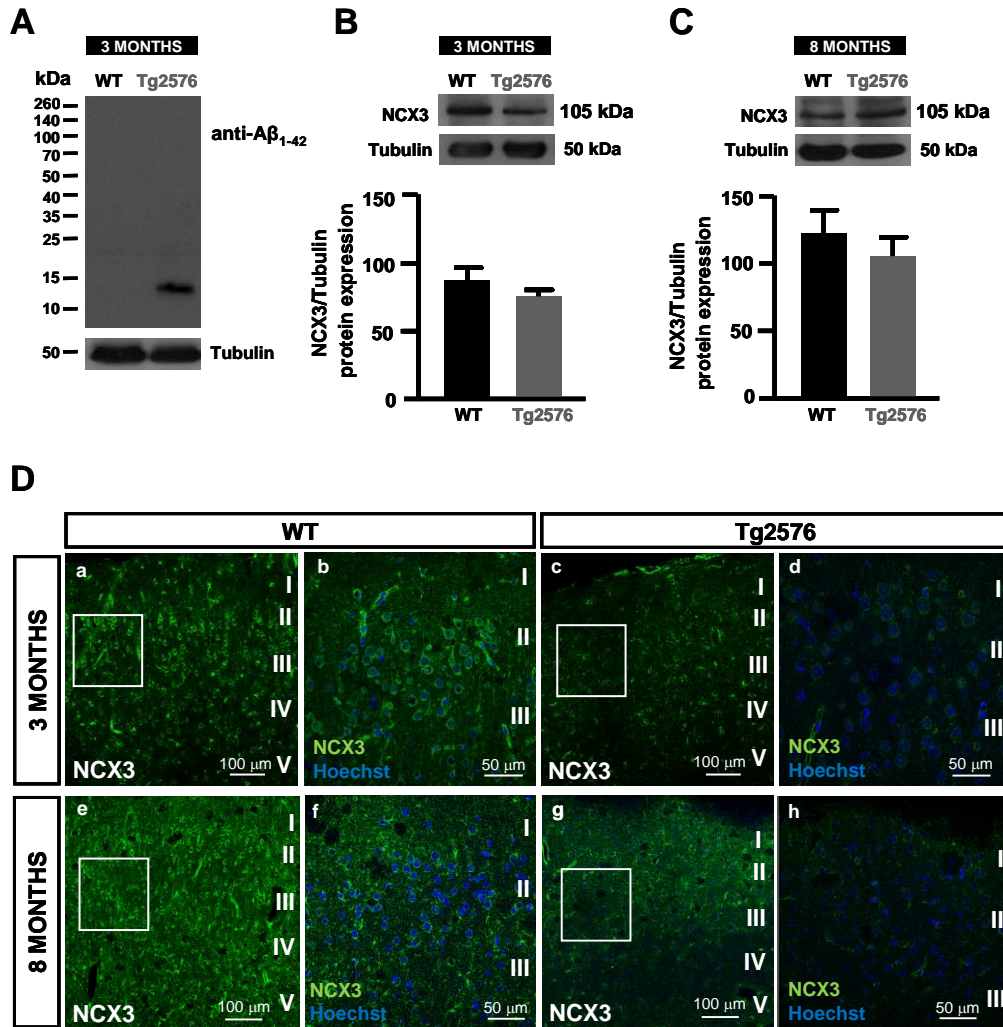


**Fig.12** (A) Representative Western blot of  $A\beta_{1-42}$  protein levels in the cerebral cortex of 3-months old WT and Tg2576 mice. (B) Representative Western blot (top) and densitometric quantification (bottom) of NCX3 protein expression normalized to  $\alpha$ -tubulin levels in the cerebral cortex of 3-months old WT and Tg2576 mice. (C) Representative Western blot (top) and densitometric quantification (bottom) of NCX3 protein expression normalized to  $\alpha$ -tubulin levels in the cerebral cortex of 8-months old WT and Tg2576 mice. (D) Confocal immunofluorescence images displaying the expression of NCX3 (green) in the cerebral cortex of 3-months old WT mice (a-b), 3-months old Tg2576 mice (c-d), 8-months old WT mice (e-f), 8-months old Tg2576 mice (g-h). Scale bars, a, c, e, g: 100  $\mu$ m; b, d, f, h: 50  $\mu$ m.

# **DISCUSSION**

The present study demonstrated that the activity of NCX3, a specific isoform of NCX, is progressively up-regulated in the reverse mode of operation in primary hippocampal neurons from Tg2576 mice. Previous studies provided evidence that NCX is involved in AD pathogenesis. In particular, Pannaccione *et al.* in 2012 reported that the selective up-regulation of NCX3 in hippocampal neurons treated with synthetic A $\beta$ <sub>1-42</sub> oligomers was associated with delayed ER stress and neuronal death. For this reason, we decided to investigate the NCX3 behaviour profile in Tg2576 hippocampal neurons, as they represent an *in vitro* model that better recapitulates AD pathology rather than the commonly used treatment with A $\beta$  oligomers.

First, the presence of intracellular A $\beta$ <sub>1-42</sub> detected in the Tg2576 neuronal lysates allowed us to validate Tg2576 hippocampal neurons, here set up for the first time, as a useful *in vitro* model of AD to investigate the effect of intracellular A $\beta$  on disease progression. Indeed, it is widely accepted that intraneuronal A $\beta$  accumulation is responsible for synaptic dysfunction and cognitive deficits even before plaque formation. In particular, western blot analyses revealed the intracellular accumulation of A $\beta$ <sub>1-42</sub> trimers, detectable as a ~ 12 kDa band, thus showing Tg2576 hippocampal neurons as an *in vitro* model particularly suitable to exploring the role of these small A $\beta$  aggregates in AD pathogenesis. In fact, it is well known that low weight, soluble A $\beta$ <sub>1-42</sub> oligomers are the critical neurotoxic entity of AD pathogenesis, since they correlate more than A $\beta$  plaques with memory deficits and cognitive dysfunction.

Ionic dysregulation is one of the metabolic consequences of A $\beta$  accumulation contributing to neuronal dysfunction and death. In particular, the dysregulation of [Ca<sup>2+</sup>]<sub>i</sub> triggers a series of events including oxidative damage and activation of apoptotic machinery. Furthermore, the dysregulation of [Na<sup>+</sup>]<sub>i</sub> affects neuronal

excitability, thus contributing to epileptogenesis in AD. NCX, coupling in a bidirectional manner the exchange of  $3\text{Na}^+$  for  $1\text{Ca}^{2+}$  across the plasma membrane, plays a relevant role in maintaining intracellular  $\text{Na}^+$  and  $\text{Ca}^{2+}$  homeostasis, especially in pathological condition in which other mechanisms regulating  $\text{Na}^+$  and  $\text{Ca}^{2+}$  fluxes across the plasma membrane are compromised. Interestingly, we did find a significant up-regulation of  $I_{\text{NCX}}$  in Tg2576 hippocampal neurons and provided evidence that this up-regulation is specifically mediated by NCX isoform 3, also in our experimental conditions. Since NCX activity and its mode of operation depend on both  $[\text{Ca}^{2+}]_i$  and  $[\text{Na}^+]_i$ , we hypothesized that the up-regulation of  $I_{\text{NCX}}$  observed in Tg2576 hippocampal neurons from 8 DIV up to 18 DIV could be related to an imbalance of  $\text{Ca}^{2+}$  or  $\text{Na}^+$  homeostasis.  $\text{Na}^+$  detection with SBF1 probe revealed a significant increase of  $[\text{Na}^+]_i$  in Tg2576 hippocampal neurons, thus showing that the up-regulation of reverse  $\text{Na}^+/\text{Ca}^{2+}$  exchange is driven by an abnormal electrochemical gradient caused by the increase of intracellular  $\text{Na}^+$  content.  $\text{A}\beta_{1-42}$ -induced membrane depolarization has been previously reported in several experimental models of AD (Mukhamedyarov *et al.*, 2009). Furthermore, the impairment of the  $\text{Na}^+/\text{K}^+$  ATPase activity, the main mechanism responsible for  $\text{Na}^+$  extrusion, has been demonstrated in AD (Hattori *et al.*, 1998; Mark *et al.*, 1995; 1997). Importantly, we here report that the abnormal increase of  $[\text{Na}^+]_i$  observed in Tg2576 hippocampal neurons is mediated by a significant up-regulation of  $\text{Na}_v$  currents, in line with previous studies that showed an intimate correlation between reverse NCX activity and  $\text{Na}^+$  influx through specific  $\text{Na}_v$  channel subunits (Estacion *et al.*, 2015; Pappalardo *et al.*, 2014; Craner *et al.*, 2004a; 2004b). Interestingly, we also found a significant over-expression of  $\text{Na}^+$  Channel  $\alpha$  subunits in Tg2576 hippocampal neurons at 12 DIV, when the maximal up-regulation of  $\text{Na}_v$  currents

has been observed. By contrast, any modulation of NCX3 protein expression has been found in our experimental conditions, thus suggesting that the up-regulation of NCX activity in the reverse mode is subsequent to the up-regulation of Nav channels without being correlated with an increased amount of exchanger on the plasma membrane. However, further experiments such as the assessment of NCX3 mRNA levels and immunocytochemical analyses are needed to confirm this aspect. NCX activity in the reverse mode has been associated to increased  $[Ca^{2+}]_i$  (Atherton *et al.*, 2009; Kortus *et al.*, 2016) but also, in other experimental conditions, to enhanced  $Ca^{2+}$  refilling into ER (Sirabella *et al.*, 2009; Pannaccione *et al.*, 2012; Sisalli *et al.*, 2014; Di Giuro *et al.*, 2017). So, we test both these hypotheses by determining  $[Ca^{2+}]_i$  and ER  $Ca^{2+}$  content of Tg2576 hippocampal neurons. Notably, we did not find any increase of  $[Ca^{2+}]_i$  but rather a significant reduction of basal  $Ca^{2+}$  content in Tg2576 hippocampal neurons at 8 DIV, whereas no significant modulations occurred with time in culture. Importantly, this result demonstrates not only that  $I_{NCX}$  up-regulation in the reverse mode does not cause an increase of  $[Ca^{2+}]_i$ , but also that  $A\beta_{1-42}$  trimers accumulating in Tg2576 neurons are not correlated with  $Ca^{2+}$  disruption. On the other hand, the up-regulation of  $Ca^{2+}$  signalling occurring in the early phases of AD pathology has been mainly associated to extracellular  $A\beta_{1-42}$  oligomers, since they may trigger  $Ca^{2+}$  influx through several mechanisms, including the formation of  $Ca^{2+}$  permeable pores, and, even more, to mutated presenilins, which can interact with  $Ca^{2+}$  transport proteins present on ER membranes. Few studies, however, have been focused on the consequences of APP mutations on  $Ca^{2+}$  signalling nor on the role of intracellular  $A\beta$ . Therefore, this result is consistent with the above-mentioned concept, according to which Tg2576 hippocampal neurons are quite different from *in vitro* models of  $A\beta$ -treatment. To emphasize this data, we also

reported that increased calpain activation does not occur in these neurons, nor we observed the activation of apoptotic cell death (data not shown). However, it is necessary to highlight that A $\beta$ -treatment is an acute stimulus, able to trigger several neurotoxic mechanisms, such as [Ca<sup>2+</sup>]<sub>i</sub> increase, ER stress and activation of the apoptotic machinery (Pannaccione *et al.*, 2012). On the other hand, primary neurons from Tg2576 are characterized by progressive and ceaseless A $\beta$ <sub>1-42</sub> oligomers secretion and accumulation. Importantly, A $\beta$ <sub>1-42</sub> oligomers naturally generated by these cultured cells are present intraneuronally and in the conditioned medium at low to sub-nanomolar concentrations, a considerably lower amount than that reached with exogenous A $\beta$  treatment (~ $\mu$ M). Therefore, it is not surprisingly that naturally secreted A $\beta$ <sub>1-42</sub> oligomers may have different effects on cell viability than synthetic preparations.

Despite ER has emerged as an important player in AD pathogenesis, few evidence has been provided about its involvement in AD pathology induced by APP mutations. Significantly, we found that ER content was significantly increased in Tg2576 hippocampal neurons in comparison with WT neurons, at 12 DIV when the first peak of *INCX* up-regulation has been observed. Previous evidence suggested that Ca<sup>2+</sup> refilling into ER constitutes a neuroprotective mechanism aimed to delay ER stress and caspase 12 activation. Moreover, ER Ca<sup>2+</sup> content can provide an important Ca<sup>2+</sup> source available for many physiological mechanisms occurring in neuronal cells. In fact, it is well known that, at dendritic level, Ca<sup>2+</sup> release from ER stores is involved in modulating postsynaptic responses and synaptic plasticity (Emptage *et al.*, 1999; Fitzjohn and Collingridge, 2002; Holbro *et al.*, 2009), whereas in axon terminals it is involved in vesicle fusion and neurotransmitter release (Emptage *et al.*, 2001; Bouchard *et al.*, 2003). Furthermore, in the soma, it is coupled to the activation of

Ca<sup>2+</sup>-sensitive signaling pathways, such as kinase and phosphatase activities (Berridge, 1998). However, in association with the increased Ca<sup>2+</sup> refilling into ER, we did not observe any activation of ER stress marker, such as caspase 12 and GRP78, in Tg2576 hippocampal neurons at various experimental time points. For this reason, we assumed that ER stress does not occur in our model. On the other hand, the significant increase of ER Ca<sup>2+</sup> content seems to be correlated with the up-regulation of NCX3 in the reverse mode of operation. Remarkably, this observation is supported by several evidence demonstrating the correlation between the reverse mode of NCX and the direct Ca<sup>2+</sup> entry into ER through SERCA pumps (Fameli *et al.*, 2007) and suggesting that it could represent a neuroprotective mechanism in several pathological conditions (Sirabella *et al.*, 2009; Pannaccione *et al.*, 2012; Sisalli *et al.*, 2014).

Importantly, we here provide for the first time preliminary evidence about NCX3 modulation in an animal model of FAD, the Tg2576 mouse. In particular, we focused our attention on the early and more advanced, but 'pre-plaques' stages of the disease, since Tg2576 mice display very early cognitive dysfunction and hyperexcitability. Importantly, western blot experiments revealed the presence of low-weight A $\beta$ <sub>1-42</sub> aggregates in the hippocampus and cerebral cortex of these mice, thereby supporting the role of soluble A $\beta$ <sub>1-42</sub> in early AD symptoms. Importantly, the significant NCX3 over-expression in the hippocampus of 3-month-old Tg2576 mice suggests the involvement of NCX3 in the early phases of AD pathogenesis. In addition, its increase in the hippocampus of 8-month-old WT mice compared to 3 month-old WT mice supports previous evidence that suggested a role for NCX in impaired calcium homeostasis during aging of the brain. Indeed, studies performed on cortical nerve endings of aged rats have demonstrated that NCX activity is significantly decreased in comparison with

young rats (Michaelis *et al.*, 1984; Canzoniero *et al.*, 1998). The situation can get worse in aged brain showing accumulation of A $\beta$ <sub>1-42</sub> aggregates. In fact, it is well known that ageing processes occur precociously in AD brains. Importantly, Tg2576 display early selective vulnerability of synaptic functions and structures (Baliatti *et al.*, 2013). Remarkably, a recent genetic study identified several genes in which variations may affect the age at onset (AAO) of FAD (Saad *et al.*, 2015). Among them, multiple rare variants in SLC8A3 have been found to be significantly associated with the AAO of AD. This finding confirms that NCX3 is implicated in AD pathogenesis and that its activity could affect the outcome of AD symptoms. In particular, based on our results, we hypothesised that the increase of reverse NCX activity reduces Na<sup>+</sup> loads mediated by the up-regulation of Nav channels activity and expression. Thereby, targeting NCX3 could represent a promising strategy to repair aberrant Na<sup>+</sup> influx and subsequent hippocampal neuronal excitability in AD.

# REFERENCES

Alkon DL (1984). Calcium-mediated reduction of ionic currents: a biophysical memory trace. *Science*; 226(4678):1037-45.

Alkon DL (1989). Memory storage and neural systems. *Sci Am*; 261(1):42-50.

Amoroso S, Tagliatela M, Canzoniero LM, Cragoe EJ Jr, di Renzo G, and Annunziato L (1990). Possible involvement of Ca<sup>2+</sup> ions, protein kinase C and Na<sup>+</sup>/H<sup>+</sup> antiporter in insulin-induced endogenous dopamine release from tuberoinfundibular neurons. *Life Sci*; 46:885–894.

Amoroso S, De Maio M, Russo GM, Catalano A, Bassi A, Montagnani S, Di Renzo GF, and Annunziato L (1997). Pharmacological evidence that the activation of the Na<sup>+</sup>-Ca<sup>2+</sup> exchanger protects C6 glioma cells during chemical hypoxia. *Br J Pharmacol*; 121:303–309.

Amoroso S, Tortiglione A, Secondo A, Catalano A, Montagnani S, Di Renzo G, and Annunziato L (2000). Sodium nitroprusside prevents chemical hypoxia-induced cell death through iron ions stimulating the activity of the Na<sup>+</sup>-Ca<sup>2+</sup> exchanger in C6 glioma cells. *J Neurochem*; 744:1505–1513.

Angulo E, Noé V, Casadó V, Mallol J, Gomez-Isla T, Lluís C, Ferrer I, Ciudad CJ, Franco R, (2004). Up-regulation of the KV3.4 potassium channel subunit in early stages of Alzheimer's disease. *J Neurochem*; 91, 547e557.

Annunziato L, Cataldi M, Pignataro G, Secondo A, Molinaro P (2007a). Glutamate-independent calcium toxicity: introduction. *Stroke*; 38:661–4.

Annunziato L, Pignataro G, Boscia F, Sirabella R, Formisano L, Saggese M, *et al.* (2007b). Di Renzo GF: ncx1, ncx2, and ncx3 gene product expression and function in neuronal anoxia and brain ischemia. *Ann N Y Acad Sci*; 1099:413–26.

Baker PF and McNaughton PA (1976). Kinetics and energetics of calcium efflux from intact squid giant axons. *J Physiol*; 259:103–144.

Ballard C and Schaffer S (1996). Stimulation of the Na<sup>+</sup>/Ca<sup>2+</sup> exchanger by phenylephrine, angiotensin II and endothelin 1. *J Mol Cell Cardiol*; 28:11–17.

Bancher C, Leitner H, Jellinger K, Eder H, Setinek U, Fischer P, Wegiel J, Wisniewski HM (1996). On the relationship between measles virus and Alzheimer neurofibrillary tangles in subacute sclerosing panencephalitis. *Neurobiol Aging*; 17(4):527-33.

Bano D, Young KW, Guerin CJ, Lefevre R, Rothwell NJ, Naldini L, Rizzuto R, Carafoli E, Nicotera P (2005). Cleavage of the plasma membrane Na<sup>+</sup>/Ca<sup>2+</sup> exchanger in excitotoxicity. *Cell*; 120(2):275-85.

Barnes KV, Cheng G, Dawson MM, Menick DR (1997). Cloning of cardiac, kidney, and brain promoters of the feline ncx1 gene. *J Biol Chem*; 272(17):11510-7.

Baulac S, LaVoie MJ, Kimberly WT, Strahle J, Wolfe MS, Selkoe DJ, Xia W (2003). Functional gamma-secretase complex assembly in Golgi/trans-Golgi network:

interactions among presenilin, nicastrin, Aph1, Pen-2, and gamma-secretase substrates. *Neurobiol Dis*; 14(2):194-204.

Bekris LM, Yu CE, Bird TD, Tsuang DW (2010). Genetics of Alzheimer disease. *J Geriatr Psychiatry Neurol*; 23:213e227.

Bers DM (2002). Cardiac excitation-contraction coupling. *Nature*; 415(6868):198-205.

Bertram L, Lill CM, Tanzi RE (2010). The genetics of Alzheimer disease: back to the future. *Neuron*; 68(2):270-81.

Bhatia R, Lin H & Lal R (2000). Fresh and globular amyloid  $\beta$  protein (1–42) induces rapid cellular degeneration: evidence for A $\beta$ P channel-mediated cellular toxicity. *FASEB J*; 14, 1233–1243.

Bjartmar C, Kidd G, Mork S, Rudick R, Trapp BD (2000). Neurological disability correlates with spinal cord axonal loss and reduced N-acetyl aspartate in chronic multiple sclerosis patients. *Ann Neurol*; 48: 893±901.

Blaustein MP and Santiago EM (1977). Effects of internal and external cations and ATP on sodium-calcium exchange and calcium-calcium exchange in squid axons. *Biophys J*; 20:79–111.

Blaustein MP (1993). Physiological effects of endogenous ouabain: control of intracellular Ca<sup>2+</sup> stores and cell responsiveness. *Am J Physiol*; 264(6 Pt 1):C1367-87.

Blaustein MP and Lederer WJ (1999). Sodium/calcium exchange: its physiological implications. *Physiol Rev*; 79:763–854.

Blumenfeld H, Lampert A, Klein JP, Mission J, Chen MC, Rivera M, Dib-Hajj S, Brennan AR, Hains BC, Waxman SG (2009). Role of hippocampal sodium channel Nav1.6 in kindling epileptogenesis. *Epilepsia*; 50: 44–55.

Boda E, Hoxha E, Pini A, Montarolo F, Tempia F(2012). Brain expression of KV3subunits during development, adulthood and aging and in a murine model of Alzheimer's disease. *J Mol Neurosci*; 46, 606e615.

Borroni B, Pilotto A, Bonvicini C, Archetti S, Alberici A, Lupi A, Gennarelli M, Padovani A (2012). Atypical presentation of a novel Presenilin 1 R377W mutation: sporadic, late-onset Alzheimer disease with epilepsy and frontotemporal atrophy. *Neurol Sc*; 33:375e378.

Boscia F, Gala R, Pignataro G, de Bartolomeis A, Cicale M, Ambesi- Impiombato A, *et al.* (2006). Permanent focal brain ischemia induces isoform-dependent changes in the pattern of Na<sup>+</sup>/Ca<sup>2+</sup> exchanger gene expression in the ischemic core, peri infarct area, and intact brain regions. *J Cereb Blood Flow Metab*;26:502–17.

Boscia F, D'Avanzo C, Pannaccione A, Secondo A, Casamassa A, Formisano L, Guida N, Sokolow S, Herchuelz A, Annunziato L (2012). Silencing or knocking out the Na<sup>+</sup>/Ca<sup>2+</sup> exchanger-3 (NCX3) impairs oligodendrocyte differentiation. *Cell Death Differ*; 19:562–572.

- Boscia F, D'Avanzo C, Pannaccione A, Secondo A, Casamassa A, Formisano L, Guida N, Scorziello A, Di Renzo G, Annunziato L (2013). New roles of NCX in glial cells: Activation of microglia in ischemia and differentiation of oligodendrocytes. *Adv Exp Med Biol*; 961:307–316.
- Boscia F, Pannaccione A, Ciccone R, Casamassa A, Franco C, Piccialli I, de Rosa V, Vinciguerra A, Di Renzo GF, Annunziato L (2017). The expression and activity of KV3.4 channel subunits are precociously upregulated in astrocytes exposed to A $\beta$  oligomers and in astrocytes of Alzheimer's disease Tg2576 mice. *Neurobiol Aging*; 54:187-198.
- Bouras C, Hof PR, Giannakopoulos P, Michel JP, Morrison JH (1994). Regional distribution of neurofibrillary tangles and senile plaques in the cerebral cortex of elderly patients: a quantitative evaluation of a one-year autopsy population from a geriatric hospital. *Cereb Cortex*; 4(2):138-50.
- Bouzon A, Reuter H (1996). A role of intracellular Na<sup>+</sup> in the regulation of synaptic transmission and turnover of the vesicular pool in cultured hippocampal cells. *Neuron*; 17(5):969-78.
- Braak H, Braak E (1991). Neuropathological staging of Alzheimer-related changes. *Acta Neuropathol*; 82:239–59.
- Braak H, Braak E (1994). Morphological criteria for the recognition of Alzheimer's disease and the distribution pattern of cortical changes related to this disorder. *Neurobiol Aging*; 15(3):355-6; discussion 379-80.
- Braak H, Thal DR, Ghebremedhin E, Del Tredici K (2011). Stages of the pathologic process in Alzheimer disease: age categories from 1 to 100 years. *J Neuropathol Exp Neurol*; 70(11):960-9.
- Buée L, Bussièrè T, Buée-Scherrer V, Delacourte A, Hof PR (2000). Tau protein isoforms, phosphorylation and role in neurodegenerative disorders. *Brain Res Rev*; 33(1):95-130.
- Busche MA, Chen X, Henning HA, Reichwald J, Staufenbiel M, Sakmann B, Konnerth A (2012). Critical role of soluble amyloid- $\beta$  for early hippocampal hyperactivity in a mouse model of Alzheimer's disease. *Proc Natl Acad Sci U S A*; 109(22):8740-5.
- Busche MA, Kekuš M, Adelsberger H, Noda T, Förstl H, Nelken I, Konnerth A (2015). Rescue of long-range circuit dysfunction in Alzheimer's disease models. *Nat Neurosci*; 18(11):1623-30.
- Busciglio J, Gabuzda DH, Matsudaira P, Yankner BA (1993). Generation of beta-amyloid in the secretory pathway in neuronal and non neuronal cells. *Proc Natl Acad Sci U S A*; 90(5):2092-6.
- Cai XD, Golde TE, Younkin SG (1993). Release of excess amyloid beta protein from a mutant amyloid beta protein precursor. *Science*; 259: 514–516.

Cairns NJ, Bigio EH, Mackenzie IR, Neumann M, Lee VM, Hatanpaa KJ, White CL 3rd, Schneider JA, Grinberg LT, Halliday G, Duyckaerts C, Lowe JS, Holm IE, Tolnay M, Okamoto K, Yokoo H, Murayama S, Woulfe J, Munoz DG, Dickson DW, Ince PG, Trojanowski JQ, Mann DM (2007). Consortium for Frontotemporal Lobar Degeneration. Neuropathologic diagnostic and nosologic criteria for frontotemporal lobar degeneration: consensus of the Consortium for Frontotemporal Lobar Degeneration. *Acta Neuropathol*; 114(1):5-22.

Canitano A, Papa M, Boscia F, Castaldo P, Sellitti S, Tagliatalata M, and Annunziato L (2002). Brain distribution of the Na<sup>+</sup>/Ca<sup>2+</sup> exchanger-encoding genes NCX1, NCX2 and NCX3 and their related proteins in the central nervous system. *Ann NY Acad Sci*; 976:394-404.

Capetillo-Zarate E, Gracia L, Yu F, Banfelder JR, Lin MT, Tampellini D, Gouras GK (2011). High-resolution 3D reconstruction reveals intra-synaptic amyloid fibrils. *Am J Pathol*; 179(5):2551-8.

Carafoli E (1985). The homeostasis of calcium in heart cells. *Mol Cell Cardiol* 17:203-212.

Castano EM, Prelli F, Wisniewski T, Golabek A, Kumar RA, Soto C, Frangione B (1995). Fibrillogenesis in Alzheimer's disease of amyloid beta peptides and apolipoprotein E. *Biochem*; 306 (Pt 2):599-604.

Chartier-Harlin MC, Crawford F, Houlden H, Warren A, Hughes D, Fidani L, Goate A, Rossor M, Roques P, Hardy J, *et al.* (1991). Early-onset Alzheimer's disease caused by Trafficking and Proteolytic Processing of APP mutations at codon 717 of the beta-amyloid precursor protein gene. *Nature*; 353: 844-846.

Cheung KH, Shineman D, Müller M, Cárdenas C, Mei L, Yang J, Tomita T, Iwatsubo T, Lee VM, Foskett JK (2008). Mechanism of Ca<sup>2+</sup> disruption in Alzheimer's disease by presenilin regulation of InsP<sub>3</sub> receptor channel gating. *Neuron*; 58(6):871-83.

Chin J (2011). Selecting a mouse model of Alzheimer's disease. *Methods Mol Biol*; 670:169-89.

Choi DW (1988). Calcium-mediated neurotoxicity: relationship to specific channel types and role in ischemic damage. *Trends Neurosci*; 11:465-469.

Chung S, Lee J, Joe EH and Uhm DY (2001). Beta-amyloid peptide induces the expression of voltage dependent outward rectifying K<sup>+</sup> channels in rat microglia. *Neurosci Lett*; 300, 67-70.

Citron M, Oltersdorf T, Haass C, McConlogue L, Hung AY, Seubert P, Vigo-Pelfrey C, Lieberburg I, Selkoe DJ (1992). Mutation of the beta-amyloid precursor protein in familial Alzheimer's disease increases beta-protein production. *Nature*; 360: 672-674.

Collin C, Ikeno H, Harrigan JF, Lederhendler I, Alkon DL (1988). Sequential modification of membrane currents with classical conditioning. *Biophys J*; 54(5):955-60.

- Colom LV, Diaz ME, Beers DR, Neely A, Xie WJ and Appel SH (1998). Role of potassium channels in amyloid-induced cell death. *J Neurochem*; 70, 1925–1934.
- Colvin RA, Bennett JW, Colvin SL, Allen RA, Martinez J, Miner GD (1991). Na<sup>+</sup>/Ca<sup>2+</sup> exchange activity is increased in Alzheimer's disease brain tissues. *Brain Res*; 543, 139-147.
- Compston A, Coles A (2008). Multiple sclerosis. *Lancet*; 372:1502–1517.
- Condrescu M, Gardner JP, Chernaya G, Aceto JF, Kroupis C, Reeves JP (1995). ATP-dependent regulation of sodium–calcium exchange in Chinese hamster ovary cells transfected with the bovine cardiac sodium–calcium exchanger. *J Biol Chem*; 270:9137–46.
- Corder EH, Saunders AM, Strittmatter WJ, Schmechel DE, Gaskell PC JR, Small GW, Roses AD, Haines JL, and Pericak-Vance MA (1993). Gene dose of apolipoprotein E type 4 allele and the risk of Alzheimer's disease in late onset families. *Science*; 261: 921–923.
- Coulson EJ, Paliga K, Beyreuther K, Masters CL (2000). What the evolution of the amyloid protein precursor supergene family tells us about its function. *Neurochem Int*; 36(3):175-84.
- Cragoe EJ Jr, Woltersdorf OW Jr, Bicking JB, Kwong SF, and Jones JH (1967). Pyrazine diuretics. II. N-amidino-3-amino-5-substituted 6-halopyrazinecarboxamides. *J Med Chem*; 10:66–75.
- Craner MJ, Lo AC, Black JA, Waxman SG (2003). Abnormal sodium channel distribution in optic nerve axons in a model of inflammatory demyelination. *Brain*; 126: 1552±61.
- Cretin B, Sellal F, Philippi N, Bousiges O, Di Bitonto L, Martin-Hunyadi C, Blanc F (2016). Epileptic Prodromal Alzheimer's Disease, a Retrospective Study of 13 New Cases: Expanding the Spectrum of Alzheimer's Disease to an Epileptic Variant. *J Alzheimers Dis*; 52(3):1125-33
- Crill WE (1996). Persistent sodium current in mammalian central neurons. *Annu Rev Physiol*; 58 349–362.
- Cruts M, Hendriks L, Van Broeckhoven C (1996). The presenilin genes: a new gene family involved in Alzheimer disease pathology. *HumMolGenet*; 5:1449e1455.
- Cruts M, Theuns J, Van Broeckhoven C (2012). Locus-specific mutation databases for neurodegenerative brain diseases. *HumanMut*; 33:1340e1344.
- Cunningham KW and Fink GR (1996). Calcineurin inhibits VCX1-dependent H<sup>+</sup>/C<sup>+</sup> exchange and induces Ca<sup>2+</sup>-ATPases in *Saccharomyces cerevisiae*. *Mol Cell Biol*; 16:2226–2237.

- Davie CA, Barker GJ, Webb S, Tofts PS, Thompson AJ, Harding AE, *et al.* (1995). Persistent functional deficit in multiple sclerosis and autosomal dominant cerebellar ataxia is associated with axon loss. *Brain*; 118: 1583±92.
- De Felice FG, Velasco PT, Lambert MP, Viola K, Fernandez SJ, Ferreira ST, Klein WL (2007). Abeta oligomers induce neuronal oxidative stress through an N-methyl-D-aspartate receptor-dependent mechanism that is blocked by the Alzheimer drug memantine. *J Biol Chem*; 282(15):11590-601.
- De Jonghe C, Zehr C, Yager D, Prada CM, Younkin S, Hendriks L, Van Broeckhoven C, Eckman CB (1998). Flemish and Dutch mutations in amyloid beta precursor protein have different effects on amyloid beta secretion. *Neurobiol Dist*; 5(4):281-6.
- DeKosky ST, Scheff SW, Styren SD (1996). Structural correlates of cognition in dementia: quantification and assessment of synapse change. *Neurodegeneration*; 5:417–21.
- Demuro A, Mina E, Kaye R, Milton SC, Parker I, Glabe CG (2005). Calcium dysregulation and membrane disruption as a ubiquitous neurotoxic mechanism of soluble amyloid oligomers. *J Biol Chem*; 280: 17294–300.
- De Strooper B, Saftig P, Craessaerts K, Vanderstichele H, Guhde G, Annaert W, Von Figura K, Van Leuven F (1998). Deficiency of presenilin-1 inhibits the normal cleavage of amyloid precursor protein. *Nature*;391(6665):387-90.
- Diochot S, Schweitz H, Beress L and Lazdunski M (1998). Sea anemone peptides with a specific blocking activity against the fast inactivating potassium channel Kv3.4. *J Biol Chem*; 273, 6744–6749.
- DiPolo R (1979). Calcium influx in internally dialyzed squid giant axons. *J Gen Physiol*;73:91–113.
- DiPolo R, Beaugé LA (1994). Cardiac sarcolemmal Na<sup>+</sup>-Ca<sup>2+</sup> inhibiting peptides XIP and FMRF-amide also inhibit Na<sup>+</sup>-Ca<sup>2+</sup> exchange in squid axons. *Am J Physiol*; 267:C307–C311
- DiPolo R, Beaugé LA (1998). Differential up-regulation of Na<sup>+</sup>-Ca<sup>2+</sup> exchange by phosphoarginine and ATP in dialysed squid axons. *J Physiol*; 507:737–747.
- Dodel RC, Du Y, Bales KR, Gao F, Eastwood B, Glazier B, Zimmer R, Cordell B, Hake A, Evans R, Gallagher-Thompson D, Thompson LW, Tinklenberg JR, Pfefferbaum A, Sullivan EV, Yesavage J, Alstiel L, Gasser T, Farlow MR, Murphy GM Jr, Paul SM (2000). Alpha2 macroglobulin and the risk of Alzheimer's disease. *Neurology*; 54(2):438-42.
- Doering AE, Nicoll DA, Lu Y, Lu L, Weiss JN, Philipson KD (1998). Topology of a functionally important region of the cardiac Na<sup>+</sup>/Ca<sup>2+</sup> exchanger. *J Biol Chem*; 273(2):778-83.
- Donnan GA, Fisher M, Macleod M, Davis SM. Stroke (2008). *Lance.*;371:1612–23.

- Driscoll HE, Muraro NI, He M, Baines RA (2013). Pumilio-2 regulates translation of Nav1.6 to mediate homeostasis of membrane excitability. *J Neurosci*; 33(23):9644-54.
- Dyck C, Omelchenko A, Elias CL, Quednau BD, Philipson KD, Hnatowich M, Hryshko LV (1999). Ionic regulatory properties of brain and kidney splice variants of the NCX1 Na(+)-Ca(2+) exchanger. *J Gen Physiol*; 114(5):701-11.
- Eriksson KS, Sergeeva O, Brown RE, and Haas HL (2001a). Orexin/hypocretin excites the histaminergic neurons of the tuberomammillary nucleus. *J Neurosci*; 21:9273–9279.
- Eriksson KS, Stevens DR, and Haas HL (2001b). Serotonin excites tuberomammillary neurons by activation of Na<sup>+</sup>/Ca<sup>2+</sup> exchange. *Neuropharmacology*; 40:345–351.
- Esch FS, Keim PS, Beattie EC, Blacher RW, Culwell AR, Oltersdorf T, McClure D, Ward PJ (1990). Cleavage of amyloid beta peptide during constitutive processing of its precursor. *Science*; 248: 1122–1124.
- Etcheberrigaray R, Matzel LD, Lederhendler II, Alkon DL (1992). Classical conditioning and protein kinase C activation regulate the same single potassium channel in *Hermissenda crassicornis* photoreceptors. *Proc Natl Acad Sci U S A*; 89(15):7184-8.
- Etcheberrigaray R, Ito E, Oka K, Tofel-Grehl B, Gibson GE, Alkon DL (1993). Potassium channel dysfunction in fibroblasts identifies patients with Alzheimer disease. *Proc Natl Acad Sci U S A*; 90(17):8209-13.
- Etcheberrigaray R, Hirashima N, Nee L, Prince J, Govoni S, Racchi M, Tanzi RE, Alkon DL (1998). Calcium responses in fibroblasts from asymptomatic members of Alzheimer's disease families. *Neurobiol Dis*; 5(1):37-45.
- Etcheberrigaray R, Bhagavan S (1999). Ionic and signal transduction alterations in Alzheimer's disease: relevance of studies on peripheral cells. *Mol Neurobiol*; 20(2-3):93-109
- Evin G, Weidemann A (2002). Biogenesis and metabolism of Alzheimer's disease Aβ amyloid peptides. *Peptides*; 23, 1285–1297.
- Fujioka Y, Matsuoka S, Ban T, and Noma A (1998). Interaction of the Na<sup>+</sup>-K<sup>+</sup> pump and Na<sup>+</sup>-Ca<sup>2+</sup> exchange via [Na<sup>+</sup>]<sub>i</sub> in a restricted space of guinea-pig ventricular cells. *J Physiol*; 509:457–470.
- Fujioka Y, Fujioka Y, Hiroe K, and Matsuoka S (2000). Regulation kinetics of Na<sup>+</sup>-Ca<sup>2+</sup> exchange current in guinea-pig ventricular myocytes. *J Physiol*; 529: 611–623.
- Gabellini N, Zatti A, Rispoli G, Navangione A, Carafoli E (1996). Expression of an active Na<sup>+</sup>/Ca<sup>2+</sup> exchanger isoform lacking the six C-terminal transmembrane segments. *Eur J Biochem*; 239(3):897-904.
- Gabellini N, Bortoluzzi S, Danieli GA, Carafoli E (2002). The human SLC8A3 gene and the tissue-specific Na<sup>+</sup>/Ca<sup>2+</sup> exchanger 3 isoforms. *Gene*; 298(1):1-7.

- Ganter P, Prince C, Esiri MM (1999). Spinal cord axonal loss in multiple sclerosis: a post-mortem study. *Neuropathol Appl Neurobiol*; 25: 459±67.
- Gasser A, Ho TS, Cheng X, Chang KJ, Waxman SG, Rasband MN, Dib-Hajj SD (2012). An ankyrinG-binding motif is necessary and sufficient for targeting Nav1.6 sodium channels to axon initial segments and nodes of Ranvier. *J Neurosci*; 32(21):7232-43.
- Gearing M, Mori H, and Mirra SS (1996). Ab-peptide length and apolipoprotein E genotype in Alzheimer's disease. *Ann Neurol*;39: 395–399.
- Glenner GG, Wong CW, Quaranta V, Eanes ED (1984). The amyloid deposits in Alzheimer's disease: their nature and pathogenesis. *Appl Pathol*;2(6):357-69.
- Goate A, Chartier-Harlin MC, Mullan M, Brown J, Crawford F, Fidani L, Guiffra L, Haynes A, Irving N, James S L, Mant R, Newton P, Rooke K, Roques P, Talbot C, Pericak-Vance M, Roses A, Williamson R, Rossor M, Owen M, and Hardy J (1991). Segregation of a missense mutation in the amyloid precursor protein gene with familial Alzheimer's disease. *Nature*; 349: 704–706.
- Goedert M (2004). Tau protein and neurodegeneration. *Semin Cell Dev Biol*; 15:45–49.
- Goodman Y & Mattson MP (1994). Secreted forms of  $\beta$ -amyloid precursor protein protect hippocampal neurons against amyloid  $\beta$ -peptide-induced oxidative injury. *Exp Neurol*;128, 1–12.
- Gopalakrishnan G, Awasthi A, Belkaid W, De Faria OJ, Liazoghli D, Colman DR, Dhaunchak AS (2013). Lipidome and proteome map of myelin membranes. *J Neurosci Res*; 91:321–334.
- Gouras GK, Tsai J, Naslund J, Vincent B, Edgar M, Checler F, Greenfield JP, Haroutunian V, Buxbaum JD, Xu H, Greengard P, Relkin NR (2000). Intraneuronal A $\beta$  42 accumulation in human brain. *Am J Pathol*; 156(1):15-20.
- Graham SF, Nasarauddin MB, Carey M, McGuinness B, Holscher C, Kehoe PG, Love S, Passmore AP, Elliott CT, Meharg A, Green BD (2015). Quantitative measurement of [Na<sup>+</sup>] and [K<sup>+</sup>] in postmortem human brain tissue indicates disturbances in subjects with Alzheimer's disease and dementia with Lewy bodies. *J Alzheimers Dis*;44(3):851-7.
- Green KN, Demuro A, Akbari Y, Hitt BD, Smith IF, Parker I, LaFerla FM (2008). SERCA pump activity is physiologically regulated by presenilin and regulates amyloid beta production. *J Gen Physiol*;132(2):i1.
- Gupta MP, Makino N, Khatter K, and Dhalla NS (1986). Stimulation of Na<sup>+</sup>-Ca<sup>2+</sup> exchange in heart sarcolemma by insulin. *Life Sci*; 39:1077–1083.
- Gyure KA, Durham R, Stewart WF, Smialek JE & Troncoso JC (2001). Intraneuronal A $\beta$ -amyloid precedes development of amyloid plaques in Down syndrome. *Arch Pathol Lab Med*; 125, 489–492

- Haass C, Scholssmacher M, Hung AY, Vigo-Pelfrey C, Mellon A, Ostaszewski B, Liederburg I, Koo F, Schenk D, Teplow D, *et al.* (1992). Amyloid b-peptide is produced by cultured cells during normal metabolism. *Nature*; 359: 322–325.
- Haass C, Hung AY, Schlossmacher MG, Teplow DB, Selkoe DJ (1993). Beta-amyloid peptide and a 3-kDa fragment are derived by distinct cellular mechanisms. *J Biol Chem*; 268: 3021–3024.
- Haass C, Selkoe DJ (1993). Cellular processing of beta-amyloid precursor protein and the genesis of amyloid beta peptide. *Cell*; 75: 1039–1042.
- Haass C (2004). Take five—BACE and the gamma-secretase quartet conduct Alzheimer’s amyloid beta-peptide generation. *EMBO J*; 23: 483–488.
- Hale CC, Bliler S, Quinn TP, and Peletskaya EN (1997). Localization of an exchange inhibitory peptide (XIP) binding site on the cardiac sodium-calcium exchanger. *Biochem Biophys Res Commun*; 236:113–117.
- Hardy J, Allsop D (1991). Amyloid deposition as the central event in the aetiology of Alzheimer’s disease. *Trends in Pharmac*; 12: 383 – 388.
- Hardy JA, Higgins GA (1992). Alzheimer's disease: the amyloid cascade hypothesis. *Science*; 256(5054):184-5.
- Hardy J (2006). Alzheimer’s disease: The amyloid cascade hypothesis: An update and reappraisal. *J Alzheimers Dis*; 9:151–53.
- Hargus NJ, Merrick EC, Nigam A, Kalmar CL, Baheti AR, Bertram EH 3rd, Patel MK (2011). Temporal lobe epilepsy induces intrinsic alterations in Na channel gating in layer II medial entorhinal cortex neurons. *Neurobiol Dis*; 41(2):361-76.
- Hargus NJ, Nigam A, Bertram EH 3rd, Patel MK (2013). Evidence for a role of Nav1.6 in facilitating increases in neuronal hyperexcitability during epileptogenesis. *J Neurophysiol*;110(5):1144-57.
- Hattori N, Kitagawa K, Higashida T, Yagyu K, Shimohama S, Wataya T, Perry G, Smith MA, Inagaki C (1998). CI-ATPase and Na<sup>+</sup>/K<sup>(+)</sup>-ATPase activities in Alzheimer’s disease brains. *Neurosci Lett*;254, 141-144.
- Hayrapetyan V, Rybalchenko V, Rybalchenko N, Koulen P (2008). The N-terminus of presenilin-2 increases single channel activity of brain ryanodine receptors through direct protein-protein interaction. *Cell Calcium*;44(5):507-18.
- He Z, Petesch N, Voges K, Roben W, and Philipson KD (1997). Identification of important amino acid residues of the Na<sup>+</sup>-Ca<sup>2+</sup> exchanger inhibitory peptide, XIP. *J Membr Biol*; 156:149–156.

He Z, Feng S, Tong Q, Hilgemann DW, and Philipson KD (2000). Interaction of PIP(2) with the XIP region of the cardiac Na<sup>+</sup>/Ca<sup>2+</sup> exchanger. *Am J Physiol Cell Physiol*; 278:C661–C666.

Hendriks L, Van Duijn CM, Cras P, Cruts M, Van Hul W, Van Harskamp F, Warren A, Mcinnis MG, Antonarakis SE, Martin J-J, Hofman A, and Van Broeckhoven C (1992). Presenile dementia and cerebral haemorrhage linked to a mutation at codon 692 of the b-amyloid precursor protein gene. *Nature Genet*; 1: 218–221.

Hensley K, Carney JM, Mattson MP, Aksenova M, Harris M, Wu JF, Floyd RA, Butterfield DA (1994). A model for beta-amyloid aggregation and neurotoxicity based on free radical generation by the peptide: relevance to Alzheimer disease. *Proc Natl Acad Sci U S A*; 91(8):3270-4.

Hilgemann DW (1990). Regulation and deregulation of cardiac Na<sup>+</sup>/Ca<sup>2+</sup> exchange in giant excised sarcolemmal membrane patches. *Nature (Lond)*; 344:242–245.

Hilgemann DW, Matsuoka S, Nagel GA, and Collins A (1992). Steady-state and dynamic properties of cardiac sodium-calcium exchange. Sodium-dependent inactivation. *J Gen Physiol*; 100:905–932.

Hilgemann DW, Ball R (1996). Regulation of cardiac Na<sup>+</sup>, Ca<sup>2+</sup> exchange and KATP potassium channels by PIP<sub>2</sub>. *Science*; 273(5277):956-9.

Hirano A, Dembitzer HM, Kurland LT, Zimmerman HM (1968). The fine structure of some intraganglionic alterations. Neurofibrillary tangles, granulovacuolar bodies and “rod-like” structures as seen in Guam amyotrophic lateral sclerosis and parkinsonism-dementia complex. *J Neuropathol Exp Neurol*; 27:167–82.

Hsiao K, Chapman P, Nilsen S, Eckman C, Harigaya Y, Younkin S, Yang F, Cole G (1996). Correlative memory deficits, Aβ elevation, and amyloid plaques in transgenic mice. *Science*; 274(5284):99-102.

Imaizumi T, Kocsis JD, Waxman SG (1998). Resistance to anoxic injury in the dorsal columns of adult rat spinal cord following demyelination. *Brain Res*; 779: 292±6.

Iwamoto T, Watano T, and Shigekawa M (1996). A novel isothioureia derivative selectively inhibits the reverse mode of Na<sup>+</sup>/Ca<sup>2+</sup> exchange in cells expressing NCX1. *J Biol Chem*; 271:22391–22397.

Iwamoto T and Shigekawa M (1998). Differential inhibition of Na<sup>+</sup>/Ca<sup>2+</sup> exchanger isoforms by divalent cations and isothioureia derivative. *Am J Physiol*; 275:C423–C430.

Iwamoto T, Uehara A, Nakamura TY, Imanaga I, and Shigekawa M (1999). Chimeric analysis of Na<sup>+</sup>/Ca<sup>2+</sup> exchangers NCX1 and NCX3 reveals structural domains important for differential sensitivity to external Ni<sup>2+</sup> or Li<sup>+</sup>. *Am J Physiol*; 275: C423–C430.

Iwamoto T, Kita S, Uehara A, Inoue Y, Taniguchi Y, Imanaga I, and Shigekawa M (2001). Structural domains influencing sensitivity to isothioureia derivative inhibitor KB-R7943 in cardiac Na<sup>+</sup>/Ca<sup>2+</sup> exchanger. *Mol Pharmacol* 59:524–531.

- Iwatsubo T, Mann DM, Odaka A, Suzuki N, Ihara Y (1995). Amyloid beta protein (A beta) deposition: A beta 42(43) precedes A beta 40 in Down syndrome. *Ann Neurol*; 37(3):294-9.
- Jalonen TO, Charniga CJ and Wielt DB (1997). beta-Amyloid peptide-induced morphological changes coincide with increased K<sup>+</sup> and Cl<sup>-</sup> channel activity in rat cortical astrocytes. *Brain Res*; 746, 85–97.
- Jarrett JT, Berger EP, Lansbury PT Jr (1993). The carboxy terminus of the beta amyloid protein is critical for the seeding of amyloid formation: implications for the pathogenesis of Alzheimer's disease. *Biochemistry*; 32(18):4693-7.
- Jicha GA, Abner EL, Schmitt FA, Kryscio RJ, Riley KP, Cooper GE, Stiles N, Mendiondo MS, Smith CD, Van Eldik LJ, Nelson PT (2012). Preclinical AD Workgroup staging: pathological correlates and potential challenges. *Neurobiol Aging*; 33(3):622.e1-622.e16.
- Juhaszova M, Shimizu H, Borin ML, Yip RK, Santiago EM, Lindenmayer GE, and Blaustein MP (1996). Localization of the Na<sup>+</sup>-Ca<sup>2+</sup> exchanger in vascular smooth muscle and in neurons and astrocytes. *Ann N Y Acad Sci*;779:318–335.
- Juhaszova M, Church P, Blaustein MP, Stanley EF (2000). Location of calcium transporters at presynaptic terminals. *Eur J Neurosci*; 12(3):839-46.
- Kaczorowski GJ, Barros F, Dethmers JK, Trumble MJ, and Cragoe EJ Jr (1985). Inhibition of Na<sup>+</sup>/Ca<sup>2+</sup> exchange in pituitary plasma membrane vesicles by analogues of amiloride. *Biochemistry*; 24:1394–1403.
- Kaczorowski GJ, Slaughter RS, King VF, and Garcia ML (1989). Inhibitors of sodium calcium exchange: identification and development of probes of transport activity. *Biochim Biophys Acta*; 988:287–302.
- Kagan BL, Hirakura Y, Azimov R, Azimova R & Lin MC (2002). The channel hypothesis of Alzheimer's disease: current status. *Peptides*;23, 1311–1315.
- Kang J, Lemaire HG, Unterbeck A, Salbaum JM, Masters CL, Grzeschik KH, Multhaup G, Beyreuther K, Muller-Hill B (1987). The precursor of Alzheimer's disease amyloid A4protein resembles a cell-surface receptor. *Nature*; 325:733–736.
- Kang TM, Hilgemann DW (2004). Multiple transport modes of the cardiac Na<sup>+</sup>/Ca<sup>2+</sup> exchanger. *Nature*; 427(6974):544-8.
- Kasir J, Ren X, Furman I, Rahamimoff H (1999). Truncation of the C terminus of the rat brain Na<sup>(+)</sup>-Ca<sup>(2+)</sup> exchanger RBE-1 (NCX1.4) impairs surface expression of the protein. *J Biol Chem*; 274(35):24873-80.
- Khachaturian ZS (1989). Calcium, membranes, aging, and Alzheimer's disease. Introduction and overview. *Ann NY Acad Sci*; 568, 1–4.
- Kiedrowski L, Brooker G, Costa E, and Wroblewski JT (1994). Glutamate impairs neuronal calcium extrusion while reducing sodium gradient. *Neuron*; 12:295–300.

Kofuji P, Hadley RW, Kieval RS, Lederer WJ, Schulze DH (1992). Expression of the Na-Ca exchanger in diverse tissues: a study using the cloned human cardiac Na-Ca exchanger. *Am J Physiol*; 263(6 Pt 1):C1241-9.

Kofuji P, WJ Lederer, and Schulze DH (1994). Mutually exclusive and cassette exons underlie alternatively spliced isoforms of the Na<sup>+</sup>/Ca<sup>2+</sup> exchanger. *J Biol Chem*; 269:5145–5149.

Kosik KS, Joachim CL, Selkoe DJ (1986). Microtubule-associated protein tau (tau) is a major antigenic component of paired helical filaments in Alzheimer disease. *Proc Natl Acad Sci U S A*; 83(11):4044-8.

Kondo J, Honda T, Mori H, Hamada Y, Miura R, Ogawara M, and Ihara Y (1988). The carboxyl third of tau is tightly bound to paired helical filaments. *Neuron*; 1: 827–834.

Koo EH, Squazzo SL (1994). Evidence that production and release of amyloid beta-protein involves the endocytic pathway. *J Biol Chem*; 269(26):17386-9

Kuchibhotla KV, Goldman ST, Lattarulo CR, Wu HY, Hyman BT, Bacskai BJ (2008). Abeta plaques lead to aberrant regulation of calcium homeostasis in vivo resulting in structural and functional disruption of neuronal networks. *Neuron*; 59:214–25.

LaFerla FM, Green KN, Oddo S (2007). Intracellular amyloid-beta in Alzheimer's disease. *Nat Rev Neurosci*; 8(7):499-509.

LaFerla FM (2002). Calcium dyshomeostasis and intracellular signalling in Alzheimer's disease. *Nat Rev Neurosci*; 3(11):862-72.

Lai A, Sisodia SS, Trowbridge IS (1995). Characterization of sorting signals in the beta-amyloid precursor protein cytoplasmic domain. *J Biol Chem*; 270: 3565–3573.

Langheinrich TC, Romanowski CA, Wharton S, *et al.* (2011). Presenilin-1 mutation associated with amnesia, ataxia, and medial temporal lobe T2 signal changes. *Neurology*; 76:1435e1436.

Lee JH, Yu WH, Kumar A, Lee S, Mohan PS, Peterhoff CM, Wolfe DM, Martinez-Vicente M, Massey AC, Sovak G, Uchiyama Y, Westaway D, Cuervo AM, Nixon RA (2010). Lysosomal proteolysis and autophagy require presenilin 1 and are disrupted by Alzheimer-related PS1 mutations. *Cell*; 141(7):1146-58.

Lee SL, AS Yu, and Lytton J (1994). Tissue-specific expression of Na<sup>+</sup>-Ca<sup>2+</sup> exchanger isoforms. *J Biol Chem*; 269:14849–14852.

Lee VMY, Balin BJ, Otvos L, and Trojanowski JQ (1991). A68: a major subunit of paired helical filaments and derivatized forms of normal tau. *Science*; 251: 675–678.

Lemere CA, Blusztajn JK, Yamaguchi H, Wisniewski T, Saido TC, Selkoe DJ (1996). Sequence of deposition of heterogeneous amyloid beta-peptides and APO E in Down syndrome: implications for initial events in amyloid plaque formation. *Neurobiol Dis*; 3(1):16-32.

- Levitsky DO, Nicoll DA, and Philipson KD (1994). Identification of the high affinity  $\text{Ca}^{2+}$ -binding domain of the cardiac  $\text{Na}^{+}$ - $\text{Ca}^{2+}$  exchanger. *J Biol Chem*; 269:22847–22852.
- Levy E, Carman MD, Fernandez-Madrid IJ, Power MD, Lieberburg I, van Duinen SG, Bots GT, Luyendijk W, Frangione B (1990). Mutation of the Alzheimer's disease amyloid gene in hereditary cerebral hemorrhage, Dutch type. *Science*; 248: 1124–1126.
- Li XF, Lytton J (1999). A circularized sodium-calcium exchanger exon 2 transcript. *J Biol Chem*; 274(12):8153-60.
- Li Z, Nicoll DA, Collins A, Hilgemann DW, Filoteo AG, Penniston JT, Weiss JN, Tomich JM, and Philipson KD (1991). Identification of a peptide inhibitor of the cardiac sarcolemmal  $\text{Na}^{+}$ / $\text{Ca}^{2+}$  exchanger. *J Biol Chem*; 266:1014–1020.
- Li Z, Matsuoka S, Hryshko LV, Nicoll DA, Bersohn MM, and Burke EP (1994). Cloning of the NCX2 isoform of the plasma membrane  $\text{Na}^{+}$ - $\text{Ca}^{2+}$  exchanger. *J Biol Chem*; 269:17434–17439.
- Lipton P (1999). Ischemic cell death in brain neuron *Physiol Rev*; 79:1431–1568.
- Lovas G, Szilagyi N, Majtenyi K, Palkovits M, Komoly S (2000). Axonal changes in chronic demyelinated cervical spinal cord plaques. *Brain*; 123: 308±17.
- Lytton J, Dong H (2002). Rat heart NCX1.1 stoichiometry measured in a transfected cell system. *Ann N Y Acad Sci*; 976:137-41.
- Lytton J, Li XF, Dong H, and Kraev A (2002).  $\text{K}^{+}$ -dependent  $\text{Na}^{+}$ / $\text{Ca}^{2+}$  exchangers in the brain. *Ann N Y Acad Sci*; 976:382–393.
- Maack C, Ganesan A, Sidor A, O'Rourke B (2005). Cardiac sodium-calcium exchanger is regulated by allosteric calcium and exchanger inhibitory peptide at distinct sites. *Circ Res*; 96(1):91-9.
- Madison DV, Malenka RC, and Nicoll RA (1991). Mechanisms underlying long-term potentiation of synaptic transmission. *Annu Rev Neurosci*; 14:379–397.
- Main MJ, Grantham CJ, and Cannell MB (1997). Changes in subsarcolemmal sodium concentration measured by  $\text{Na}^{+}$ - $\text{Ca}^{2+}$  exchanger activity during  $\text{Na}^{+}$  pump inhibition and  $\beta$ -adrenergic stimulation in guinea pig ventricular myocytes. *Pflugers Arch*; 435:112–118.
- Makino N, Zhao D, and Dhalla NS (1988). Stimulation of heart sarcolemmal  $\text{Na}^{+}$ - $\text{Ca}^{2+}$  exchange by concanavalin A. *Biochem Biophys Res Commun*; 154:245–251.
- Mark RJ, Hensley K, Butterfield DA & Mattson MP (1995). Amyloid  $\beta$ -peptide impairs ion-motive ATPase activities: evidence for a role in loss of neuronal  $\text{Ca}^{2+}$  homeostasis and cell death. *J. Neurosci*; 15, 6239–6249.

- Mark RJ, Pang Z, Geddes JW, Uchida K, Mattson MP (1997). Amyloid beta-peptide impairs glucose transport in hippocampal and cortical neurons: involvement of membrane lipid peroxidation. *J Neurosci*; 17(3):1046-54.
- Masliah E (1995). Mechanisms of synaptic dysfunction in Alzheimer's disease. *Histol Histopathol*; 10:509–19.
- Masters CL, Simms G, Weinman NA, Multhaup G, McDonald BL, Beyreuther K (1985). Amyloid plaque core protein in Alzheimer disease and Down syndrome. *Proc Natl Acad Sci U S A*; 82(12):4245-9.
- Matsuoka S, Nicoll DA, Reilly RF, Hilgemann DW, and Philipson KD (1993). Initial localization of regulatory regions of the cardiac sarcolemmal Na<sup>+</sup>-Ca<sup>2+</sup> exchanger. *Proc Natl Acad Sci USA*;90:3870–3874.
- Matsuoka S, Nicoll DA, Hryshko LV, Levitsky DO, Weiss JN, and Philipson KD (1995). Regulation of the cardiac Na<sup>(+)</sup>-Ca<sup>2+</sup> exchanger by Ca<sup>2+</sup>: mutational analysis of the Ca<sup>2+</sup>-binding domain. *J Gen Physiol*;105:403–420.
- Matsuoka S, Nicoll DA, He Z, and Philipson KD (1997). Regulation of cardiac Na<sup>+</sup>-Ca<sup>2+</sup> exchanger by the endogenous XIP region. *J Gen Physiol*; 109:273–286.
- Mattson MP, Cheng B, Davis D, Bryant K, Lieberburg I, Rydel RE (1992). beta-Amyloid peptides destabilize calcium homeostasis and render human cortical neurons vulnerable to excitotoxicity. *J Neurosci*;12(2):376-89.
- Mattson MP (1994). Calcium and neuronal injury in Alzheimer's disease. Contributions of  $\beta$ -amyloid precursor protein mismetabolism, free radicals, and metabolic compromise. *Ann NY Acad Sci*; 747, 50–76.
- Mattson, MP (1995). Free radicals and disruption of neuronal ion homeostasis in AD: a role for amyloid  $\beta$ -peptide? *Neurobiol Aging*;16, 679–682.
- Mattson MP, LaFerla FM, Chan SL, Leissring MA, Shepel PN, Geiger JD (2000). Calcium signaling in the ER: its role in neuronal plasticity and neurodegenerative disorders. *TrendsNeurosci*; 23(5):222-9.
- Mattson MP, Chan SL (2003). Neuronal and glial calcium signaling in Alzheimer's disease. *Cell Calcium*; 34:385–97.
- Meyer-Luehmann M, Spires-Jones TL, Prada C, Garcia-Alloza M, de Calignon A, Rozkalne A, Koenigsknecht-Talboo J, Holtzman DM, Bacskai BJ, Hyman BT (2008). Rapid appearance and local toxicity of amyloid-beta plaques in a mouse model of Alzheimer's disease. *Nature*; 451(7179):720-4.
- Milo R, Kahana E (2010). Multiple sclerosis: geoeidemiology, genetics and the environment. *Autoimmun Rev*; 9:A387–A394.
- Minkeviciene R, Banerjee P & Tanila H (2004). Memantine improves spatial learning in a transgenic mouse model of Alzheimer's disease. *J Pharmacol Exp Ther*; 311, 677–682

Minkeviciene R, Rheims S, Dobszay MB, Zilberter M, Hartikainen J, Fülöp L, Penke B, Zilberter Y, Harkany T, Pitkänen A, Tanila H (2009). Amyloid beta-induced neuronal hyperexcitability triggers progressive epilepsy. *J Neurosci*; 29(11):3453-62.

Miura Y, Kimura J (1989). Sodium-calcium exchange current. Dependence on internal Ca and Na and competitive binding of external Na and Ca. *J Gen Physiol*; 93(6):1129-45.

Molinaro P, Pannaccione A, Sisalli MJ, Secondo A, Cuomo O, Sirabella R, Cantile M, Ciccone R, Scorziello A, di Renzo G, Annunziato L (2015). A new cell-penetrating peptide that blocks the autoinhibitory XIP domain of NCX1 and enhances antiporter activity. *Mol Ther*; 23(3):465-76.

Montine TJ, Phelps CH, Beach TG, Bigio EH, Cairns NJ, Dickson DW, Duyckaerts C, Frosch MP, Masliah E, Mirra SS, Nelson PT, Schneider JA, Thal DR, Trojanowski JQ, Vinters HV, Hyman BT (2012). National Institute on Aging; Alzheimer's Association. National Institute on Aging-Alzheimer's Association guidelines for the neuropathologic assessment of Alzheimer's disease: a practical approach. *Acta Neuropathol*; 123(1):1-11.

Mullan M, Crawford F, Axelman K, Houlden H, Lilius L, Winblad B, Lannfelt L (1992). A pathogenic mutation for probable Alzheimer's disease in the APP gene at the N-terminus of beta-amyloid. *Nat Genet*; 1: 345-347.

Murata Y, Harada K, Nakajima F, Maruo J, and Morita T (1995). Non-selective effects of amiloride and its analogues on ion transport systems and their cytotoxicities in cardiac myocytes. *Jpn J Pharmacol*; 68:279-285.

Nagele, RG, D'Andrea MR, Anderson WJ & Wang HY (2002). Intracellular accumulation of  $\beta$ -amyloid1-42 in neurons is facilitated by the  $\alpha 7$  nicotinic acetylcholine receptor in Alzheimer's disease. *Neuroscience*; 110, 199-211.

Namane A, Gouyette C, Fillion MP, Fillion G, and Huynh-Dinh T (1992). Improved brain delivery of AZT using a glycosyl phosphotriester prodrug. *J Med Chem*; 35:3039-3044.

Naruse S, Thinakaran G, Luo JJ, Kusiak JW, Tomita T, Iwatsubo T, Qian X, Ginty DD, Price DL, Borchelt DR, Wong PC, Sisodia SS (1998). Effects of PS1 deficiency on membrane protein trafficking in neurons. *Neuron*; 21(5):1213-21.

Nelson PT, Alafuzoff I, Bigio EH, Bouras C, Braak H, Cairns NJ, Castellani RJ, Crain BJ, Davies P, Del Tredici K, Duyckaerts C, Frosch MP, Haroutunian V, Hof PR, Hulette CM, Hyman BT, Iwatsubo T, Jellinger KA, Jicha GA, Kövari E, Kukull WA, Leverenz JB, Love S, Mackenzie IR, Mann DM, Masliah E, McKee AC, Montine TJ, Morris JC, Schneider JA, Sonnen JA, Thal DR, Trojanowski JQ, Troncoso JC, Wisniewski T, Woltjer RL, Beach TG (2012). Correlation of Alzheimer disease neuropathologic changes with cognitive status: a review of the literature. *J Neuropathol Exp Neurol*; 71(5):362-81.

Nicholas SB, Yang W, Lee SL, Zhu H, Philipson KD, Lytton J (1998). Alternative promoters and cardiac muscle cell-specific expression of the Na<sup>+</sup>/Ca<sup>2+</sup> exchanger gene. *Am J Physiol*; 274(1 Pt 2):H217-32.

- Nicoll DA, Longoni S, and Philipson KD (1990). Molecular cloning and functional expression of the cardiac sarcolemmal Na<sup>+</sup>-Ca<sup>2+</sup> exchanger. *Science (Wash DC)*; 250:562–565.
- Nicoll DA, Hryshko LV, Matsuoka S, Frank JS, and Philipson KD (1996). Mutation of amino acid residues in the putative transmembrane segments of the cardiac sarcolemmal Na<sup>+</sup>-Ca<sup>2+</sup> exchanger. *J Biol Chem*; 271:13385–13391.
- Nicoll DA, Ottolia M, Lu L, Lu Y, and Philipson KD (1999). A new topological model of the cardiac sarcolemmal Na<sup>+</sup>-Ca<sup>2+</sup> exchanger. *J Biol Chem*; 274:910–917.
- Niggli E, Lederer WJ (1993). Activation of Na-Ca exchange current by photolysis of caged calcium". *Biophys J*; 65(2):882-91.
- Nilsberth C, Westlind-Danielsson A, Eckman CB, Condron MM, Axelman K, Forsell C, Sten H, Luthman J, Teplow DB, Younkin SG, et al. (2001). The “Arctic” APP mutation (E693G) causes Alzheimer’s disease by enhanced A-beta protofibril formation. *Nat Neurosci*; 4: 887–893.
- Nixon RA, Saito KI, Grynspan F, Griffin WR, Katayama S, Honda T, Mohan PS, Shea TB, Beermann M (1994). Calcium-activated neutral proteinase (calpain) system in aging and Alzheimer's disease. *Ann N Y Acad Sci*; 747:77-91.
- Nunomura A, Castellani RJ, Zhu X, Moreira PI, Perry G, Smith MA (2006). Involvement of oxidative stress in Alzheimer disease. *J Neuropathol Exp Neurol*; 65(7):631-41.
- Ohm TG, Müller H, Braak H, Bohl J (1995). Close-meshed prevalence rates of different stages as a tool to uncover the rate of Alzheimer's disease-related neurofibrillary changes. *Neuroscience*; 64(1):209-17.
- Olney JW (1973). Status of monosodium glutamate revisited. *Am J Clin Nutr*; 26:683–5.
- Ottolia M, John S, Qiu Z, Philipson KD (2001). Split Na<sup>+</sup>-Ca<sup>2+</sup> exchangers. Implications for function and expression. *J Biol Chem*; 276(22):19603-9.
- Palop JJ, Chin J, and Mucke L (2006). A network dysfunction perspective on neurodegenerative diseases. *Nature*; 443, 768–773.
- Palop JJ, Chin J, Roberson ED, Wang J, Thwin MT, Bien-Ly N, Yoo J, Ho KO, Yu GQ, Kreitzer A, Finkbeiner S, Noebels JL, Mucke L (2007). Aberrant excitatory neuronal activity and compensatory remodeling of inhibitory hippocampal circuits in mouse models of Alzheimer's disease. *Neuron*; 55(5):697-711.
- Palop JJ, Mucke L (2009). Epilepsy and cognitive impairments in Alzheimer disease. *Arch Neurol*; 66(4):435-40.
- Palop JJ, Mucke L (2010). Amyloid-beta-induced neuronal dysfunction in Alzheimer's disease: from synapses toward neural networks. *Nat Neurosci*; 13(7):812-8.
- Pannaccione A, Secondo A, Scorziello A, Cali G, Tagliatela M, Annunziato L (2005). Nuclear factor-kappaB activation by reactive oxygen species mediates voltage-gated K

current enhancement by neurotoxic beta-amyloid peptides innervate growth factor-differentiated PC-12 cells and hippocampal neurones. *J Neurochem*; 94, 572e586.

Pannaccione A, Boscia F, Scorziello A, Adornetto A, Castaldo P, Sirabella R, Tagliatalata M, Di Renzo GF, Annunziato L (2007). Up-regulation and increased activity of KV3.4 channels and their accessory subunit MinK-related peptide 2 induced by amyloid peptide are involved in apoptotic neuronal death. *Mol Pharmacol*; 72, 665e673.

Pannaccione A, Secondo A, Molinaro P, D'Avanzo C, Cantile M, Esposito A, Boscia F, Scorziello A, Sirabella R, Sokolow S, Herchuelz A, Di Renzo G, Annunziato L (2012). A new concept: A $\beta$ 1-42 generates a hyperfunctional proteolytic NCX3 fragment that delays caspase-12 activation and neuronal death. *J Neurosci*; 32(31):10609-17.

Papa M, Canitano A, Boscia F, Castaldo P, Sellitti S, Porzig H, Tagliatalata M, and Annunziato L (2003). Differential expression of the Na<sup>+</sup>-Ca<sup>2+</sup> exchanger transcripts and proteins in rat brain regions. *J Comp Neurol*; 461:31-48.

Penniston JT, Enyedi A, Verma AK, Adamo HP, Filoteo AG (1997). Plasma membrane Ca<sup>2+</sup> pumps. *Ann N Y Acad Sci*; 834:56-64.

Perez RG, Soriano S, Hayes JD, Ostaszewski B, Xia W, Selkoe DJ, Chen X, Stokin GB, Koo EH (1999). Mutagenesis identifies new signals for beta-amyloid precursor protein endocytosis, turnover, and the generation of secreted fragments, including Abeta42. *J Biol Chem*; 274(27):18851-6.

Philipson KD, Bersohn MM, Nishimoto AY (1982). Effects of pH on Na<sup>+</sup>-Ca<sup>2+</sup> exchange in canine cardiac sarcolemmal vesicles. *Circ Res*;50(2):287-93.

Philipson KD, Nishimoto AY (1984). Stimulation of Na<sup>+</sup>-Ca<sup>2+</sup> exchange in cardiac sarcolemmal vesicles by phospholipase D. *J Biol Chem*; 59(1):16-9.

Philipson KD, Longoni S, and Ward R (1988). Purification of the cardiac Na<sup>+</sup>-Ca<sup>2+</sup> exchange protein. *Biochim Biophys Acta*; 945:298-306.

Philipson KD and Nicoll DA (2000). Sodium-calcium exchange: a molecular perspective. *Ann Rev Physiol*; 62:111-133.

Pignataro G, Tortiglione A, Scorziello A, Giaccio L, Secondo A, Severino B, Santagada V, Caliendo G, Amoroso S, Di Renzo GF, *et al.* (2004b) Evidence for a protective role played by the Na<sup>+</sup>/Ca<sup>2+</sup> exchanger in cerebral ischemia induced by middle cerebral artery occlusion in male rats. *Neuropharmacology*; 46:439-448.

Pike CJ, Balazs R and Cotman CW (1996). Attenuation of beta-amyloid neurotoxicity in vitro by potassium-induced depolarization. *J Neurochem*; 67, 1774-1777.

Pozos TC, Sekler I, and Cyert MS (1996). The product of HUM1, a novel yeast gene, is required for vacuolar Ca<sup>2+</sup>/H<sup>+</sup> exchange and is related to mammalian Na<sup>+</sup>/Ca<sup>2+</sup> exchangers. *Mol Cell Biol*;16:3730-3741.

- Quednau BD, Nicoll DA, and Philipson KD (1997). Tissue specificity and alternative splicing of the Na<sup>+</sup>/Ca<sup>2+</sup> exchanger isoforms NCX1, NCX2 and NCX3 in rat. *Am J Physiol*; 272:C1250–C1261.
- Querfurth HW & Selkoe DJ (1994). Calcium ionophore increases amyloid  $\beta$  peptide production by cultured cells. *Biochemistry*;33, 4550–4561.
- Ramsden M, Plant LD, Webster NJ, Vaughan PF, Henderson Z and Pearson HA (2001). Differential effects of unaggregated and aggregated amyloid beta protein (1–40) on K<sup>+</sup> channel currents in primary cultures of rat cerebellar granule and cortical neurones. *J Neurochem*; 79, 699–712.
- Reeves JP and Hale CC (1984). The stoichiometry of the cardiac sodium-calcium exchange system. *J Biol Chem*; v259(12):7733-9.
- Reeves JP, Bailey CA, and Hale CC (1986). Redox modification of sodium-calcium exchange activity in cardiac sarcolemmal vesicles. *J Biol Chem*; 261:4948–4955.
- Reeves JP, Poronnik P (1987). Modulation of Na<sup>+</sup>-Ca<sup>2+</sup> exchange in sarcolemmal vesicles by intravesicular Ca<sup>2+</sup>. *Am J Physiol*; 252(1 Pt 1):C17-23.
- Reisberg B, Doody R, Stöffler A, Schmitt F, Ferris S, Möbius HJ (2003). Memantine Study Group. Memantine in moderate-to-severe Alzheimer's disease. *N Engl J Med*; 348(14):1333-41.
- Reitz C, Mayeux R (2009). Use of genetic variation as biomarkers for Alzheimer's disease. *Ann N Y Acad Sci*; 1180:75–96.
- Reitz C, Brayne C, Mayeux R (2011). Epidemiology of Alzheimer disease. *Nat Rev Neurol*; 7(3):137-52.
- Ren X, Philipson KD (2013). The topology of the cardiac Na<sup>+</sup>/Ca<sup>2+</sup> exchanger, NCX1. *J Mol Cell Cardiol*; 57:68-71.
- Reuter H, Porzig H (1995). Localization and functional significance of the Na<sup>+</sup>/Ca<sup>2+</sup> exchanger in presynaptic boutons of hippocampal cells in culture. *Neuron*; 15(5):1077-84.
- Ruknudin A, He S, Lederer WJ, Schulze DH (2000). Functional differences between cardiac and renal isoforms of the rat Na<sup>+</sup>-Ca<sup>2+</sup> exchanger NCX1 expressed in *Xenopus* oocytes. *J Physiol*; 529 Pt 3:599-610.
- Samson WN, van Duijn CM, Hop WC, Hofman A (1996). Clinical features and mortality in patients with early-onset Alzheimer's disease. *Eur Neurol*; 36(2):103-6.
- Sanchez PE, Zhu L, Verret L, Vossel KA, Orr AG, Cirrito JR, Devidze N, Ho K, Yu GQ, Palop JJ, Mucke L (2012). Levetiracetam suppresses neuronal network dysfunction and reverses synaptic and cognitive deficits in an Alzheimer's disease model. *Proc Natl Acad Sci U S A*; 109(42):E2895-903.

- Possin KL, Sanchez PE, Anderson-Bergman C, Fernandez R, Kerchner GA, Johnson ET, Davis A, Lo I, Bott NT, Kiely T, Fenesy MC, Miller BL, Kramer JH, Finkbeiner S (2016). Cross-species translation of the Morris maze for Alzheimer's disease. *J Clin Invest*; 126(2):779-83.
- Saad M, Brkanac Z, Wijsman EM (2015). Family-based genome scan for age at onset of late-onset Alzheimer's disease in whole exome sequencing data. *Genes Brain Behav*; 14(8):607-17.
- Sanchez-Andres JV, Alkon DL (1991). Voltage-clamp analysis of the effects of classical conditioning on the hippocampus. *J Neurophysiol*; 65(4):796-807.
- Sanchez-Armass S, Blaustein MP (1987). Role of sodium-calcium exchange in regulation of intracellular calcium in nerve terminals. *Am J Physiol*; 252(6 Pt1):C595-603.
- Santacruz-Tolozza L, Ottolia M, Nicoll DA, and Philipson KD (2000). Functional analysis of a disulfide bond in the cardiac Na<sup>+</sup>/Ca<sup>2+</sup> exchanger. *J Biol Chem*; 275:182–188.
- Santos SF, Pierrot N, Morel N, Gailly P, Sindic C, Octave JN (2009). Expression of human amyloid precursor protein in rat cortical neurons inhibits calcium oscillations. *J Neurosci*; 29(15):4708-18.
- Saunders AM, Strittmatter WJ, Schmechel D, George-Hyslop PH, Pericak-Vance MA, Joo SH, Rosi BL, Gusella JF, Crapper-MacLachlan DR, Alberts MJ, et al. (1993). Association of apolipoprotein E allele epsilon 4 with late-onset familial and sporadic Alzheimer's disease. *Neurology*; 43(8):1467-72.
- Saunders AM (2000). Apolipoprotein E and Alzheimer disease: an update on genetic and functional analyses. *J Neuropathol Exp Neurol*; 59(9):751-8.
- Schenk D, Basi GS, Pangalos MN (2011). Treatment strategies targeting amyloid beta-protein. *Cold Spring Harb Perspect Med*.
- Schnetkamp PP, Basu DK, and Szerencsei RT (1989). Na<sup>+</sup>/Ca<sup>2+</sup> exchange in bovine rod outer segments requires and transports K<sup>+</sup>. *Am J Physiol*; 257:C153–C157.
- Schulze DH, Polumuri SK, Gille T, Ruknudin A (2002). Functional regulation of alternatively spliced Na<sup>+</sup>/Ca<sup>2+</sup> exchanger (NCX1) isoforms. *Ann N Y Acad Sci*;976:187-96.
- Secondo A, Staiano RI, Scorziello A, Sirabella R, Boscia F, Adornetto A, et al. (2007). BHK cells transfected with NCX3 are more resistant to hypoxia followed by reoxygenation than those transfected with NCX1 and NCX2: possible relationship with mitochondrial membrane potential. *Cell Calcium*;42:521–35.
- Selkoe DJ, Ihara Y, and Salazar F (1982). Alzheimer's disease: insolubility of partially purified helical filaments in sodium dodecyl sulfate and urea. *Science*; 215: 1243–1245.
- Selkoe DJ (1991). The molecular pathology of Alzheimer's disease. *Neuron*; 6:487 – 498.

- Selkoe DJ (1994). Cell biology of the amyloid beta-protein precursor and the mechanism of Alzheimer's disease. *Annu Rev Cell Biol*; 10:373-403.
- Selkoe DJ (1999). Translating cell biology into therapeutic advances in Alzheimer's disease. *Nature*; 399(6738 Suppl):A23-31.
- Selkoe DJ (2001). Alzheimer's disease: genes, proteins, and therapy. *Physiol Rev*; 81(2):741-66.
- Selkoe DJ (2008). Biochemistry and molecular biology of amyloid  $\beta$ -protein and the mechanism of Alzheimer's disease. *Handb Clin Neurol*; 89:245-60.
- Selkoe DJ (2011). Alzheimer's disease. *Cold Spring Harb Perspect Biol*; 3(7).
- Serrano-Pozo A, Qian J, Monsell SE, Blacker D, Gómez-Isla T, Betensky RA, Growdon JH, Johnson KA, Frosch MP, Sperling RA, Hyman BT (2014). Mild to moderate Alzheimer dementia with insufficient neuropathological changes. *Ann Neurol*; 75(4):597-601.
- Seubert P, Vigo-Pelfrey C, Esch F, Lee M, Dovey H, Davis D, Sinha S, Schlossmacher M, Whaley J, Swindlehurst C, *et al.* (1992). Isolation and quantification of soluble Alzheimer's beta-peptide from biological fluids. *Nature*; 359: 325-327.
- Seubert P, Oltersdorf T, Lee MG, Barbour R, Blomquist C, Davis DL, Bryant K, Fritz LC, Galasko D, Thal LJ, *et al.* (1993). Secretion of b-amyloid precursor protein cleaved at the amino-terminus of the b-amyloid peptide. *Nature*; 361: 260-263.
- Sharikabad MN, Cragoe EJ Jr, and Brors O (1997). Inhibition by 5-N-(4-chlorobenzyl)-2',4'-dimethylbenzamil of Na<sup>+</sup>/Ca<sup>2+</sup> exchange and L-type Ca<sup>2+</sup> channels in isolated cardiomyocytes. *Pharmacol Toxicol*; 80:57-61.
- Shaul O, Hilgemann DW, de-Almeida-Engler J, Van Montagu M, Inz D, and Galili G (1999). Cloning and characterization of a novel Mg(2+)/H(+) exchanger. *EMBO (Eur Mol Biol Organ) J*;18:3973-3980.
- Sherzai D, Losey T, Vega S, Sherzai A (2014). Seizures and dementia in the elderly: Nation wide In patient Sample 1999-2008. *Epilepsy Behav*; 36:53-6.
- Shigekawa M, Iwamoto T, Uehara A, and Kita S (2002). Probing ion binding sites in the Na<sup>+</sup>-Ca<sup>2+</sup> exchanger. *Ann N Y Acad Sci*; 976:19-30.
- Sisodia SS, Koo EH, Beyreuther K, Unterbeck A, Price DL (1990). Evidence that b-amyloid protein in Alzheimer's disease is not derived by normal processing. *Science*; 248: 492-495.
- Smith BN and Armstrong WE (1996). The ionic dependence of the histamine-induced depolarization of vasopressin neurones in the rat supraoptic nucleus. *J Physiol*; 495:465-478.

Snyder EM, Nong Y, Almeida CG, Paul S, Moran T, Choi EY, Nairn AC, Salter MW, Lombroso PJ, Gouras GK, Greengard P (2005). Regulation of NMDA receptor trafficking by amyloid-beta. *Nat Neurosci*; 8(8):1051-8.

Stafstrom CE (2007). Persistent sodium current and its role in epilepsy. *Epilepsy Curr*; 7: 15–22.

Stengl M, Mubagwa K, Carmeliet E, and Flameng W (1998). Phenylephrine-induced stimulation of Na<sup>+</sup>/Ca<sup>2+</sup> exchange in rat ventricular myocytes. *Cardiovasc Res*; 38:703–710.

Strittmatter WJ, Saunders AM, Schmechel D, Pericak-Vance M, Enghild J, Salvesen GS, Roses AD (1993). Apolipoprotein E: high-avidity binding to  $\beta$ -amyloid and increased frequency of type 4 allele in late-onset familial Alzheimer disease. *Proc Natl Acad Sci*; 90: 1977–1981.

Stutzmann GE (2005). Calcium dysregulation, IP<sub>3</sub> signaling, and Alzheimer's disease. *Neuroscientist*; 11: 110–5.

Stutzmann GE, Smith I, Caccamo A, Oddo S, Laferla FM, Parker I (2006). Enhanced ryanodine receptor recruitment contributes to Ca<sup>2+</sup> disruptions in young, adult, and aged Alzheimer's disease mice. *J Neurosci*; 26(19):5180-9.

Stys PK, Waxman SG, Ransom BR (1991). Na<sup>+</sup>-Ca<sup>2+</sup> exchanger mediates Ca<sup>2+</sup> influx during anoxia in mammalian central nervous system white matter. *Ann Neurol*; 30: 375±80.

Stys PK, Waxman SG, Ransom BR (1992). Ionic mechanisms of anoxic injury in mammalian CNS white matter: role of Na<sup>+</sup> channels and Na<sup>+</sup>-Ca<sup>2+</sup> exchanger. *J Neurosci*; 12: 430±9.

Stys PK, Lopachin RM (1998). Mechanisms of calcium and sodium fluxes in anoxic myelinated central nervous system axons. *Neuroscience*; 82: 21±32.

Suzuki N, Cheung TT, Cai XD, Odaka A, Otvos L Jr, Eckman C, Golde TE, Younkin SG (1994). An increased percentage of long amyloid beta protein secreted by familial amyloid beta protein precursor (beta APP717) mutants. *Science*; 264: 1336–1340.

Tagliatela M, Amoroso S, Di Renzo GF, and Annunziato L (1988). Membrane events and ionic processes involved in dopamine release from tuberoinfundibular neurons. II. Effect of the inhibition of the Na<sup>+</sup>Ca<sup>2+</sup> exchange by amiloride. *J Pharmacol Exp Ther*; 246:689–694.

Tagliatela M, Canzoniero LM, Cragoe EJ, Di Renzo, and Annunziato L (1990). Na<sup>+</sup>-Ca<sup>2+</sup> exchange activity in central nerve endings. II. Relationship between pharmacological blockade by amiloride analogues and dopamine release from tuberoinfundibular hypothalamic neurons. *Mol Pharmacol*; 38:393–400.

Tagliavini F, Giaccone G, Frangione B, Bugiani O (1988). Pre-amyloid deposits in the cerebral cortex of patients with Alzheimer's disease and non demented individuals. *Neurosci Lett*; 93: 191–196.

- Takahashi RH, Milner TA, Li F, Nam EE, Edgar MA, Yamaguchi H, Beal MF, Xu H, Greengard P, Gouras GK (2002). Intraneuronal Alzheimer abeta42 accumulates in multivesicular bodies and is associated with synaptic pathology. *Am J Pathol*; 161(5):1869-79.
- Takahashi RH, Capetillo-Zarate E, Lin MT, Milner TA, Gouras GK (2013). Accumulation of intraneuronal  $\beta$ -amyloid 42 peptides is associated with early changes in microtubule-associated protein 2 in neurites and synapses. *PLoS One*; 8(1):e51965.
- Tamagnini F, Scullion S, Brown JT, Randall AD (2015). Intrinsic excitability changes induced by acute treatment of hippocampal CA1 pyramidal neurons with exogenous amyloid  $\beta$  peptide. *Hippocampus*;25(7):786-97.
- Tanzi RE, Bertram L (2005). Twenty years of the Alzheimer's disease amyloid hypothesis: a genetic perspective. *Cell*; 120(4):545-55.
- Terry RD, Masliah E, Salmon DP, Butters N, DeTeresa R, Hill R, Hansen LA, Katzman R (1991). Physical basis of cognitive alterations in Alzheimer's disease: synapse loss is the major correlate of cognitive impairment. *AnnNeurol*; 30(4):572-80.
- Thal DR, Rüb U, Schultz C, Sassin I, Ghebremedhin E, Del Tredici K, Braak E, Braak H (2000). Sequence of A $\beta$ -protein deposition in the human medial temporal lobe. *J Neuropathol Exp Neurol*; 59(8):733-48.
- Thal DR, Capetillo-Zarate E, Del Tredici K, Braak H (2006). The development of amyloid beta protein deposits in the aged brain. *Sci Aging Knowledge Environ*; (6):re1.
- Thal DR, Del Tredici K, Ludolph AC, Hoozemans JJ, Rozemuller AJ, Braak H, Knippschild U (2011). Stages of granulovacuolar degeneration: their relation to Alzheimer's disease and chronic stress response. *Acta Neuropathol*; 122(5):577-89.
- Tokuda T, Fukushima T, Ikeda S, Sekijima Y, Shojis S, Yanagisawa N, and Tamaoka A (1997). Plasma levels of amyloid beta proteins Ab1-40 and Ab1-42(43) are elevated in Down's syndrome. *Ann Neurol*; 41: 271-273.
- Tolosa de Talamoni N, Smith CA, Wasserman RH, Beltramino C, Fullmer CS, Penniston JT (1993). Immunocytochemical localization of the plasma membrane calcium pump, calbindin-D28k, and parvalbumin in Purkinje cells of avian and mammalian cerebellum. *Proc Natl Acad Sci U S A*; 90(24):11949-53.
- Van Eylen F, Kamagate A, Herchuelz A (2001). A new Na/Ca exchanger splicing pattern identified
- Verkhatsky A (2002). The endoplasmic reticulum and neuronal calcium signaling. *Cell Calcium*; 32: 393-404.
- Vitvitsky VM, Garg SK, Keep RF, Albin RL, Banerjee R (2012). Na<sup>+</sup> and K<sup>+</sup> ion imbalances in Alzheimer's disease. *Biochim Biophys Acta*;1822, 1671-1681.

Vogt DL, Thomas D, Galvan V, Bredesen DE, Lamb BT, Pimplikar SW (2011). Abnormal neuronal networks and seizure susceptibility in mice overexpressing the APP intracellular domain. *Neurobiol Aging*; 32(9):1725-9.

Vossel KA, Beagle AJ, Rabinovici GD, Shu H, Lee SE, Naasan G, Hegde M, Cornes SB, Henry ML, Nelson AB, Seeley WW, Geschwind MD, Gorno-Tempini ML, Shih T, Kirsch HE, Garcia PA, Miller BL, Mucke L (2013). Seizures and epileptiform activity in the early stages of Alzheimer disease. *JAMA Neurol*; 70(9):1158-66.

Walsh DM, Tseng BP, Rydel RE, Podlisny MB & Selkoe DJ (2000). The oligomerization of amyloid  $\beta$ -protein begins intracellularly in cells derived from human brain. *Biochemistry* 39, 10831–10839.

Wang X, Zhang XG, Zhou TT, Li N, Jang CY, Xiao ZC, Ma QH, Li S (2016). Elevated Neuronal Excitability Due to Modulation of the Voltage-Gated Sodium Channel Nav1.6 by A $\beta$ 1-42. *Front Neurosci*;10:94.

Weidemann A, Konig G, Bunke D, Fischer P, Salbaum JM, Masters CL, Beyreuther K (1989). Identification, biogenesis, and localization of precursors of Alzheimer's disease A4 amyloid protein. *Cell*; 57: 115–126.

Wertkin AM, Turner RS, Pleasure SJ, Golde TE, Younkin SG, Trojanowski JQ, Lee VM (1993). Human neurons derived from a teratocarcinoma cell line express solely the 695-amino acid amyloid precursor protein and produce intracellular beta-amyloid or A4 peptides. *Proc Natl Acad Sci U S A*; 90(20):9513-7.

Wild-Bode C, Yamazaki T, Capell A, Leimer U, Steiner H, Ihara Y, Haass C (1997). Intracellular generation and accumulation of amyloid beta-peptide terminating at amino acid 42. *J Biol Chem*; 272(26):16085-8.

Wischik CM, Novak M, Thogersen HC, Edwards PC, Runswick MJ, Jakes R, Walker JE, Milstein C, Rother M, and Klug A (1988). Isolation of a fragment of tau derived from the core of the paired helical filament of Alzheimer's disease. *Proc Natl Acad Sci USA*; 85: 4506– 4510.

Wittmack EK, Rush AM, Craner MJ, Goldfarb M, Waxman SG, Dib-Hajj SD (2004). Fibroblast growth factor homologous factor 2B: association with Nav1.6 and selective colocalization at nodes of Ranvier of dorsal root axons. *J Neurosci*; 24(30):6765-75.

Wittmack EK, Rush AM, Hudmon A, Waxman SG, Dib-Hajj SD (2005). Voltage-gated sodium channel Nav1.6 is modulated by p38 mitogen-activated protein kinase. *J Neurosci*; 25(28):6621-30

Woo SH and Morad M (2001). Bimodal regulation of Na<sup>+</sup>/Ca<sup>2+</sup> exchanger by beta-adrenergic signaling pathway in shark ventricular myocytes. *Proc Natl Acad Sci USA*; 98:2023–2028.

Wood JG, Mirra SS, Pollock NL, Binder LI (1986). Neurofibrillary tangles of Alzheimer's disease share antigenic determinants with the axonal microtubule-associated protein tau. *Proc Natl Acad Sci USA*; 83: 4040–4043.

Wujek JR, Bjartmar C, Richer E, Ransohoff RM, Yu M, Tuohy VK, *et al.* (2002). Axon loss in the spinal cord determines permanent neurological disability in an animal model of multiple sclerosis. *J Neuropathol Exp Neurolol*; 61: 23±32.

Yamoah EN, Lumpkin EA, Dumont RA, Smith PJ, Hudspeth AJ, Gillespie PG (1998). Plasma membrane Ca<sup>2+</sup>-ATPase extrudes Ca<sup>2+</sup> from hair cell stereocilia. *J Neurosci*; 18(2):610-24.

Yu LP, Edalji R, Harlan JE, Holzman TF, Lopez AP, Labkovsky B, Hillen H, Barghorn S, Ebert U, Richardson PL, *et al.* (2009). Structural characterization of a soluble amyloid b-peptide oligomer. *Biochemistry*; 48: 1870–1877.

Yu SP (2003). Regulation and critical role of potassium homeostasis in apoptosis. *Prog Neurobiol*; 70, 363–386.

Yu XM, Askalan R, Keil GJ, and Salter MW (1997). NMDA channel regulation by in situ leads to a functionally active 70kDa NH(2)-terminal protein. *Cell Calcium*; 30(3):191-8.

Yue C, Remy S, Su H, Beck H, Yaari Y (2005). Proximal persistent Na<sup>+</sup> channels drive spike after depolarizations and associated bursting in adult CA1 pyramidal cells. *J Neurosci*; 25(42):9704-20.

Yuste R, Majewska A, Holthoff K (2000). From form to function: calcium compartmentalization in dendritic spines. *Nat Neurosci*; 3:653–659.

Zhang X, Garbett K, Veeraraghavalu K, Wilburn B, Gilmore R, Mirnics K, Sisodia SS (2012). A role for presenilins in autophagy revisited: normal acidification of lysosomes in cells lacking PSEN1 and PSEN2. *J Neurosci*; 32(25):8633-48.

Zozulya AL, Wiendl H (2008). The role of regulatory T cells in multiple sclerosis. *Nat Clin Pract Neurol*; 4:384–398.